



**Development of a microfluidic sample preparation system for bacteria  
magnetic labelling and capture in clinical samples**

**Davide Carta**

Thesis to obtain the Master of Science Degree in  
**Bioengineering and Nanosystems**

Supervisors: Prof. Susana Isabel Pinheiro Cardoso de Freitas  
Dra. Verónica Cristina Martins Romão

**Examination committee**

Chairperson: Prof. Gabriel António Amaro Monteiro  
Supervisor: Dra. Verónica Cristina Martins Romão  
Member of the committee: Dra. Elisabete Fernandes

**December 2020**

## Contents

Acknowledgments .....	4
Preface .....	5
Declaration .....	5
Abstract .....	5
List of Figures.....	6
List of Tables.....	9
List of Formulas .....	10
List of Acronyms .....	11
1. Introduction.....	1
1.1. Aim of the project.....	1
1.2. State of the art.....	4
1.2.1. State of the art of sample pre-treatment: passive mixing and microfluidics.....	4
1.2.2. State of the art of bacteria detection.....	11
1.2.3. State of the art of magnetic cytometry .....	15
2. Materials and methods .....	21
2.1. Materials and tools.....	21
2.2. Methods .....	22
2.2.1. Immobilization protocol .....	22
2.2.2. Bacteria inoculum preparation.....	23
2.2.3. Protocol for bench-top capture.....	23
2.2.4. Microfluidic device fabrication .....	24
2.2.5. Protocol for microfluidic capture .....	25
2.2.6. Plating.....	28
2.2.7. Protocol for cytometric platform .....	29
3. Theoretical Background.....	30
3.1. Bench-top assay: immobilization of antibodies and bacteria capture.....	30
3.2. Microfluidic Device Fabrication .....	31
3.2.1. Hard Mask.....	31
3.2.2. SU-8 mold .....	33
3.2.3. PDMS production.....	36
3.3. Cytometer output signal simulation.....	37
3.4. Sample detection in a magnetic cytometric platform.....	42
4. Results .....	44
4.1. Benchtop optimization for antibody immobilization and bacteria capture.....	44
4.2. Fluidic simulations and design.....	55

4.3.	Microfluidic device fabrication .....	60
4.3.1.	Hard Mask.....	60
4.3.2.	SU-8 mold .....	62
4.3.3.	PDMS Device.....	69
4.4.	Microfluidic testing.....	71
5.	Conclusions and Discussion .....	80
5.1.	Importance of results .....	80
5.2.	Future optimization of the studied platform: modification, improvements and integration in an automatic system .....	80
6.	References .....	83
7.	Appendix.....	90
7.1.	Appendix A: Ademtech beads Datasheet.....	90
7.2.	Appendix B: table with summarized bench results .....	91
7.3.	Appendix C: table with microfluidic and bench results comparison .....	94
7.4.	Appendix D: Su-8 Datasheet.....	96
7.5.	Appendix E: Microfluidic device production Runsheet (provided by INESC-MN) .....	100
7.6.	Appendix F: Antibodies AbCam Datasheets .....	115

## Acknowledgments

To begin with, I would like to thank my supervisor Professor Susana Cardoso, for her support and enthusiasm in the project as well as for introducing me to the inspiring and eclectic environment that INESC MN represents, and PhD Verónica C. Martins, my daily guide through the complexity that a thesis work can represent, who always had the right advice to push the project further.

I would like to thank all the colleagues at Bioneer lab, Rita Soares, for all the knowledge she shared and the time she dedicated to mentor me for the whole period of the thesis, Ana Francisca, that transferred to me her previous work in the project, Débora Albuquerque, Sara Viveiros and the new acquired Raffaele Campanile, for making my time at INESC-MN not only a work but also a pleasure. I acknowledge PhD Vania Silverio and PhD Sofia Martins, who supported my work with some of their previous results and never missed to provide extra tips.

I want to thank Eng. Virgínia Soares, Eng. Fernando Silva and Eng. José Bernardo for managing all the processes that require expertise in the use of fabrication tools.

I also want to thank Professor Ana Azevedo and my colleagues Marta Patinha and Inés Simoes for the weekly meetings and discussions.

And not to forget a thank to all the people at INESC-MN who created a friendly and supportive environment.

I acknowledge Tecnofage for the provided material.

In conclusion, a thank to everyone that is far, but never missed to support me through these two years spent in Lisbon, my family and friends in Italy and my brother in UK, always there for a comforting call and some life tips.

## Preface

The work presented in this thesis was performed at the company Instituto de Engenharia de Sistemas e Computadores–Microsistemas e Nanotecnologias INESC-MN (Lisbon, Portugal), during the period February-December 2020, under the supervision of Dra. Verónica C. Martins Romão. The thesis was co-supervised at Instituto Superior Técnico by Prof. Susana Isabel Pinheiro Cardoso de Freitas.

## Declaration

I declare that this document is an original work of my own authorship and that it fulfills all the requirements of the Code of Conduct and Good Practices of the Universidade de Lisboa.

## Abstract

Hospital infections represent one of the novel health care challenges of the new century and rapid, economic and efficient technique for their detection are essential for rapid isolation of the patient and limited diffusion. Magnetic cytometry represents an emerging platform for bacteria detection, but complexity of the sample matrix and necessity of bacteria cell labelling require a preparative step. In the frame of a LoC (Lab on Chip) device PoC-oriented (Point of Care), such sample pre-treatment must be integrated in the cytometer and thus realized as a microfluidic component. Needed steps are bacteria labelling with magnetic particles and their concentration in a smaller volume, while unwanted components of the original sample, as other bacteria or residues, are discarded; labelling requires that recognition elements (here antibodies) specific for the target bacteria are immobilized on magnetic particles.

As concerning the following study, a bench-top assay for antibodies immobilization and bacteria capture and concentration has been optimized. A PDMS based microfluidic device, in two variants, have been produced and the parameters from the previous optimized protocol, such as ratios between antibodies, particles and bacteria have been applied to automatize sample pre-treatment through a new assay based on the device.

Devices ability on bacteria labelling and concentration have been evaluated and compared with results from bench-top assay, verifying if the former could be a substitute for the latter.

Microfluidic devices have been tested with spiked samples at different concentrations, as controlled solution of target bacteria in buffer, and with clinical samples, representing all the complexity of the real matrix. Efficiency in processing spiked sample is quantified and a mean capture efficiency of  $86\% \pm 9\%$  is obtained at a concentration of  $2 \cdot 10^5$  CFU/ml, while the lowest concentration capture with reasonable difference between positive and negative control is  $2 \cdot 10^3$  CFU/ml. Processing of clinical sample offered limited results due to high variability in sample concentration and limited tests, even though capture is observed and qualitative results are promising.

**Keywords:** sample preparation; sample pre-treatment; microfluidics; clinical sample; labelling; capture; immunomagnetic separation

## List of Figures

Figure 1- General flow for standard approach .....	3
Figure 2- General flow for proposed approach: in red, area of competence of presented work.....	3
Figure 3- Above: produced devices with outlined features; Below: CAD files reporting relative measures ....	4
Figure 4-Split and recombine mixer [16] .....	6
Figure 5-Split T-mixer design [17].....	6
Figure 6- Planar Asymmetric Split-And-Recombine PASAR mixer [18] .....	7
Figure 7- Planar view of the mixer with example of water-glycerol mixing at different stages [19].....	7
Figure 8- SHM configuration of the mixer [21] .....	8
Figure 9- SME mixer, top view [23] .....	9
Figure 10-Comparison in efficiency of a T-shape mixer with different number of obstacles [24]. Color code refers to specie A concentration, during specie A and specie B mixing.....	9
Figure 11-Top view and obstacles details of the mixer [15].....	10
Figure 12-Representation of photoresist mold fabrication: hard mask is taped on the holder, put in contact with photoresist on silicon substrate and exposed by UV light [25].....	11
Figure 13- GMR effect visually explained; F stays for Ferromagnetic while NM stays for Non Magnetic; White arrows indicates the Magnetic field direction in the layer and long arrows represents electron path moving from one layer to the other. [48] .....	16
Figure 14- Representation of MR effect and dependence from measured magnetic field with linear range evidenced by red dashed circle [48].....	16
Figure 15 - Transfer curve of sensor used for preliminary detection on processed sample, refer to section 5.2 .....	16
Figure 16-Example of the fringe field emitted by a superparamagnetic bead, in the case of vertical magnetization [26] .....	17
Figure 17-Simulation of normalized fringe field planar component on sensor surface, used parameters in Table 1 .....	18
Figure 18-Corresponding normalized output voltage of the sensor, used parameters in Table 1 .....	19
Figure 19- Set up of the device during testing .....	26
Figure 20-Detail of the device connections during testing .....	26
Figure 21- Device during mixing, red colored die is used to outline the process .....	27
Figure 22- Left: device during capture/retention, red colored die used to outline the process; right: Example of retained and resuspended beads.....	27
Figure 23-Left: device during elution, red colored die used to outline the process; right: example of eluted beads .....	28
Figure 24- Magnetic cytometric platform set-up [5].....	29
Figure 25 - Biotin structure [56] .....	30
Figure 26- Positive and negative photoresist [58].....	32
Figure 27 – General scheme for SU-8 mold production [59] .....	33
Figure 28- Exposure in photolithography [60].....	33
Figure 29-example of non-vertical walls due to high exposure dose [59] .....	35
Figure 30-example of undercut in SU-8 due to low exposure dose [59].....	35
Figure 31 - General schema for PDMS production, adapted from [62] .....	36
Figure 32- Oxygen plasma treatment for PDMS/glass sealing [63].....	37
Figure 33-Magnetic fingerprint of a particle detected with sensors half-bridge configuration [28] .....	37
Figure 34- Example of spherical beads distribution: left, 64 beads; right, 128beads .....	38
Figure 35 - Example of spheroidal beads distribution: left, 64 beads; right, 128 beads.....	39
Figure 36 – Example of rod-like beads distribution: left, 64 beads; right:128 beads .....	40

Figure 37 - Matlab output window for set parameters.....	41
Figure 38 - Fringe field and corresponding sensor output for a spherical distribution of beads on single bacteria with a coverage equal to 64 beads, other parameters as shown in Figure 37 .....	41
Figure 39- PtP and PW parameters for the example signal presented in Figure 38 .....	42
Figure 40-Code output for extracted parameters .....	42
Figure 41- Top view of sensor and microfluidic from cytometric platform [4] .....	43
Figure 42- Benchtop protocol schematics, only first washing step is represented, adapted from [64] .....	44
Figure 43- Superparamagnetic beads covered with antibodies, adapted from [64] .....	44
Figure 44 - Streptavidin/Biotin interaction: left, tetrameric streptavidin structure [65]; right, active site and evidenced hydrogen bonds [66].....	45
Figure 45- Bacteria surrounded by magnetic beads, adapted from [67] .....	46
Figure 46- Example of bacteria CFU counting: left, Klebsiella pneumoniae; right: Pseudomonas aeruginosa .....	51
Figure 47 - Example of bench protocol optimized: comparison between specific (positive) and aspecific (negative) antibody for Klebsiella pneumoniae capture at -1 dilution ( $10^7$ CFU/ml); NC refers to Non Countable. ....	52
Figure 48 - Graph representing mean results from bench experiments, data from Table 7 .....	55
Figure 49- Distribution of beads(red) and bacteria(green) at the outlet. (A) No obstacles (B) Alternated cylindrical pillars (C) Triangular obstacles at the channel walls (D) Rectangular obstacles at the channel walls with curved end.....	56
Figure 50- Distribution of beads(red) and bacteria(green) along channel width when close to obstacles (A) No obstacles (B) Alternated cylindrical pillars (C) Triangular obstacles at the channel walls (D) Rectangular obstacles at the channel walls with curved end.....	56
Figure 51- Distribution of beads(red) and bacteria(green) for rectangular obstacles at the channel walls with triangular end .....	57
Figure 52-CAD file of the first design of the microfluidic device produced, on the right zoom on channel and obstacles. (all measures are in $\mu\text{m}$ if not differently specified) .....	58
Figure 53- CAD file of the second design of the microfluidic device produced, on the right zoom on channel and obstacles. (all measures are in $\mu\text{m}$ if not differently specified) .....	58
Figure 54- Chambers and relative measures. Upper: first design; lower: second design.....	59
Figure 55-Microscope picture of hard mask of first design, first version .....	60
Figure 56-Picture of the hard mask of first design, first version .....	61
Figure 57- Picture of the hard mask of first design, second version .....	61
Figure 58-Microscope picture of hard mask of second design, first version .....	61
Figure 59- Picture of the hard mask of second design, first version .....	62
Figure 60-Picture of the hard mask of second design, second version.....	62
Figure 61-Graph showing relation between spin speed during coating and obtained thickness, from section 7.4, annex D.....	63
Figure 62-Experimental spin coating curve .....	64
Figure 63- A. First design SU-8 mold; B. Second design SU-8 mold .....	69
Figure 64- Microscope images of PDMS device for the first design, sectioned transversally: left, inclined at 90deg respect to line of sight; right, inclined >90deg respect to line of sight .....	69
Figure 65- Microscope images of PDMS device for the first design, sectioned transversally: upper, edge of the serpentine; lower: area of the serpentine with obstacles low definition.....	70
Figure 66- Microscope images of PDMS device for the second design, sectioned transversally: left, inclined at 90deg respect to line of sight; right, inclined >90deg respect to line of sight.....	70
Figure 67-Microscope image of PDMS device for the second design, top view .....	71
Figure 68 - Graph representing mean results for capture efficiency of K.pneumoniae solution comparing different methods, data presented in Table 16. ....	72

Figure 69- Graph on results for capture of bacteria Klebsiella pneumoniae at different dilutions; Concentration as CFU/ $\mu$ l. ....	74
Figure 70-First clinical sample plated in Lb agar media Petri dish ,see legend Figure 71 .....	76
Figure 71-Spiked clinical sample with initial sample (resuspended swab with added colony) compared with retained and non-retained collected volume.....	76
Figure 72-Result of plating sample aliquot and microfluidic non-retained outcome from three of the four clinical sample testing .....	78
Figure 73- Result of plating microfluidic retained outcome from three of the four clinical sample testing ..	78
Figure 74-Analysis of output from first sensor as correlation between peak to peak time interval and peak to peak amplitude of the bipolar signal .....	81



## List of Tables

Table 1- Parameters applied for magnetic particles fringe field and relative sensor output .....	19
Table 2-Computation of volume used to prepare second inoculum .....	23
Table 3- Factors involved in bench protocol optimization and their influence .....	31
Table 4-Parameters and results of a series of experiment on antibody immobilization and bacteria capture by bench-top assay. In red: parameters that change compared to previous experiment. Legend below .....	49
Table 5- Optimized bench parameters for bacteria capture (on samples of 100µl); o/n refers to overnight.	51
Table 6- Example of identification of outliers with quartile method: data on Wash I (WI) sample from -3 dilution Klebsiella pneumoniae specific capture.....	53
Table 7- Mean results from bench experiments, refer to appendix 7.2 for complete results.....	55
Table 8- Main parameters for simulated models.....	57
Table 9- Relation between spin speed and thickness of the polymeric substrate during spin coating, from section 7.4, annex D .....	63
Table 10-Measured values of thickness at different spin speed.....	63
Table 11-Relation between thickness and needed exposure dose, from section 7.4 , annex D.....	64
Table 12-Results on different exposition dose applied, first design .....	65
Table 13-Microscope picture of molds at different exposure dose.....	67
Table 14-Results on different exposition dose applied, second design .....	68
Table 15-Parameters of the final device .....	68
Table 16- Summarized results from comparison in capture efficiency of K.pneumoniae solution for bench and 2 microfluidic design devices, refer to appendix 7.3 for complete results. HBC is equal to $3.8 \cdot 10^{10}$ beads/ml, and LBC is equal to $1.9 \cdot 10^{10}$ beads/ml.....	71
Table 17-Results for capture of bacteria Klebsiella pneumoniae at different dilutions with specific antibody .....	73
Table 18- Results for capture of bacteria Klebsiella pneumoniae at different dilutions with non-specific antibody.....	73
Table 19-Parameters and result of spiked clinical sample capture.....	76
Table 20-Results from four clinical sample testing, as shown in Figure 72 and Figure 73.....	77

## List of Formulas

Equation 1 – Reynolds number .....	5
Equation 2 – Hydraulic diameter for a rectangular duct.....	5
Equation 3 – Diffusion time .....	5
Equation 4 – Mixing index at x distance from inlet .....	6
Equation 5 – Mixing efficiency .....	9
Equation 6 – Standard deviation of pixel intensity at distance x from inlet .....	9
Equation 7 - Magnetoresistance .....	15
Equation 8 – Sensitivity of transfer curve .....	15
Equation 9 – Stray field produced by a superparamagnetic bead when approximated to a dipole .....	17
Equation 10 – XY plane component of the stray field produced by a magnetic particle approximated to a dipole.....	17
Equation 11 – Sensor voltage output.....	18
Equation 12 – Proportion for the computation of needed volume for second inoculum preparation .....	23
Equation 13 – diffraction limit in photolithography.....	33
Equation 14 - Spherical beads distribution .....	38
Equation 15 - Spheroidal beads distribution .....	38
Equation 16 – Rod-like beads distribution, 1 <sup>st</sup> emisphere .....	39
Equation 17 – Rod-like beads distribution, cylinder.....	39
Equation 18 – Rod-like beads distribution, 2 <sup>nd</sup> cylinder.....	39
Equation 19 – Bacteria coverage.....	40
Equation 20- Mean velocity of fluid in the channel .....	40
Equation 21- Time to space relationship.....	40
Equation 22 – Antibodies to bead ratio based on geometrical parameters .....	44
Equation 23 - Antibodies to bead ratio based on number of available interaction sites.....	45
Equation 24 – Coverage.....	46
Equation 25 – Percentage of capture, first method .....	54
Equation 26 – Percentage of capture, second method.....	54
Equation 27 – Percentage of capture, third method .....	54
Equation 28 – Relation between exposition time and absorbed dose .....	65
Equation 29 – Aspect ratio of an element.....	70

## List of Acronyms

Ab- Antibody	NC-Non Countable
ADC- Analog to Digital Converter	OD600 – Optical Density at 600nm
AMR- Anisotropic MagnetoResistance	O/N - OverNight
ASSURED- Affordable, Sensitive, Specific, User-friendly, Rapid and robust, Equipment-free and Deliverable to end users	PASAR-Planar Asymmetric Split and Recombine Mixer
BSA- Bovine Serum Albumin	PB- Phosphate Buffer
CAD- Computer Aided Design	PBS-Phosphate Buffer Saline
CFD- Computational Fluid Dynamics	PBT20- Phosphate Buffer plus Tween 20
CFU- Colony Forming Unit	PCB- Printed Circuit Board
DC- Direct Current	PCR – Polymerase Chain Reaction
DI water- DeIonized water	PDE-Partial Differential Equation
DNA – DeoxyriboNucleic Acid	PDMS- Poly DiMethyl Siloxane
DWL- Direct Laser Writing	PEB – Post-Exposure Bake
EBA- Ethidium Bromide monoAzide	PGMEA- polyethylene glycol methyl ether acetate
ELISA- Enzyme-linked ImmunoSorbent Assay	PHE- Planar Hall Sensor
FC- Flow Cytometry	PMMA- Poly(Methyl MethAcrylate)
FCC- Face-Centered Cubic	PoC - Point of Care
FDTSS- Perfluorodecyltrichlorosilane	PR – PhotoResist
FRET- Fluorescence Resonance Energy Transfer	PtP- Peak to Peak
GFP- Green Florescent Protein	PW-Peak Width
GMI- Giant Magnetic Impedence	RF-RadioFrequency
GMR- Giant MagnetoResistance	RT- Room Temperature
HIV - Human Immunodeficiency Virus	SGM-Slanted Groove Micromixer
IAC- Internal Amplification Control	SHM-Staggered Herringbone Micromixer
IMS- ImmunoMagnetic Separation	SNR- Signal to Noise Ratio
IPA- Isopropyl Alcohol	SPM- SuperParaMagnetic
LAN-Locked Nucleic Acid	SV-Spin Valve
LB media- Luria Bertani media	TMR- Tunnel MagnetoResistance
LFI – Later Flow Immunoassay	ToF-(Time of Flight)
LoC - Lab on a Chip	UV-UltraViolet
LoD – Limit of Detection	WBD- Wall Binding Domain
MNP- Magnetic Nano Particles	WHO- World Health Organization
MR- MagnetoResistance	
MRB - MultiResistant Bacteria	
MRSA - Methicillin-Resistant <i>Staphylococcus aureus</i>	
MTJ-Magnetic Tunnel Junction	

# 1. Introduction

## 1.1. Aim of the project

In recent years, miniaturization and implementation of detection systems in portable device have grown, with a major impulse in chemical and biological detection [1]; innovative systems have been developed with the aim of discriminating the analyte of interest from its surroundings, with an attempt to ensure the lowest limit of detection while maintaining high accuracy and specificity. All with the aim to develop a device which guarantees what WHO (World Health Organization) defined as the goal for PoC-LoC (Point of Care - Lab on Chip) systems, namely the ASSURED criteria, or Affordable, Sensitive, Specific, User-friendly, Rapid and robust, Equipment-free and Deliverable to end users [2]. Such trend is not entirely mirrored in the area of sample pre-treatment, which contains all the sample processing required, previous to the detection, to ensure minimal interference with the latter. As a matter of fact, sample matrix, defined as all the components forming the sample except for the detection target, on numerous times may have a negative effect on the interaction between analyte and sensor, and their elimination is advised, if not essential.

One limiting factor is related to the tendency of many sample processing steps to be performed off-chip [1], thus hampering complete integration of a device, while representing a high-cost, time-consuming and equipment-dependent [2] feature. Sample pre-processing is typically represented by filtration, centrifugation, dilution, mixing, target amplification and extraction [1]; in addition, any sample treatment process must guarantee that analytes are present in a form compatible with the detection system, or alternatively, such approach limits the type of detection method that can be applied downstream. Besides, small volumes for sample and reagents, in the order of pL to  $\mu$ l are sought in most miniaturized systems [1].

In order to guarantee all the above-mentioned characteristics, microfluidic implementation represents the best approach to achieve the development of PoC-LoC device which integrates sample preparation and target detection. As a matter of fact a microfluidic system generally provides reduced sample/reagents consumption, minor cost requirements per single analysis, reduced power consumption, low contamination risk, improved sensitivity/sensibility and high reliability [3]. Fabrication of the device can be achieved with well characterized photolithographic and soft-lithographic techniques, which include the formation of a mold that can be repeatedly used; PDMS is the most chosen material for the final device given, among others, properties as flexibility, optically transparency, and biocompatibility [3].

When designing a similar complete system, sample preparation and detection inter-dependence cannot be neglected, as a result their characteristics have to be taken into consideration in a choral approach.

Specifically, INESC MN in collaboration with INESC ID [4] [5] have been studying and developing a magnetic cytometer platform oriented, among other objectives, to bacteria detection in clinical sample as part of a project for rapid hospital bacterial infection detection, named “*Bacteriófagos no Diagnóstico e Prevenção de Infecções Multiresistentes em Portugal e no Mundo (Phage4BacID)*”. Preferential targets of the project are antimicrobial resistant bacteria, specifically carbapenem resistant *Escherichia coli*, *Klebsiella pneumoniae* and *Pseudomonas aeruginosa*, as such class of antibiotics represents the last resort for treating multidrug resistant infections [6]. In particular number of cases for carbapenem resistant *K.pneumoniae* in Portugal has raised from 3.4% to almost 11% from 2015 to 2019 [7], with even higher percentages for *P.aeruginosa* and *Acinetobacter* species, generating an increased demand on efficient detection systems for patient rapid isolation. The role of this work is thus to cooperate and support the cytometric platform, designing, producing and testing a coupled microfluidic device for sample preparation, applied to bacteria solutions

(*K.pneumoniae*, *P.aeruginosa* and *E.coli*) and refined for resuspended rectal swab samples, provided by Hospital Beatriz Ângelo and tested positive for carbapenem resistant *K.pneumoniae*. This coupling defines the requirements the device must fulfil. Firstly, given the absence of natural magnetic activity of biological samples, target bacteria cells need to be labelled with magnetic particles. This effect is achieved in the device by mixing a solution of superparamagnetic particles covered with a specific recognition element, namely antibodies, with the solution containing the target, eventually represented by the resuspended swab. Secondly, the analyte requires to be separated by the complex matrix where it is contained and it also requires to be concentrated in a smaller volume. The retaining of magnetic particles, along with captured bacteria, is implemented to fulfil such demand. Given the characteristics of the phenomena involved and the elements exploited, the device represents an implementation of an immunomagnetic separation process. One convenient aspect is represented by the exploitation of the magnetic elements for the segregation, lately also required for the detection. This does not limit the use of the sample preparation device to downstream magnetic detection, as other detection methods may be implemented with minimal device adaptation. Nonetheless, the device is designed with the explained frame in mind. A deeper description of magnetic detection fundamentals is presented in section 1.2.3.

Coupling together the sample preparation method here described with the detection method developed at INESC MN can potentially provide an answer for the demand of a fast all in one device able to detect bacteria infections. Bacteria detection can be applied in many different areas, such as biohazard, microbial forensic, environmental studies, and more [8], among which clinical diagnosis. As for clinical samples, represented by blood, urine, saliva or different collected body fluids, a significant obstacle is represented by matrix complexity, whose components are able to affect the efficiency in detection or in other steps of the process. For example, contained lipids can interfere with antibody/antigen interaction. For such kind of matrix pre-treatment steps as sample collection and storage, separation, extraction and concentration are generally required [2], as proposed by the discussed system. In addition, limited time is given for the detection, in order to achieve patient rapid isolation if needed.

Targeted characteristics are thus lower than 3h processing time (to be compared to the 24 to 72h needed with classical culture-based methods already in use), all in one approach with the ability to include sample pre-processing, Point of Care (PoC) solution integrating all the step in a single Lab on a Chip (LoC) device, ability to deal with complex biological samples, high sensitivity (very low number of false negative) and specificity (reduced false positives, even if less relevant for the possibility of further, longer, detection method) and able to process sample volumes in the order of 500µl.

The necessity of such device arises from the novel menace health care systems worldwide are facing in the new century, represented by highly diffused hospital infections. Such infections cause patients mortality and morbidity, in a considerable number; for example, in 2005 approximately 19.000 patients in USA lost their life due to a MRB (MultiResistant Bacteria) infection caused by methicillin-resistant *Staphylococcus aureus* (MRSA), more than the sum of deaths due to HIV, cancer and homicide [9]. Situation in Europe is similar, where European Centre for Disease prevention and Control (ECDC) estimated that 33.000 died for infections occurring due to resistant bacteria, a number comparable to the sum of deaths caused by influenza, tuberculosis and HIV/AIDS combined, based on a study of 2015 [10]. Such organisms, as the name suggests, are bacterial cells which are immune to the more than one antibiotic, or, at least, at human body accepted doses, where such resistance is confirmed *in vitro*. This condition also puts additional limitations and risks in many fields of medicine, as organs implantation, premature infant care, chemotherapy, surgery and all areas where infections are expected and already critical. In addition, very few amounts of new antibiotics

are being developed recently, both due to the already highly explored field and to the lowest income respect to chronic diseases treatment. Two are the core aspects of hospital infections, respectively limiting infection diffusion and extreme fast recognition. In order to achieve patient isolation though, it is requested to discriminate between different bacterial strains in a straightforward manner and limited time. This is hardly achieved with current methods for bacteria detection applied in an hospital setting, representing by plating, selective cultivation and CFUs count (Figure 2). A discussion on different bacteria detection method is presented in section 1.2.2.

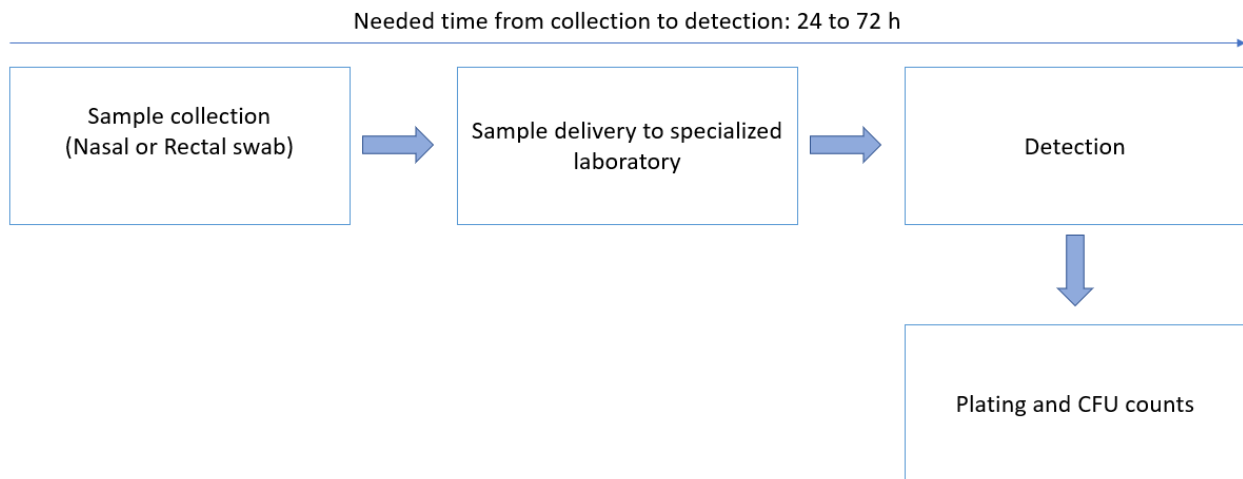


Figure 1- General flow for standard approach

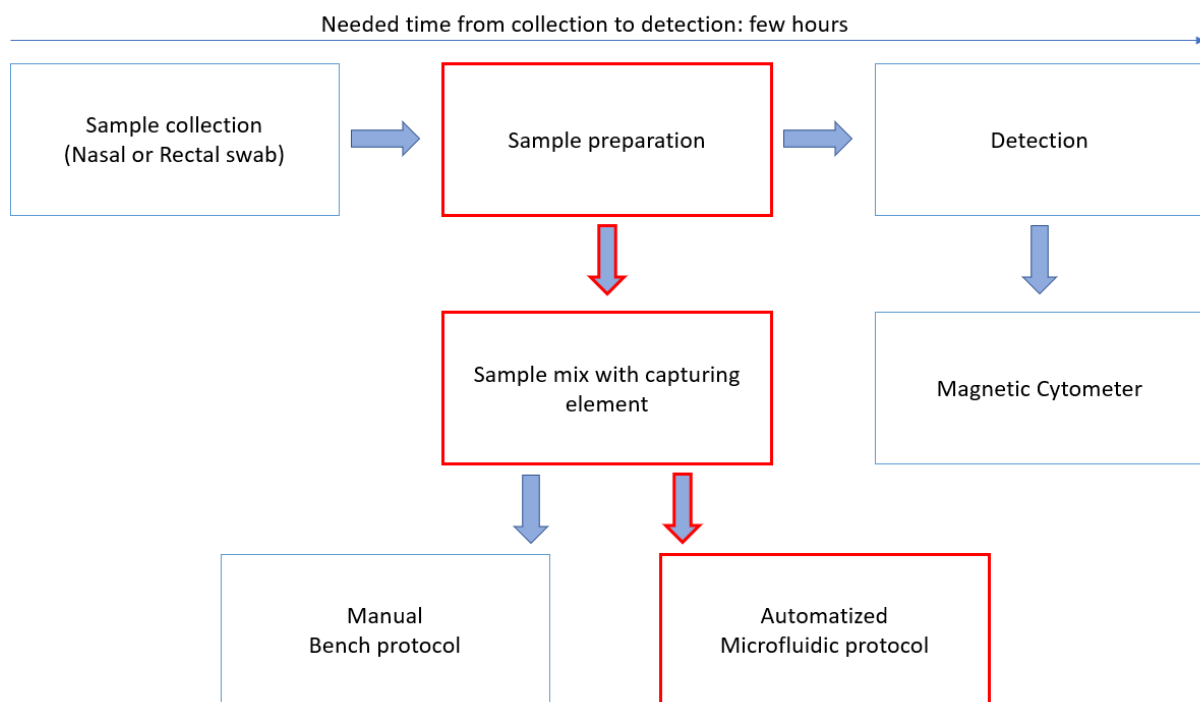


Figure 2- General flow for proposed approach: in red, area of competence of presented work

In Figure 1 and Figure 2 general schematics of the standard used approach and proposed new approach are represented. As also reinforced in section 1.2.2 plating method represent the current

golden standard for bacteria detection and it is the main tool exploited for clinical sample analysis nowadays. Competing with such cheap and effective tool, given the low limit of detection, involves the proposal of a system that ensures extremely better timing requirement, true big limitation of such method, while competing on the other aspects. Cytometric approaches can represent the researched tool, among which magnetic cytometry rises in importance for its portability, relative reduced costs, absence of background noise in biological sample, ease of sample pre-processing and good microfluidic integration. Nevertheless, while the sample needs negligible preparation in the case of plating method, if magnetic cytometry is exploited as a mean of detection, sample pre-processing represents a core aspect, as involves the actual process by which magnetic properties of a specific target among the sample are tuned to the wanted level, or in other words, the target is made magnetically “visible” to the sensor.

Within the frame presented above, such step must be integrated in the final device (ie. the aimed LoC), and that is the major focus of this work, providing a device able to accomplish such preparatory step with characteristics displayed in Figure 3.

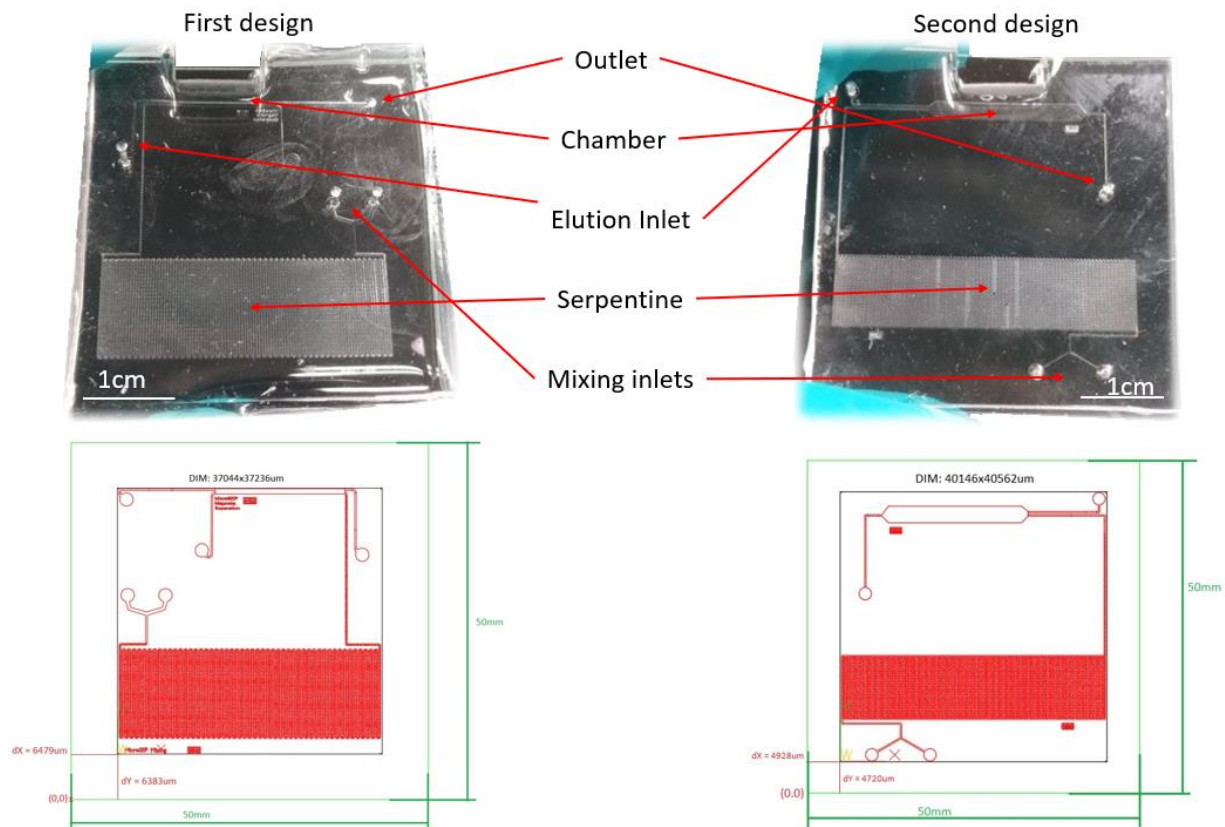


Figure 3- Above: produced devices with outlined features; Below: CAD files reporting relative measures

## 1.2. State of the art

### 1.2.1. State of the art of sample pre-treatment: passive mixing and microfluidics

As anticipated in section 1.1 sample pre-treatment represents the core topic of the work.

Steps that are usually included in sample preparation are mixing, separation, concentration, purification, labelling and cell lysis [11].

Relatively to the device here developed and discussed, mixing and concentration are sought.

As for the first, a solution with recognition elements immobilized on magnetic particles and a solution containing target bacteria are involved; as for the second, particles that interacted with bacteria are the target.

Mixing in microfluidic has a long story of different approaches, that can be summarised in two macro-classes: active and passive mixing. Where in the former an external source of energy is needed in order to achieve mixing through injection of energy in form of sound waves, kinetic energy, thermal energy and electromagnetic energy through different phenomena [12], in the latter mixing is obtained by exploiting some fluid dynamic effect.

If mixing is not specifically addressed, it generally occurs, in a microfluidic device where two or more streams are in contact, at low rates, since it solely relies on diffusion to allow species from one flow to migrate to a second flow; this is because for the common range of speed of the fluid and adopted cross-section of channels, given a fluid with similar characteristics to water as concerning density and viscosity, flow is characterized by a low Reynolds number (Equation 1), generally lower than one [13] [14], which implies the establishing of a laminar flow, characterized by ordered fluid streams with no transversal advection, or no bulk mass motion in the direction perpendicular to the flow.

$$Re = \frac{\rho * V_{mean} * D_h}{\mu}; \quad (1)$$

*Equation 1 – Reynolds number*

where  $\rho$  is the fluid density,  $V_{mean}$  is the mean velocity of the flow in the channel,  $\mu$  is the dynamic viscosity of the fluid and  $D_h$  represents the hydraulic diameter, equal to  $\frac{4 * Area}{Perimeter}$ , or for a rectangular cross-section.

$$D_h = \frac{2 * width * height}{width + height}; \quad (2)$$

*Equation 2 – Hydraulic diameter for a rectangular duct*

To verify that such considerations applies also for the device presented in this work, Reynolds number can be computed, considering a target flow rate  $Q=10\mu\text{l}/\text{min}$ , channel width  $W=200\mu\text{m}$ , channel height  $H=100\mu\text{m}$ , water based fluid with viscosity  $\mu=0.001 \text{ Ns}/\text{m}^2$  and density  $\rho=1\text{g}/\text{cm}^3$ , which implies a cross section  $A=W*H=2*10^4\mu\text{m}^2$ , a mean velocity  $V_{mean}=Q/A=8.3*10^{-3}\text{m}/\text{s}$  and a hydraulic diameter according to Equation 2  $D_h=133.33 \mu\text{m}$ , leading to a value of Reynolds number  $Re = 1.11$ ; this value agrees with the range of laminar flows and justifies the requirements of specialized mixing structure to overcome mixing limitations when based on diffusion only.

In fact, in such case, the diffusion time is proportional to the square of diffusion distance with a proportionality constant represented by the diffusivity of the fluid, as reported in Equation 3

$$t_D = \frac{\delta_D^2}{D}; \quad (3)$$

*Equation 3 – Diffusion time*

where  $t_D$  is the diffusion time,  $\delta_D$  is the diffusion length here equal to half of the channel width and  $D$  is the diffusion coefficient. Since in the case of biological samples of dimensions between  $0.1\mu\text{m}$  and  $1\mu\text{m}$  such coefficient can vary in the order of  $10^{-12}$  to  $10^{-13} \text{ m}^2/\text{s}$  [15], diffusion time for the given dimensions would span values between  $10^4\text{s}$  to  $10^5$ , more than 2h in the case of smaller samples. At the given flow rate of  $10 \mu\text{l}/\text{min}$ , this would require a channel longer than 80m to reach complete mixing. Such times and lengths are not compatible with LOC devices, that are meant, at least in the



frame of this work, to be fabricated in a surface that should be limited to 100cm<sup>2</sup>, thus marking again the need of exploiting different phenomena rather than diffusion to accomplish mixing.

While generally more performant, active mixing involves a series of limitation as complex fabrication, poor integration with other LOCs components, high power consumption and increased heat generation, of particular interest when biological samples are considered [15], characteristic that made passive mixing to be preferred if fabrication simplicity is a requirement.

Passive mixing is divided in two major categories, namely lamination-based and chaotic advection based [14] [13]. The former is characterized by flow segmentation and formation of multiple streams, with the aim to reduce the diffusion path and increase contact area between the two fluids to be mixed. The latter is based on flow rotation and formation of transversal mass motion.

Exploring scientific literature many examples of both approaches can be found, and here few are reported with the goal of evidencing some properties and define and support the approach chosen in this work.

As for lamination based mixers, Tofterberg et al. [16] realized a device based on a 90° rotation of the flow, obtained through grooves implementation, with consequential flow splitting; after a further 90° flow rotation, split streams are recombined thus doubling the contact area and reducing diffusion length, as represented in Figure 4. This configuration was tested with a solution of a florescent compound in water and proved to reach a mixing efficiency of 0.9, defined as the normalized difference between florescence deviation at device inlet and florescence deviation at structure outlet, after 4 repeated structures. Differently, Roudgard et al. [17] analysed the possibility of exploiting a well-characterizing T-mixer, while introducing split streams at its inlets, in a vertical or horizontal configuration (refer to Figure 5). Simulations obtained a mixing performance, computed as integration along the width of the channel of the difference between concentration at a certain distance from the inlet and concentration of completed mixed solutions normalized to the integration along the width of the channel of the difference between fully unmixed and fully mixed solution (Equation 4), equal to 0.6 at a distance of 500um.

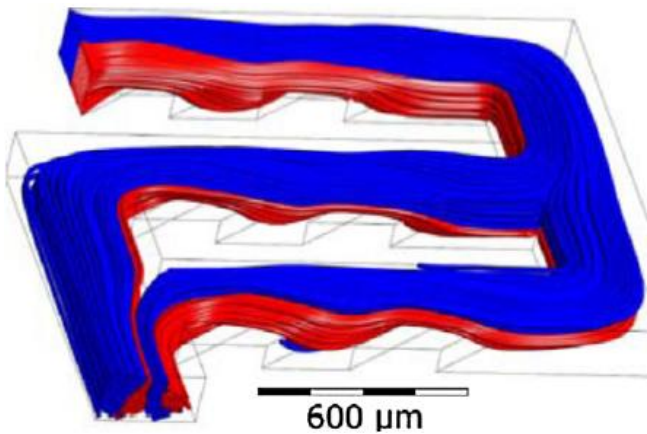


Figure 4-Split and recombine mixer [16]

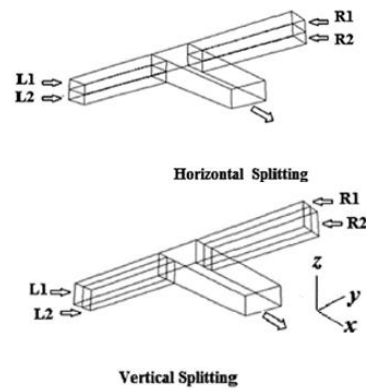


Figure 5-Split T-mixer design [17]

$$\text{mixing index} = \sigma(x) = 1 - \frac{\int_0^W |C(x) - C_\infty| dy}{\int_0^W |C_0 - C_\infty| dy}; \quad (4)$$

Equation 4 – Mixing index at x distance from inlet

where C(x) is concentration at a certain distance from inlet, C<sub>∞</sub> is concentration at complete mixing, C<sub>0</sub> is concentration at inlet or unmixed and W is channel width. Such formulation of mixing index is shared among the followed presented papers.

These and other lamination based mixers all share one major limitation in their need of a more complex fabrication, as organized on multiple level and thus requiring alignment procedures; even though such characteristic does not prevent their realization, it is in the intention of this work to realize a device based on very simple fabrication procedures, able to be easily replicated with consistent properties and reduced costs.

Relatively to the second category, which is chaotic advection-based mixers, various approaches have been attempted.

Li et al. [18] studied efficiency of a Planar Asymmetric Split-and-Recombine mixer, based on vortexes generation at sub-channel reconnection and as a result of unbalanced collision between the two different streams, as displayed in Figure 6. Mixing efficiency up to 86% have been reached.

Xia et al. [19] exploited both stream split as seen in lamination based mixing, with advection mixing through vertical re-injection of one fluid into the other in a so called expansion chamber that triggers viscosity instabilities; higher mixing performances are in fact obtained when difference in viscosity of the two mixed fluids are present, even if also in the case of equal viscosity, complete mixing is achieved after seven units. In Figure 7 it is shown how initially laminar, the flow converts to a more turbulent state at the third unit C3, increasing mixing, and is restored to a laminar state seventh unit C7.

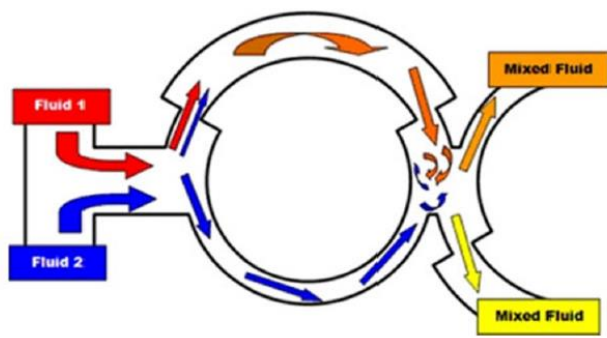


Figure 6- Planar Asymmetric Split-And-Recombine PASAR mixer [18]

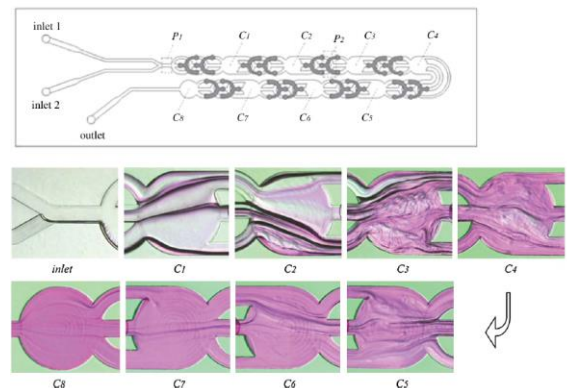


Figure 7- Planar view of the mixer with example of water-glycerol mixing at different stages [19]

Both designs are efficient in mixing fluids, but their effect on particles solution may be detrimental as effect of collisions induced on biological sample is not known; in addition, as already commented for lamination based devices, these approaches brings similar complexity at production level.

Another approach involves the use of grooves on the floor of the channel in order to induce vortexes formation; Cortes-Quiroz et al. [20] realized and tested a staggered herringbone structure and verify the dependence of mixing efficiency on parameters like the aspect ratio of the mixing channel ( $w/h$ ), the ratio of the groove depth to the channel height ( $d_g/h$ ), the ratio of the groove width to the groove pitch ( $w_g/k$ ), the asymmetry factor of the groove ( $b$ ), the angle of the groove ( $h$ ), and the numbers of grooves per half channel ( $N_g$ ), reached for the best configuration a mixing index equal to 0.83 (Equation 4)

Du et al [21] instead performed a numerical simulation comparing performances on two different configurations of grooves, namely slanted groove micromixer (SGM), as shown in Figure 8, and a staggered herringbone micromixer (SHM), verifying that for the SHM, due to the alternance of the structure as shown in Figure 8, two transvers vortices are formed, compared with a single helical

stream present in the slanted version SGM, thus resulting in continue alternating mix between the two solutions. Such configuration allowed mixing index up to 0.95(Equation 4)

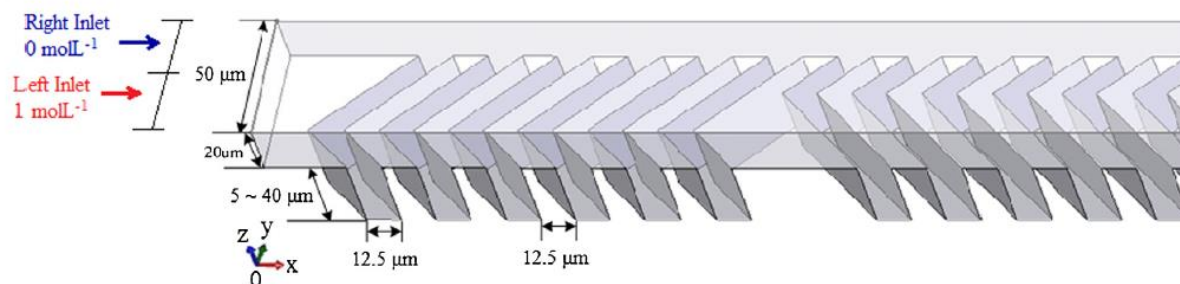


Figure 8- SHM configuration of the mixer [21]

In addition to already discussed limitation relative to fabrication process complexity given the multilayer character of such devices, the use of similar structures may cause a important particle loss; both bacteria( $\rho \sim 1.1\text{g/cm}^3$  [22]) and nanoparticles( $\rho \sim 2\text{g/cm}^3$ , see 7.1, Appendix A) have higher density than water or used buffers (which have very close properties to water,  $\rho \sim 1\text{g/cm}^3$ ), which causes their sedimentation and accumulation at the bottom of the tube in which the solution is contained. If the bottom of the channel in which they are loaded is interrupted by grooves, they can form a space were particles accumulated and are subtracted from the stream, thus reducing the number of available recognition elements, in the case of the sole magnetic particles, or the loss of part of the target bacteria, which may produce false negatives if its concentration, as expected, is low. This effect will be dependent on applied flow rate, but it must be considered that, in order to maximize magnetic retention, flow rate will be chosen in the order of  $10\mu\text{l/min}$ .

Finally, some approaches based on obstacles insertion in the fluidic channel are discussed; Wong et al. [23] compared mixing performance of a three inlet mixer with and without the presence of two static mixing elements(SME); their role demonstrated to provoke a stretching of the contact area between the two solutions, in an asymmetric scheme, thus creating some transversal mass transport (refer to Figure 9). Mixing index of 0.9 is obtained at the outlet (according to Equation 4).

Fang et al. [24] applied single periodically alternated geometric structures, as displayed in Figure 10, to a T shaped linear mixer and compared mixing performance in their absence; simulations and experimental data agreed that a mixing index of 0.79(Equation 4)could be obtained with a repetition of 28 units, hence in total 56 obstacles inserted.

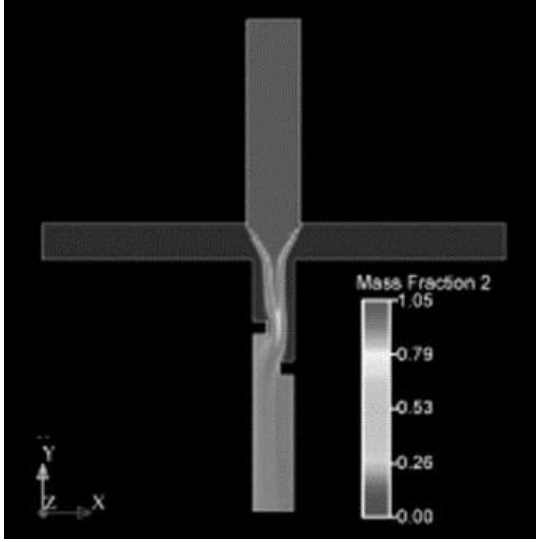


Figure 9- SME mixer, top view [23]

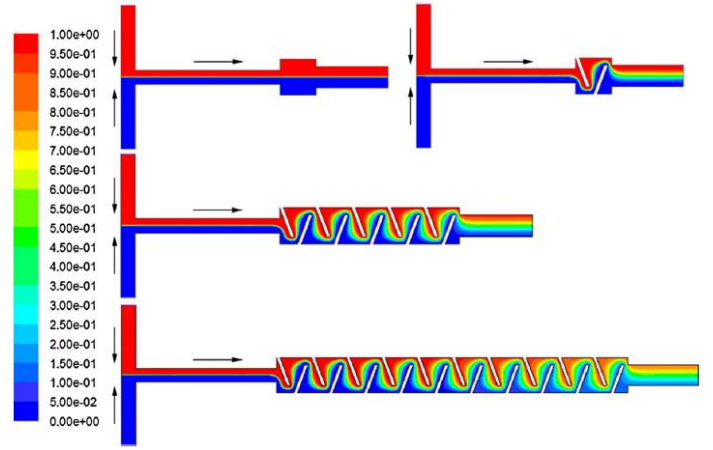


Figure 10-Comparison in efficiency of a T-shape mixer with different number of obstacles [24]. Color code refers to specie A concentration, during specie A and specie B mixing

Bhagat et al. [15] exploited similarly the presence of obstacles in the flow to trigger transversal mass transport and enhance fluids distribution along channel width, but positioned them at the center of the channel, instead of at its walls, as displayed in Figure 11. The angle at which obstacles are positioned, namely  $45^\circ$  respect to flow direction, as well as the choice of splitting the obstacles in two part at  $1/3$  of their length creating a space between them, have been evaluated as a compromise between the pressure drop induced by the mixer and the mixing efficiency. Once again, obstacles cover the role of introducing a component in the velocity of the fluid or particles in the transversal direction, thus forcing a mass flow between the two fluids that are wanted to be mixed. Most interesting aspect of this study lies in the comparison effectuated between displayed configuration in Figure 11 and a mixer structure called Tesla mixer, also based on chaotic advection mixing, known in the micromixer field for its high efficiency at the cost of a high complexity. What was demonstrated in the study is that, for the novel design based on obstacles, performance where higher compared with Tesla mixer in both cases of fluids or particles mixing; 90% mixing efficiency is reached in a 5 mm long channel ( 7 mm for Tesla mixer) for fluid mixing while 90% particle dispersion (60% for Tesla mixer) is reached in a 3mm long channel (refer to Equation 5 and Equation 6 ). Mixing efficiency are computed by simulating mixing between water and water/fluorescent particles solution.

$$\text{mixing efficiency}(x) = \left(1 - \frac{\sigma_x}{\sigma_{\text{unmixed}}}\right) * 100 ; \quad (5)$$

Equation 5 – Mixing efficiency

where  $\sigma_x$  (Equation 6) represents the standard deviation of the pixel intensity at a given cross-section at an  $x$  distance from inlet and  $\sigma_{\text{unmixed}}=0.5$  represent the standard deviation that corresponds to a complete unmixed solution.

$$\sigma_x = \sqrt{\frac{\sum_1^{N_{\text{pixel}}} (I - \bar{I})^2}{N_{\text{pixel}}}} ; \quad (6)$$

Equation 6 – Standard deviation of pixel intensity at distance  $x$  from inlet

where  $I$  represents pixel intensity in grayscale value from 0 (no fluorescence) to 1 (maximum fluorescence) and  $\bar{I}$  represents average pixel intensity in the image, relative to a cross section of the channel at a distance  $x$  from inlet;  $N_{\text{pixel}}$  instead represents total number of pixel composing the image.

This difference is explained by the authors on the bases of the fact that the introduction of a transversal component of fluid velocity it is not sufficient to form a consistent flow of particles in the same direction, and that the presence of obstacles that interrupt particles flow and force them to move on the other half of the channel is essential for high particle dispersion in the channel.

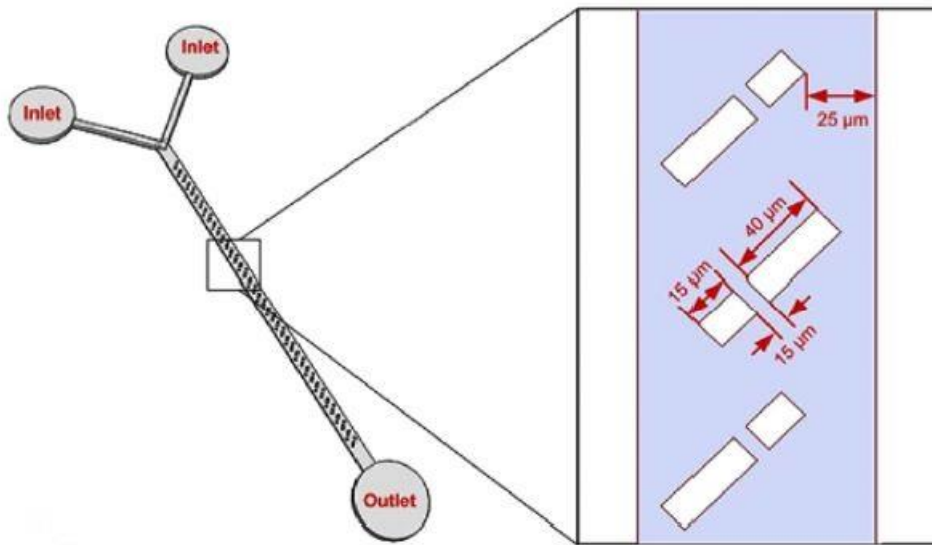


Figure 11-Top view and obstacles details of the mixer [15]

Microfluidic again is also an important component for the cytometric platform itself, constituting the channels below which sensors are positioned and where processed sample flows. For this purpose its design is generally simpler, but fabrication methods involved are equivalent to the ones required for sample preparation device fabrication.

Undoubtedly, the most chosen material to produce microfluidic components at a laboratory scale is PDMS, due to its easy moldability, low cost, transparency to visible frequencies, low autofluorescence, high biocompatibility, gas permeability (oxygen and  $\text{CO}_2$  exchange) and simplicity in sealing, as well as its compatibility with soft lithography fabrication methods. Briefly, fabrication steps are reported for relevant studies in the same frame as this work is inserted, while a more complete presentation of the method is reported in section 3.2.

Fernandes et al. [25] realized their microfluidic system in PDMS (Polydimethylsiloxane) through cast-molding with three main steps.

First, a hard mask of  $\text{Al}_{98.5}\text{Si}_{1.0}\text{Cu}_{0.5}$  (wt%) deposited on glass was produced by Physical Vapour Deposition on glass in Nordiko 7000 and subsequent Direct Laser Writing patterning and chemical etching in solution of acetic acid (3.3%), nitric acid (3.1%) and phosphoric acid (3.0%). Second, a negative photoresist SU-8 mold is produced by contact microlithography, with UV exposure of SU-8 spun silicon substrate, visualized in Figure 12. Finally, mix of DMS and silicon elastomer (10:1 w/w) is conserved in vacuum to remove any possible air bubble and after poured on the SU-8 mold and kept at  $70^\circ\text{C}$  to favour polymerization. After, the microfluidic is peeled out from the mold.

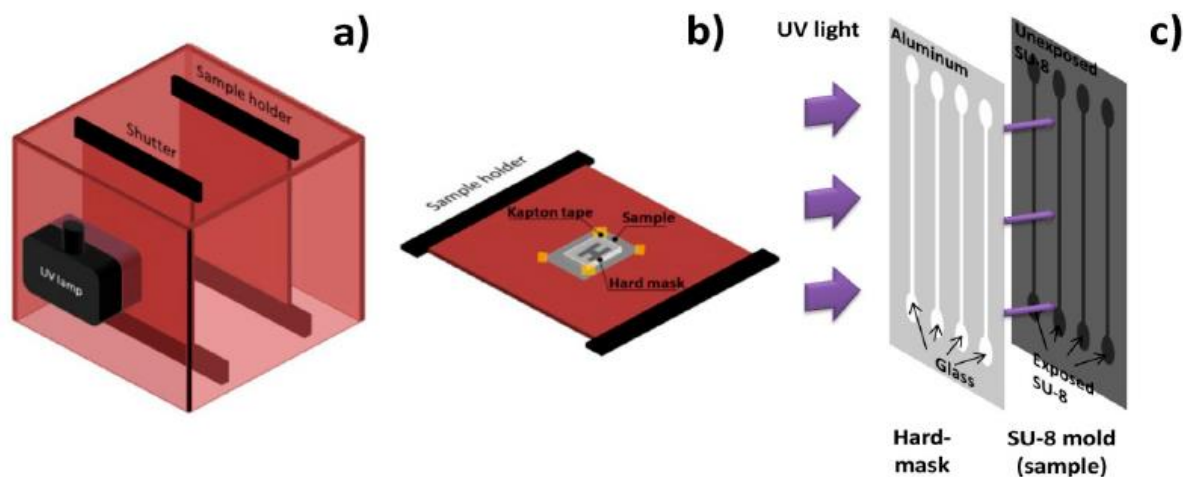


Figure 12-Representation of photoresist mold fabrication: hard mask is taped on the holder, put in contact with photoresist on silicon substrate and exposed by UV light [25]

At this point, the produced PDMS structure must be joint to the microfabricated sensor substrate, achieved by  $\text{Si}_3\text{N}_4$  and PDMS irreversible bonding by ultraviolet/ozone. Alignment is a critical step of the procedure, and it is manually performed exploiting alignment marks and delay the bond formation with ethanol. PDSM-Silicon substrate bonding is completed at  $70^\circ\text{C}$  and in conclusion the system can be glued to a PCB board and contacts can be wired to connection pads to allow access to the metal lines.

Loureiro et al [26] and Duarte et al [27] produced the microfluidic system similarly.

Same polymer is chosen as the material for the structure, realized with a micro molding technique.

Hard mask is microfabricated and photoresist (AZ4562 MicroChemicals GmbH) is shaped as wanted mold by contact lithography with UV exposure. A PMMA (Poly(methyl methacrylate)) master is micromachined to guide the PDMS casting, with metal pins to define inlets and outlets. PDMS is prepared by mixing monomeric base and curing agent (10:1 w/w) and degassed in void. After casting, the polymeric structure is cured at  $60^\circ$  and then peeled off from mold. Finally, PDMS-silicon bond is obtained by surface activation through oxygen plasma and surfaces contact at room temperature, with manual alignment under microscope.

M.Reisbeck et al. [28], D.Issadore et al. [29] and W.Shen et al. [30] [31] once again, exploited PDMS as a material for the microfluidic structure, produced through mold-casting with a contact lithography produced SU-8 mold through microfabricated glass-aluminium hard-mask. PDMS-substrate bonding with deposited  $\text{SiO}_2$  is achieved by  $\text{O}_2$  plasma surface treatment and contact under positive pressure.

### 1.2.2. State of the art of bacteria detection

Final application sought with the fabricated device coupled with the magnetic cytometric platform is the detection of infection in clinical samples; the method applied thus requires to be competitive with current methods and overcome some of their limitations. Here, an insight of the present detection approaches is reported.

Bacteria detection methods through history can be separated into different macro-classes: culture based and non-culture based methods. The second one has been developed with the idea of decrease detection time and sample volume, up to extreme cases such as the design of biosensors, promising tools for cheap, Point of Care, fast, automatic, sample reduced, portable and expertise-free detection. In additions, methods can be distinguished regarding the need of sample pre-treatment or pre-enrichment, or the absence of pre-processing steps [32].

Culture based methods are considered a “gold standard” since they allow the detection up to a single pathogenic cell for a large variety of samples type and quantity, from micrograms to different grams. Its major advantages are the cost effectiveness, sensitivity, cell viability confirmation and the methods are already widely standardized. The drawback is the almost complete lack of quantitative evaluation and the high amount of time needed for the detection, on average 16h to 72h. Culture based techniques are characterized by a pre-treatment step, aiming to amplify and differentiate the sample, selection and differential plating and strain typing. In order, first step is realized by feeding the sample to allow pathogens amplification (enrichment) followed by a selective media able to let only desired bacteria to grow or suppress concurring strains; amplification at this point can reach million-fold. After differential agents are supplied, able to discriminate the researched pathogens and allowing isolation. Finally, in the absence of colonies, the analysis is considered negative, while in their presence, identification of the recovered bacteria is needed as confirmation.

First Generation rapid detection methods tries to overcome time limitations given by culture based approaches, thus maintaining its sensitivity, or the ability to discriminate true positives and so detect the pathogens in any compromised sample, and specificity, as relative to true negatives avoiding detection in clean samples, both high for culture based techniques. In addition, detection at single cell level is also requested. Emerged approaches in this direction are Lateral Flow Immunoassay, ELISA (Enzyme-linked Immunosorbent Assay), PCR (Polymerase Chain Reaction) and DNA hybridization.

In order, LFI is a cheap and quick (5 to 10 minutes) method for bacterial detection, but it lacks specificity (many false positives respect to ELISA approach). It consists of the use of antibodies blocked on a membrane at a defined distance from sample inlet. Antibodies of two types are used, detection antibodies are present at the inlet, they are labelled with a reporter in order to be visually recognised (eg. Gold nanoparticles) and can bind the target and flow with it according to capillary forces imposed by the substrate; capture antibodies are fixed at a certain position in the substrate and they can recognise target as well; more far, a second line of fixed antibodies can recognise detection antibodies. So, depending on the presence or absence of the target in the sample, the fluid will be captured at both lines (double line, positive test) or only at the second line (one line, negative test). Many assays of this kind are commercially available and studied [33], but usually concentrated samples are needed in the order of  $10^7$ - $10^9$  CFU, making the pre-enrichment a vital step.

ELISA exploits the specificity of antibodies to antigens expressed at the bacterial surface level; many different configurations are available (competitive or non-competitive detection, as example) but in general, the device surface is functionalised with primary immunoglobulin, with the aim of recognising the target pathogen once the sample is poured, and a second antibody covalently bonded to an enzyme is subsequently added after a washing step. The enzyme has the role of catalyse a reaction with a specific substrate, forming as a result, a coloured compound. Being an antibody-based method, it shares limitations with other immunoassays, represented by cross-reactivity and interferences from matrix components. Moreover, ELISA method is time-limited as the enzymatic reaction must be identified and quantified in a specific time frame

PCR is based on nucleic acid amplification by DNA polymerase reaction, and it can be widened to a quantitative method if real-time PCR (qPCR) is implemented. In such approach, a fluorophore is used to quantify the de novo synthesized DNA and with a calibration, detecting the increase in fluorescence in time, it is possible to compute the initial concentration of the pathogen in addition to its detection, which is confirmed in case of amplification since the primers are designed to be unique for the target pathogen. Different fluorescent molecules are used, briefly SYBR green intercalates in double stranded DNA unspecifically, producing false positives in the case of unspecific amplification. Detections up to 1 CFU/10g are reported [34] if enrichment step is present. Taqman™ probes relies on FRET (Förster Resonance Energy Transfer), hybridizing with single stranded DNA and containing

a fluorophore and a quencher (reduces emission); when Polymerase performs its exonuclease activity, the probe is broken and quencher and fluorophores are released, causing increasing in fluorescence. Detection of 10 CFU/ml have been confirmed [35].

Molecular beacon also relies on FRET, but with a different architecture. When connected to the single stranded DNA they form a harpin like structure putting quencher and fluorophore in close contact; when exonuclease activity is performed, the beacon is released and an open configuration is obtained, causing the quencher to be positioned far from the fluorophore and so increase emission. Such technique has been successfully applied for clinical samples detection [36]. With the last two techniques, multiplexity can be achieved, using different probes and emission wavelengths. Major limitations of polymerase based techniques are the low specificity due to unspecific amplification and the lack of an intrinsic control to verify correct proceeding of the polymerization, which is fixed by the introduction of Internal Amplification Controls (IAC), basically a second amplification of a known sequence to verify that the lack of amplified DNA is due to the absence of the target and not of different problems in the procedures, and the inability to distinguish between living or dead cells, also overcome by the use of binding dyes like Ethidium Bromide Monoazide (EBA) that penetrates dead cells only, cross-linking DNA and avoiding polymerase replication.

Another largely used method for bacterial identification in a culture free manner are DNA microarrays. They consist of glass or silicon substrate on which numerous copies of target-specific nucleotide sequences are spotted. Sample containing DNA fragments is poured on the device and if target sequences are present, they hybridize with the probes and are detected.

DNA based technique shares the major limitation in requiring sample pre-processing for extraction of the nucleic acid content, and probably enrichment in the case of microarrays since detection limit is proved up to  $10^4$  copies.

Even though rapidity of detection has been undoubtedly increased by such methods, some limitations still needs to be overcome. Some elements of the complex matrix of the sample such as fats, background microflora, big particulates and other bioactive molecules can be incompatible with analytical methods, and having in mind the aim of processing clinical samples such restrictions became critical; as example, fats can interfere with antibodies binding and carbohydrates with nucleic acid amplification. Also, many of these methods can only accommodate small sample volumes which in some situation can be counterproductive. In addition, sublethal injured cells may be not detected and, on the other hand, presence of antigens and nucleic acid do not always equal presence of viable pathogens, that may be wrongly detected. Finally, single cell in sample is rarely detected with such methods.

In such optic, pre-treatment steps can be applied to a wide range of applications of such methodologies; the development and inclusion of pre-processing device becomes of central importance and directly affects the downstream detection. For this reason, even if tuned and finely adapted to the detection method chosen, sample pre-treatment devices can be applied to different context, and their development be independent.

The aim of the upstream sample processing is relative to obtain mainly intact and viable cells with isolation and concentration of the target, reduced matrix complexity and reduced sample volume. Both nonspecific and specific methods can be implemented. Between the former category are widely used centrifugation, which differentiate bacteria based on diameter, volume, density of fluid and cell and speed centrifugation; such method is widened through differential centrifugation or density gradient centrifugation, allowing finer separation of cells and matrix. Filtering is easily implemented, as well as dielectrophoresis, relying on bacterial negative charged attracted to the positive polarity if a non-uniform electric field is applied. Such technique has been successfully implemented on a microfluidic device for upstreaming separation of bacteria from human blood cell [37]. Similarly, ion exchange resins are based on charged resins able to retrieve negatively charged bacteria while metal



oxide particles are based on the natural affinity of superficial bacterial amino acids with exposed hydroxyl groups, giving a large surface for clustering.

Instead, as specific separation method, Antibodies (concerning as example ImmunoMagnetic Separation-IMS and Flow Cytometry-FC), Bacteriophage, Nucleic Acid Aptamers and Lectins are worth mentioning; to be noticed that many of the intermediate species used for recognition of the target can be adapted as a mean to conjugated magnetic labels and target in a magnetic cytometric device.

In order, IMS is based on paramagnetic particles coupled with immunoglobulins to conjugate with the target. The recovery of the method depends on bacterial antigenic expression and antibody affinity, as well as on matrix elements that can disturb the interaction. If monoclonal antibodies are used, the selectivity is higher, but their design and manufacture is more expensive, compared to polyclonal antibodies, who are not epitope specific, leading to more false positives. When coupled with PCR it showed detection limits up to 1.1 CFU/g [38]. If coupled with fluorescence, particularly with quantum beads, the limit can be used for quantitative detection [39].

FC is another widely applied technique; it is based on fluorescent detection of single cells by conjugation with a fluorophore, usually driven by antibody specificity. It can be used to identify and to sort particles in liquid samples and it has been successfully exploited bacterial (*S. Typhimurium*) detection at 1 CFU/ml [40], and also introduced in a microfluidic device with only 30 minutes processing [41]. Limitations of such technique are complex alignment process, high cost equipment, need of well-trained operators, background autofluorescence of samples and partial loss of cell viability in sorting.

Bacteriophages have been reported in methodologies used for selective separation and concentration of bacterial cells. Their advantages are represented by the simplicity in production (phage are self-reproductive), the high affinity and the relative low influence of environment on bacteria recognition. Different approaches have been developed to exploit such organisms; capture systems are designed, where the identification of the target is delegated to other methods. Virus can be also used as a vehicle for reported genes, such as GFP (Green Fluorescent Protein) [42], LacZ (promoter for an enzyme called  $\beta$ -galactosidase) and Lux+ (gene for luciferase, linked to bioluminescence), be fluorescently stained, or being exploited in its natural lytic amplifying cycle, where new phage are used as an indirect signal for target detection, as in the detection of *P.aeruginosa* with limit of detection of 10 CFU/ml with live/ dead exogenous fluorochromic cell staining in 4h with no need of enrichment [43] or also coupled with cELISA (competitive ELISA) for detection of multi-antibiotic resistant *S. enterica* [44] .

Another possibility is to use phage fragments, instead of the whole virus, as an affinity ligand; endolysins are phage Wall Binding Domains (WBD) with affinity with bacterial peptidoglycans and can thus only be exploited against gram positive bacteria. Major problems are identification of necessary phage, understanding of the correct orientation for effective recognition and minimization of cell damage due to phage interaction.

Aptamers are universally recognised as possible substitutes of antibodies. Where the latter are aminoacid polymers, the former are nucleic acid polymers, and in a similar way presents a three-dimensional structure. By in vitro random libraries aptamer with a 3D structure specific for wanted epitope are isolated and can be used in the role of antibodies. The advantages of such species are the smaller size, ease of synthesis, smaller cost yet maintaining high specificity. It has been proved their efficiency in detecting *S.enterica* when used to functionalize magnetic beads with detection limit of 1CFU/10ml [45]. A drawback is represented by its nuclease sensitivity that can limit their used, even if stabilization methods can be applied like the insertion of LAN (Locked Nucleic Acid) in the structure.

Lectins proteins with high specificity for carbohydrates that can be used to target bacteria external, like the N-acetyl glucosamine residue of the peptidoglycan. Major limitations are shared with antibodies and aptamers, regarding the sensitivity to environment conditions which may influence target recognition, and in addition, the necessity to isolate them from biological sources, which makes them expensive.

### 1.2.3. State of the art of magnetic cytometry

In this section some properties of magnetic cytometry are presented as such detection system is recognised as optimal to be coupled with the sample pre-treatment device developed in this work and in the frame of the project for bacterial hospital infection detection.

Even if optical flow cytometry is considered a golden standard in single cell identification, the need of multiplexity, high sensitivity and microfluidic integration leads to the need of a different type of cytometry, among which magnetic cytometry appeared to be one of the most promising, due to the relatively inexpensive materials involved, reduced sizes of the detection system, limited sample preparation (reduced to the magnetic labelling), higher possibility of automation due to integration, almost complete absence of magnetic background in biological samples and possibility of multichannel design [46].

The general working principle of such technique is the detection of magnetic species, which can be represented by naturally magnetic materials or, more often and almost exclusively as concerns biological materials, by magnetically labelled entities; both labels and sensors can be of many kinds, the former as ferromagnetic but more usually showing superparamagnetic behaviour, especially to avoid aggregation, but with possibility of tuneable characteristics important for multiplexity [47], while the latter exploiting different phenomena as GMR(Giant Magnetic Resistance), TMR (Tunnel Magnetic Resistance), Hall effect and GMI(Giant Magnetic Impedance). Depending on the array architecture, more than simple detection can be achieved, and further information like velocity, size, labelling density and rotational movements could be inferred.

All the sensors used in the context of microfluidic magnetic flow cytometry are magnetic field to voltage transducers in a direct or indirect way, with a linear proportion between the two quantities. Among them, Magnetoresistive sensors are a well-known class, referring to sensors which are based on AMR (Anisotropic Magnetic Resistance), TMR and GMR; all present a variation in their resistance to an electric current due to the application of a magnetic field. This characteristic is called Magnetoresistance (Equation 7)

$$MR = \frac{R_{max} - R_{min}}{R_{min}}; \quad (7)$$

*Equation 7 - Magnetoresistance*

and the sensitivity (Equation 8) of the transfer curve of such sensors, representing the slope of the linear range, is function of

$$S = \frac{1}{R_{min}} * \frac{\Delta R}{\Delta H} = \frac{MR}{\Delta H}; \quad (8)$$

*Equation 8 – Sensitivity of transfer curve*

Due to the fact that higher MR are reached, GMR and TMR are the most explored elements among Megnetoresistive sensors for the area of magnetic cytometry. Main differences between the implementation of the two effects is due to the separation layer between two magnetic layers, where GMR (Figure 13) are characterized by a conductor separator and the TMR rely on an insulation layer.

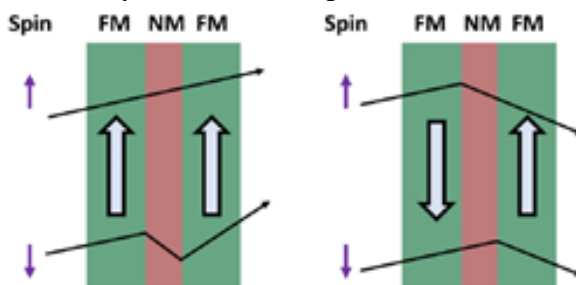


Figure 13- GMR effect visually explained; F stays for Ferromagnetic while NM stays for Non Magnetic; White arrows indicates the Magnetic field direction in the layer and long arrows represents electron path moving from one layer to the other. [48]

Due to their high signal to noise ratio (SNR), MR based sensors are preferred in PoC applications. The MR sensors used in biochip platforms are essentially of two types: spin valves (SV) and magnetic tunnel junctions (MTJ).

The MR sensors are characterized by a linear change in electrical resistance under an external magnetic field (refer to Figure 14 and Figure 15).

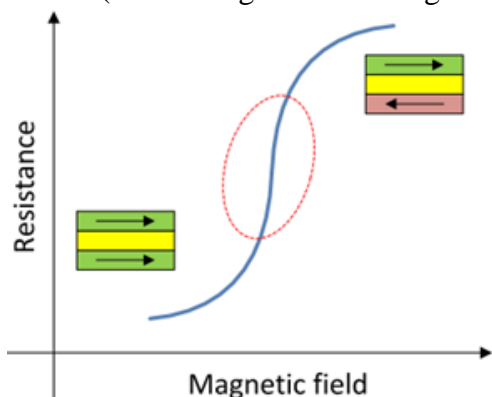


Figure 14- Representation of MR effect and dependence from measured magnetic field with linear range evidenced by red dashed circle [48]

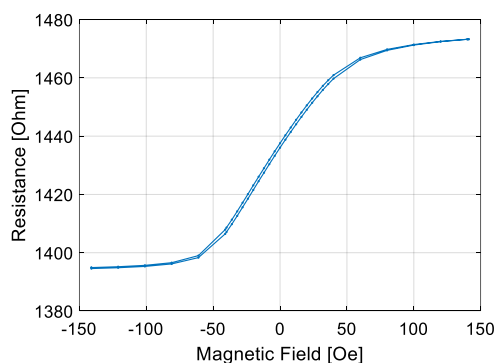


Figure 15 - Transfer curve of sensor used for preliminary detection on processed sample, refer to section 5.2

For the biochip application the more commonly used sensors are the SV due to their high signal to noise ratio and their simpler fabrication process. Since an increase of sensitivity is needed for some applications (i.e. direct analysis of unamplified biological samples), MTJs are started to be used in biochips [49]. However, since the current is flowing through the MTJ in a perpendicular to plane configuration, the sensors need a top contact which increases the distance between the sensing layer and the particles. This fact reduces the fringe field created by the particles on the sensor leading to a lower signal when compared with a sensor with a current in-plane configuration, as the SV [50].

For the mentioned reasons, Spin Valve sensors have been the choice for the magnetic flow cytometer developed by INESC-MN in collaboration with INESC ID [4] [5], on which in section 5.2 a preliminary test for the evaluation of the microfluidic device performance have been verified, as a mere sight on device future perspectives.

Another aspect involved is the magnetic label, not only essential for the capturing process required by the sample treatment process discussed in section 1.2.1, but also off extreme importance for the efficacy of the detection system, once the field created by the labels allows the detection by

the sensors. This means that different factors are relevant, the produced magnetic field, their connection with the sample, the size and the positioning respect to the sensor.

As concerns the field, it can be permanently produced, like in ferromagnetic particles, or induced by a second external field, as for superparamagnetic particles. The major used materials are iron oxides of magnetite ( $\text{Fe}_3\text{O}_4$ ) and maghemite ( $\gamma\text{-Fe}_2\text{O}_3$ ) as well as pure ferromagnetic materials as Fe, Ni, Co and oxide ferrites [51].

Superparamagnetic particles result more appealing as concerning magnetic separation and magnetic labelling and detection due to their zero remanent magnetization; this property avoids magnetic interactions between particles when not influenced by an external magnetic field and thus reduces phenomena of clustering and aggregation. For the mentioned reason, such type of particles has been chosen to be exploited in this work, provided by Ademtech and organized as a magnetic core of iron oxide encapsulated by a highly cross-linked hydrophilic polymer shell (refer section 7.1).

Due to the reduced dimension of the superparamagnetic particles, a first and easy approach for the mathematical treatment of its produced field is considering each element as an elementary dipole centred in the particle centre [46]. The stray field produced is governed by Equation 9 and it is visually displayed in Figure 16

$$\mathbf{H}(\mathbf{r}) = \frac{1}{4\pi} * \left( \frac{3(\mathbf{r} * \mathbf{m})\mathbf{r}}{r^5} - \frac{\mathbf{m}}{r^3} \right); \quad (9)$$

Equation 9 – Stray field produced by a superparamagnetic bead when approximated to a dipole

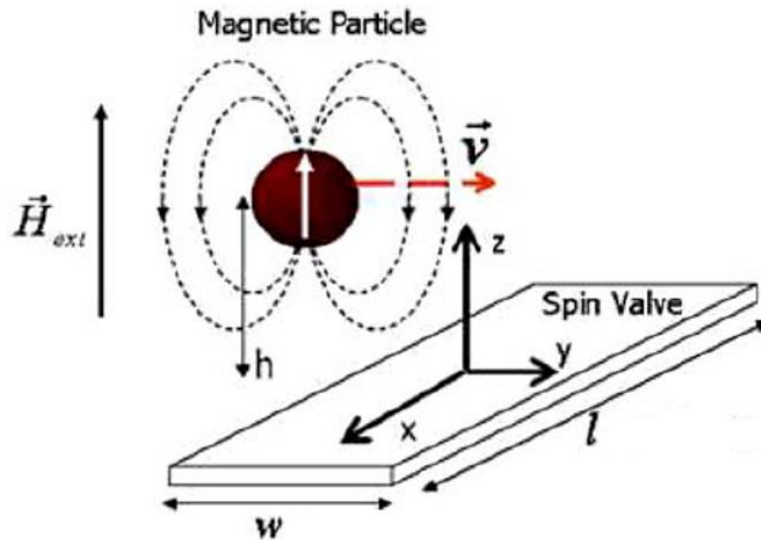


Figure 16-Example of the fringe field emitted by a superparamagnetic bead, in the case of vertical magnetization [26]

while its component in the plane of the sensor along y axis (the only component affecting the free layer magnetization, parallel to such direction) is described by Equation 10

$$H_y(x, y, z) = \frac{m_z}{4\pi} * \frac{3xz}{(x^2 + y^2 + z^2)^{\frac{5}{2}}}; \quad (10)$$

Equation 10 – XY plane component of the stray field produced by a magnetic particle approximated to a dipole

where  $m_z$  is the component of bead magnetic moment along vertical direction and  $x$ ,  $y$  and  $z$  are the distance from the centre of the sensor, according to the system of reference reported in the figure.

The signal generated at the sensor level, related to a spin valve, will then be bipolar, due to the inversion of the direction of the fringe field affecting the sensor it-self. In fact, depending on the chosen system of reference, the field produced from the bead will be negative at the beginning, when only first half of the bead influence the sensor; then other half will compensate with a field in opposite direction, thus reaching zero at the centre of the sensor. Finally, the field will become positive when the bead is leaving the sensor surface and goes to zero once bead is far enough. The sensor is sensitive to the average field over its area, so an integration of the equation of the area of the sensor returns the measured signal. Its shape is then predicted to be bipolar (refer to Figure 17)

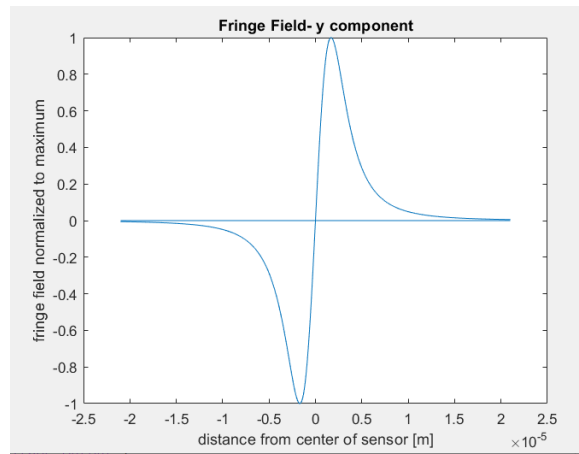


Figure 17-Simulation of normalized fringe field planar component on sensor surface, used parameters in Table 1

while the voltage output of the sensor is defined by Equation 11 and visualized in Figure 18.

$$V = -I * S * H_y; \quad (11)$$

Equation 11 – Sensor voltage output

where  $I$  is the applied current to the sensor,  $S$  is sensor sensitivity ( $\frac{\Omega}{Oe}$ , or  $S' * R_{minimum}$ ) and  $H_y$  is the fringe field of the beads in the plane of the sensor and along the easy axis direction.

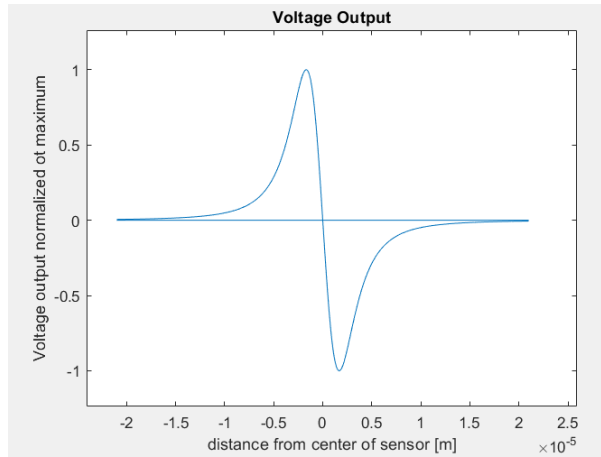


Figure 18-Corresponding normalized output voltage of the sensor, used parameters in Table 1

Table 1- Parameters applied for magnetic particles fringe field and relative sensor output

Parameter	Description	Value
$m_{tot}[\text{Am}^2]$	Total beads magnetic moment (64 beads)	$-6.12 \cdot 10^{-14}$
$Q[\mu\text{l}/\text{min}]$	Flow rate	10
$W[\text{m}]$	Sensor width	$10^{-4}$
$L[\text{m}]$	Sensor length	$2 \cdot 10^{-6}$
$S_{ch}[\text{m}^2]$	Channel cross-section	$10^{-8}$
$I[\text{mA}]$	Sensor biasing current	1
$S[\text{Ohm}/\text{Oe}]$	Sensor sensitivity	0.4
$D[\text{m}]$	Vertical distance from sensor	$2 \cdot 10^{-6}$

Label and its link to the sample is another relevant step to be taken into account and can be achieved in different ways. Since generally a reversible interaction is needed, a third element is exploited to link magnetic entity and sample, among which aptamers and antibodies (or their fragments); the latter are surely the most used for magnetic cytometry since they ensure high specificity towards exposed domains of a cell, with good stability and being already well-developed [27] [25]. In addition, the chemistry to connect antibodies to beads is also deeply explored, varying from covalent bonds with carboxyl or amino group, as well as side-chain groups, to the use of biotin-streptavidin bond in modified antibodies, or protein A and G affinity to  $F_c$  antibody domain, making antibodies a perfect model recognition element to be used.

One interesting recognition element that is recently emerging is represented by bacteriophages with some properties quite appealing, like the natural selectivity and ability to self-duplicate which reduced production costs, limited interactions with other biological molecules as other proteins or lipids and interaction with living cells only [52]. Nevertheless, the lack of well-characterized protocol, few literature studies on similar application, and its natural cycle involving cell lysis, causing the loss of the sample in a short term, makes them a poor model recognition element to be explored at the beginning.

Following, one additional factor to be considered is the size of the particle due to the possibilities of false positive detections, of aggregation and eventually clogging, of deposition in the channel, or inlets/outlets and different pressures needed to be applied to achieve wanted flowrate. Dimensions can cover a range from few micro-meters to few nano-meters [51] [26]; related to the

produced pre-treatment device and for further preliminary detection test, particles in the size of 250nm have been used(refer to section 7.1).

One additional advantage of introducing magnetic particles for separation and detection is the possibility to exploit magnetophoresis as a sample focusing technique, in addition to the well-known hydrodynamic focusing, in order to force the sample in a specific position without changing channel dimensions or geometry, and so avoiding clogging or obtaining a separation procedure [53]. This effect can be an advantage in both sample preparation step and downstream sensing element in order to collect differentiated samples. Specifically, a combination of lateral hydrodynamic focusing and vertical magnetophoretic focusing would concur to increase the signal intensity, where the first would allow only one target in the plane and the second only one target in the vertical direction to cross the sensor and avoid missing detection, allowing a more freely disposition of the sensor, in its size and number, no more forced to occupy the total width of the channel, reducing its noise and so increasing the signal to noise ratio. Some drawbacks, though, lead to the decision to not include mentioned approach in the final device, given the increase of complexity in external systems required to achieve it; nonetheless, it is possible to introduce magnetophoresis/hydrodynamic focusing coupling in future designs of the device to increase separation and detection yield.

## 2. Materials and methods

### 2.1. Materials and tools

The section covers the role to collect information characterizing the material used, divided for each specific process. All the material reported as sterile is either already sterilized by the supplier or sterilized in autoclave (UNICLAVE 88 from AJC) at 121°C for 21min, and used under sterile conditions only.

#### *Benchtop protocol*

Buffers: PB (pH=7.4; 0.1M; Disodium phosphate from FisherScientific), PB-T20 (pH=7.4;0.1M; Tween20 from FisherScientific), LB agar (40g/L<sub>H2O</sub>, FisherScientific), LB broth (25g/L<sub>H2O</sub>, FisherScientific), SuperBlock(PBS)T20 (FisherScientific), BSA5% w/v(pH = 6.5 to 7.5, FischerScientific, sterilized by filtration: Whatman GE healthcare 0.2um sterile)

Flow hood (Scanlab Mars from Labogene), magnetic column (dynamag-2 invitrogen), agitator (ika MS 3 basics), incubator (Heratherm by ThermoFisher)

Beads (Bio-Adembeads Streptavidin plus 0322 200nm)

Antibody stock: ab69468 Rb pAb to *Klebsiella spp* (biotin), ab68539 Rb pAb to *Pseudomonas aeruginosa* (biotin) from AbCam.

Bacteria (kindly provided by Tecnophage): *Klebsiella pneumoniae* and *Pseudomonas aeruginosa*

#### *Hard Mask production*

Glass (50\*50 mm<sup>2</sup>, 0.7mm thick) covered in aluminium (composition: Al98.5Si1.0Cu0.5, thickness: 3000Å)

Lasarray DWL 2.0 (Direct Write Laser system, Heidelberg), Nordiko 7000, SGV track

PFR7790G27cP positive photoresist, TMA283WA PR Developer, TechniEtch Al 80 MOS Aluminium Etchant

Buffers: IPA (LabChem), Alconox(LabChem), Acetone(LabChem), DI water

#### *SU-8 production*

Silicon substrate (60\*60 mm<sup>2</sup>, 0.7mm thick)

Flow hood (Faster BSC EN2.6), Spin coater (Technology Corporation model WS 650MZ 23NPP lite), UV exposition setup (lamp from UV light technology), Hot plate (Torrey Pines scientific), degasser (Bel Arts Products model 1 800 4)

SU-8-50 negative photoresist (Microchem), PGMEA SU-8 developer (MW=132.16g/mol, SigmaAldrich), FDTs (SigmaAldrich)

Buffers: IPA (LabChem), Alconox (LabChem), Acetone (LabChem), DI water

#### *PDMS production*

DMS monomeric solution (Sylgard 184 Silicone Elastomer Kit, Dow Corning), Fossil 184 silicon elastomer curing agent)

Oven (Mettmert model 100-800)

Punch pen for inlets/outlets (WPI 1.25mm plunge)

Glass substrate for sealing (50\*50 mm<sup>2</sup>, 0.7mm thick)

Buffers: IPA (LabChem), Alconox (LabChem), Acetone (LabChem), DI water



### Microfluidic testing

2xMechanical pumps (NewEraPumpSystem model NE300), Vortex (FisherBrand)  
1ml syringes (Codan), connectors LS20 20ga\*1/2 inch (Instech), Tubing BTPE90: Polyethylene, internal diameter 0.86 mm, external diameter 1.27 mm (Instech)  
BSA5% g/v (pH = 6.5 to 7.5, FischerScientific, not autoclavable, sterilizing filter: Whatman GE healthcare 0.2um sterile), Ethanol 70% v/v

## 2.2. Methods

In this section protocols are reported and discussed in detail; they are presented in their final structure, as a result of an optimization process, while evidencing adaptation that occurred where needed

### 2.2.1. Immobilization protocol

Immobilization refers to the process of covering the superparamagnetic particles with the proper amount of recognition element, or antibodies as concerns this study, in order to be later exploited to recognize and capture the target bacteria. A specific ratio of antibodies per particle is needed to maximise the efficiency in interaction with the bacteria; this parameter is discussed in section 4.1.

The immobilization has been performed on a variable number of samples per experiment, depending on the amount of beads required, and always under sterile conditions as guaranteed by the flow hood. For a single aliquot of 100µl particles covered with antibodies, needed for the capture of 100µl of bacteria solution, 10µl of beads from stock are resuspended in 100µl PB-T20 in an Eppendorf tube, and further washed two time in the magnetic column; this process involves the insertion of the tube in the column, and after a 5 min waiting time the extraction of the supernatant with proper tip and pipette, which can be discarded. The pellet formed on the wall of the tube due to the magnetic force of the column is then resuspended in 100µl PB-T20.

After, antibodies are added to the particle solution, in a volume of 1µl from the stock. The volume of beads (10µl) and the volume of antibodies(1µl) here reported refer to the optimized ratio of antibodies to beads, thus these two volumes have been altered during different protocol to verify the best condition.

Once antibodies are added, the solution is incubated at RT for 2h under 250rpm agitation. Solution is later washed again, as already explained, and resuspended in 300µl SuperBlock™ or 5% w/v BSA solution in DI water; this represents the blocking step, and the volume of used blocking agent have been varied to verify optimal conditions.

Follows incubation of the sample at RT for 1h under 250rpm agitation. Effects of incubation temperature at 37°C for both incubation steps reported have also been evaluated.

A final wash of the solution is then performed, with resuspension in 200µl PB added to 100µl SuperBlock™ or 5% w/v BSA solution in DI water. The solution is so stored overnight at 4°C, better performance is obtained when immediately exploited while shelf life shouldn't pass the 5 days, as it is estimated that the immobilized antibody can lose their efficiency in interacting with the epitope on the bacteria after such time interval at given storing condition. An example of the decreasing of interaction efficiency of the antibodies is given by the decreasing capture efficiencies in experiment 5, 6 and 7 from Table 4 (section 4.1. *parameters during capture*), where same parameters are maintained with the only difference being storage time for antibodies covered magnetic particles, produced the day before experiment 5 for all three experiments.

Before being used to perform a capture protocol in a bench-top assay or in the microfluidic device, particle solution is washed twice and resuspended in 100µl PB.

### 2.2.2. Bacteria inoculum preparation

In order to be able to test the efficiency in the prepared magnetic particle solution with immobilized antibodies to interact with bacteria, a solution of target bacteria at wanted concentration is needed. Bacteria are grown following standard laboratorial procedure. All the procedures are performed under sterile conditions, in a flow hood. Target bacteria stock is stored at 6°C in a Petri dish filled with LB agar media; one colony is moved from the stock to a falcon tube containing 5ml LB broth media and incubated overnight (16h to 18h) at 37°C under 250rpm agitation. After first incubation, 155 µl (see Table 2) of the solution are added to 4845µl of LB broth media in a falcon tube and incubated a second time at 37°C under 250rpm agitation, for 1h in the case of *Klebsiella pneumoniae* and for 1.5h in the case of *Pseudomonas aeruginosa*.

The volume of 155 µl is chosen as average between volume computed in different experiments in which OD<sub>600</sub> was measured (Table 2); this parameter, in fact, is related to the concentration of bacteria in a solution. The wanted concentration of 2\*10<sup>8</sup> CFU/ml is equivalent to an OD<sub>600</sub> of 0.3; knowing bacteria growth curve, which relates OD<sub>600</sub> to growing time, a solution at OD<sub>600</sub> equal to 0.1 is be prepared and then incubated for the amount of time extracted from the curve to reach the wanted OD<sub>600</sub>, ie. 0.3. To prepare the solution at OD<sub>600</sub> equal to 0.1 a solution of bacteria at high concentration, resulting from an overnight incubation, is measured for its OD<sub>600</sub> and a proportion is made (Equation 12) to compute the volume need for an OD<sub>600</sub> of 0.1 in a 5000µl solution in LB broth.

$$\frac{OD_{600}^{1st\,inoc}}{5000} = \frac{0.1}{V_x}; \quad (12)$$

Equation 12 – Proportion for the computation of needed volume for second inoculum preparation

where  $OD_{600}^{1st\,inoc}$  is the measured OD<sub>600</sub> of the first inoculum while V<sub>x</sub> is the volumed added to LB broth so that V<sub>x</sub>+V<sub>LB broth</sub>=5000µl and 0.1 is the value of OD<sub>600</sub> wanted in the second inoculum, chosen according to the specific growth curve of the bacteria. Following it, the time needed for a specific bacteria to reach a target concentration under incubation is known.

Table 2-Computation of volume used to prepare second inoculum

$OD_{600}^{1st\,inoc}$	V <sub>x</sub> (µl)
2.8	178.6
3.43	145.8
3.34	149.7
3.6	138.9
3.22	155.3
2.995	166.9
3.27	152.9
<b>Mean V<sub>x</sub></b>	<b>155.4±13</b>

### 2.2.3. Protocol for bench-top capture

This protocol represents the bench-top assay performed as a comparison with the protocol performed in the produced microfluidic device, as presented later. It involves the mixing of particles with immobilized antibodies and bacteria solution and retention of the labelled bacteria, and are thus performed by the operator in a manual procedure.

Once solution of particles with immobilized antibodies and inoculum are prepared, as described in the previous section, capture can be performed.

Dilutions of the inoculum are prepared in order to obtain solutions at wanted concentrations, starting from a nominal concentration expected in the inoculum of  $2 \cdot 10^8$  CFU/ml and proceeding with serial dilutions, where 100 $\mu$ l from a more concentrated dilution are added to 900 $\mu$ l of PB in an Eppendorf tube, thus leading to a 1/10 dilution; this is repeated until a  $10^{-7}$  dilution (or  $10^{-7}$  dilution from original inoculum, with expected concentration of  $2 \cdot 10^1 = 20$  CFU/ml)

Beads solution with immobilized antibodies is washed, as explained in the section 2.2 *immobilization protocol*, and resuspended in 100 $\mu$ l of bacteria solution from the tested concentration, depending on the aim of the single experiment.

Sample is incubated at RT for 15min at 250rpm; different values of these parameters have been tested to verify better performance.

The solution is then washed 2 times (3 times in earlier experiments), but supernatants are not discarded and are collected instead, as they represent the solution containing bacteria that have not been proficiently captured; at every wash, the pellet is resuspended in 100 $\mu$ l PB. After such washing step, three samples are obtained: the first supernatant, called SB, the second supernatant, called WI, and the resuspended pellet, called CM. If three washes are performed, an additional supernatant, called WII, is present.

#### 2.2.4. Microfluidic device fabrication

The role of this section is to present to the reader the mean by which the microfluidic device production can be achieved, thus exploiting the already mentioned (section 1.2.1) soft lithography technique.

This process involves three main steps, the production of a hard mask, the creation of a polymeric mold and finally the realization of the microfluidic device itself; this steps are preceded by another essential component of the process, the software device design, discussed in section 4.2.

Here a summarized version of the production protocol is presented, while the complete procedure with all parameters can be consulted in section 7.5 appendix E. In addition, in the following section, when parameters are reported, they will refer to the final optimized protocol.

##### *Hard Mask*

All step reported in the section are performed inside a cleanroom facility (*class 10000 and class 1000*).

Initially a glass slab of 0.7mm thickness is cut with dicer in order to obtain squares of 50\*50mm<sup>2</sup>. After properly cleaned in Alconox (1h at 65°C under ultrasounds) and rinsed with IPA, DI water and blow dried, metal (Al98.5Si1.0Cu0.5 wt%) is deposited on its top with a thickness of 3000Å in Nordiko 7000. Positive photoresist PFR7790G27cP is then spin coated at SGV track on it to obtain a ~1.45 $\mu$ m thick layer. Follows a soft bake at 85°C for 1 min.

Substrate is after exposed and photoresist patterned with DWL (Direct Laser Writing) tool at a wavelength of 442 nm based on NeAr laser. Photoresist development is performed at SGV track and consists of a baking step at 110°C for 1 min, cooling for 30s and contact with developer TMA283WA for 1 min.

Once the pattern is developed and metal uncovered in selective areas, etching of the metal layer is performed. Substrate is immersed for 5 min in TechniEtch Al 80 MOS Aluminium etchant at RT and under manual agitation, then washed in DI water. To complete the procedure, photoresist removal is achieved by acetone wash (2 min at RT under manual agitation) and cleaning with IPA, DI water and blow dried.

##### *SU-8 mold*

Following steps are performed inside a cleanroom facility (*class 10000*).

Silicon substrate 0.7mm thick is manually cut as a square of 60\*60mm<sup>2</sup> and cleaned in Alconox (1h at 65°C under ultrasounds) and rinsed with IPA, DI water and blow dried. Surface is lately treated

with oxygen plasma for 1min at a pressure of 800mTorr and with an RF power of 11W in Plasma Cleaner (model PDC 022 CE from Harrick Plasma) and moved out from cleanroom facility while properly stored in a clean plastic box.

Following steps are performed inside a flow hood (Faster BSC EN 2.6).

Sample is baked at 110°C for 5 min to be dehydrated on hot plate(Torrey Pines Scientific) and cooled down to RT. Follows negative photoresist SU-8-50 spin coating in order to reach a nominal thickness of 100um; parameters involved in the spin coating process have been varied to achieve aimed thickness(final values can be verified in section 7.5, appendix E). Soft baking of the sample is performed at 65°C for 10 min and 95°C for 30 min on hot plate. After cooled down to RT, exposition takes place in proprietary tool from INESC MN™, based on a lamp filtered at wavelength of 365nm, exploiting previously produced hard mask; exposure dose have been varied in the study to reach good features definition and final dose have been set to 166.5mJ/cm<sup>2</sup>.

Post exposure bake is performed on hot plate at 65°C for 1 min and at 95°C for 10 min, following cooling down to RT.

In conclusion, sample is developed in PGMEA developer for 15 min at RT under manual agitation, rinsed with IPA to verify complete development (transparent solution of IPA and PGMEA turns white if development is not completed) and checked under microscope. If development is satisfying, sample is rinsed in IPA and blow dried.

Eventually, the newly fabricated mold can be treated with FDTs for 20 min under vacuum to increase surface hydrophobicity.

#### *PDMS production*

PDMS is prepared by mixing DMS and curing agent in a proportion 10:1 (w/w) in a clean plastic cup, for an approximated mass of 15g of DMS and consequently approximately 1.5g of curing agent. The solution is manually mixed with a disposable plastic spoon and degassed for 1h at low pressure in degasser (Bel Arts Products). When no air bubbles are present in the solution, it is manually poured in the previously fabricated SU-8 mold and baked at 70°C for 1h in oven (Memmert model 100-800).

Once removed from the oven, sample is let cool down to RT and manually peeled off from the mold with the help of a tweezer. A proper hole punch pen for desired measures is used to produce inlet/outlet holes in the device, which is later cleaned with DI water and blow dried to remove any residue.

A glass substrate of 50\*50mm<sup>2</sup> area and 0.7mm thickness is cleaned in Alconox (1h at 65°C under ultrasounds) and rinsed with IPA, DI water and blow dried. Both glass substrate and PDMS are treated with oxygen plasma for one minute and finally put in contact with gentle manual pressure to achieve device sealing. Device is stored 24h before being tested.

#### 2.2.5. Protocol for microfluidic capture

When the produced microfluidic device is tested, the following protocol is followed, depending if the sample tested is a simple solution of target bacteria in PB buffer at a controlled concentration, or if complex clinical samples are tested; in both cases, immobilization of antibodies on particles is performed as reported in section 2.2 *immobilization protocol*.

The following protocol are performed in sterile condition inside a flow hood.

### Buffer based bacteria solutions

For device characterization, bacteria solutions in PB buffer at controlled concentration have been used as a sample, together with magnetic particle solution with immobilized antibodies, obtained as described before.

Different sample concentration, as concerning bacteria, are tested; here is reported the protocol applied independently on this factor. Such protocol was applied multiple time to the same device if its behaviour at different concentrations was to be evaluated.

The device was stored filled with 70% v/v ethanol solution from one to several days, up to the moment it was tested following the described sequence of steps.

At first, elution inlet is closed by a proper metallic rod, while mixing inlets and outlet are connected with suitable tubing. Tubes are then connected to syringes through proper connectors, which are inserted in the mechanical pumps. Figure 19 and Figure 20 shows the discussed set up.

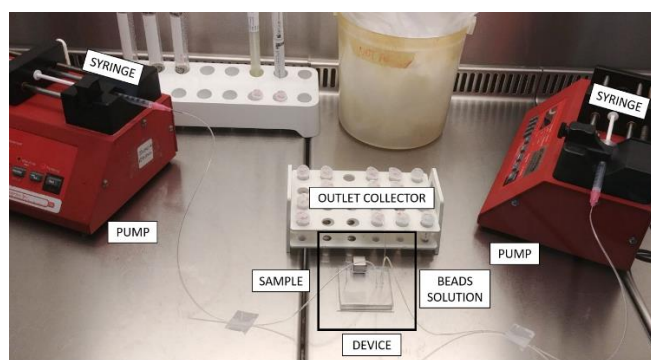


Figure 19- Set up of the device during testing

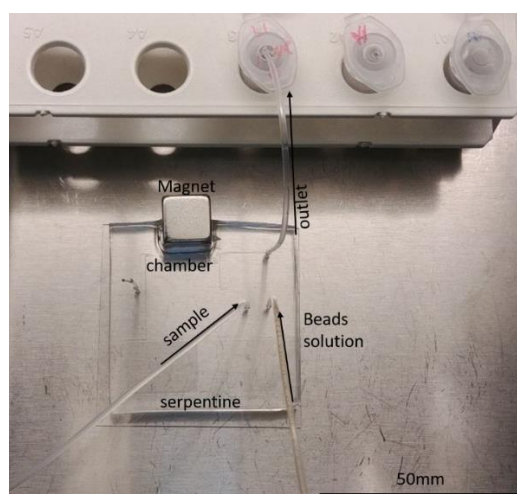


Figure 20-Detail of the device connections during testing

The device is first sterilized with 200 $\mu$ l an ethanol solution 70% v/v in DI water at a flow rate of 50 $\mu$ l/min (per single inlet).

After, a washing step is performed with 200 $\mu$ l DI water at flow rate of 50 $\mu$ l/min (per single inlet).

To conclude the preparation steps, system is primed with 100 $\mu$ l of a blocking solution, SuperBlock™ or 5% v/v BSA in DI water, at a flow rate of 50 $\mu$ l/min (per single inlet); volume is completely released and discarded before next step is started. No tests have been performed to evaluate the possibility to the device to be stored after priming, as all devices were stored in ethanol 70% v/v and priming and washing were performed immediately before sample testing.

Mixing and capture/retain steps can now begin, as displayed in Figure 21, evidenced with the use of a red colored die; The magnet is positioned in the suitable location, close to the chamber, and 100 $\mu$ l of magnetic particle with immobilized antibodies are injected from one inlet, while bacteria solution sample is injected from the other, at a flow rate of 10 $\mu$ l/min. The outgoing volume is collected in an Eppendorf tube and marked as non-retained (NR), until the whole volume is released.

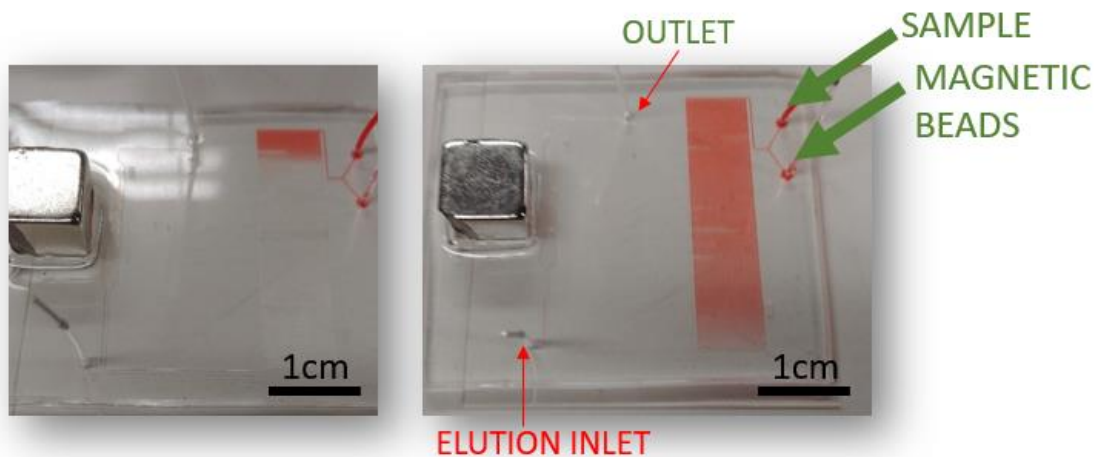


Figure 21- Device during mixing, red colored die is used to outline the process

Once completed, elution step can take place; mixing inlets are closed with proper metal rods, while elution inlet is connected to a tube, and 40 $\mu$ l PB are injected in the microfluidic device at a flow rate of 10 $\mu$ l/min, filling the elution channel, chamber (where particles are retained) and outlet channel, as well as part of the outlet tube.

Magnet is now removed, and a time interval of 5 min is waited in order to allow particles to resuspend in the buffer. An example is shown in Figure 22

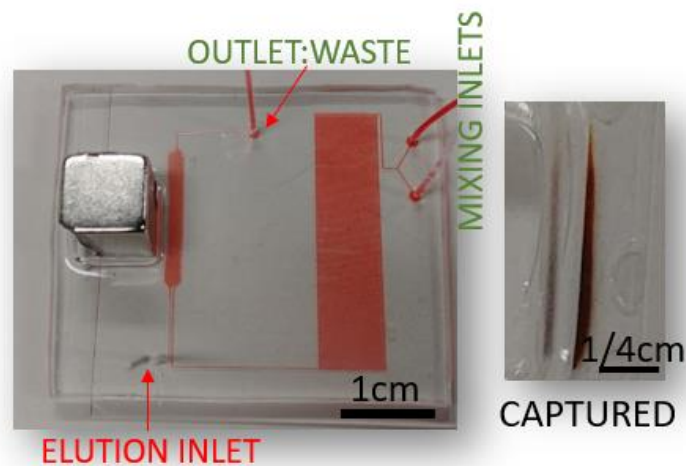


Figure 22- Left: device during capture/retention, red colored die used to outline the process; right: Example of retained and resuspended beads

The solution in the device is then released, as presented in Figure 23, at a flow rate of 100 $\mu$ l/min to limit particles depositions at the outlet, and collected in an Eppendorf tube as retained(R).

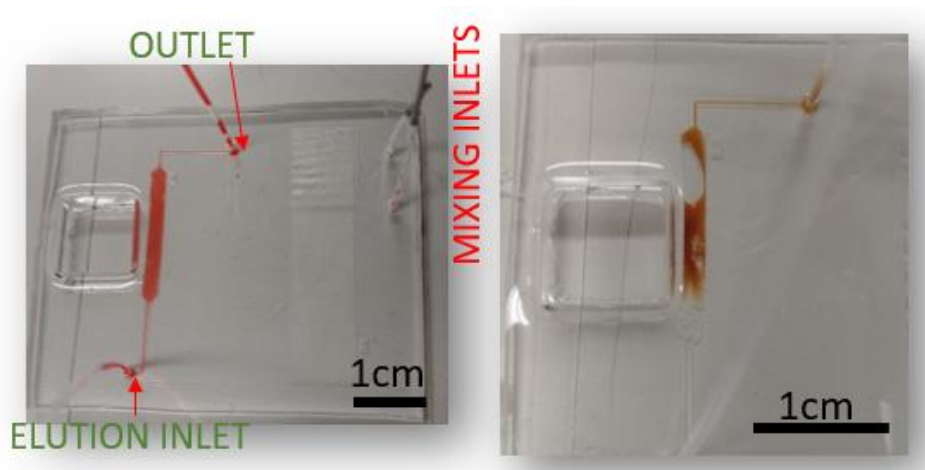


Figure 23-Left: device during elution, red colored die used to outline the process; right: example of eluted beads

Preparation steps comprising of sterilization, washing and priming of the device can be performed again if a new sample is wanted to be tested; the reusability of the device is simply for testing purposes, as final device applied to real samples is meant to be disposable, at least for the component discussed in this section.

#### Clinical samples

Clinical samples are stored at 6°C before being tested. The swab is stored in a gelatine-based matrix, representing the storage media which supports viability of organisms of various species among which *Enterobacteriaceae* of which *K.pneumoniae* is part, and thus needs to be resuspended in a liquid buffer before being tested in the platform. Resuspension is obtained in an Eppendorf tube filed with 500µl PB and the solution is then homogenized with vortexing at 1600rpm. 100µl of the solution are thus separated and will represent the tested sample. All further steps are equivalent to protocol reported in the previous section related to buffer based bacteria solution.

The microfluidic device is disposed after a single test and autoclaved to ensure sterilization.

#### 2.2.6. Plating

After samples are collected from different washing steps, as regarding the bench-top assay protocol for bacteria capture, or as non-retained and retained solution, for microfluidic device testing, the concentration of bacteria in each sample have be assessed; at the same time, also the initial concentration of bacteria, present in the original sample which is the specific inoculum dilution or the resuspended clinical sample swab, depending on test, is wanted to be quantified.

Plating and CFU counting is chosen as a mean to evaluate the number of bacteria in the samples, being a well-characterized reference technique for such role and not limited by the required time in the frame of laboratorial testing and bacteria used. Other approaches like RT-PCR or florescence would have required expensive tools, expertise in the sector and may have been suffered from interference of magnetic particles more than colony count method.

Main limitation of the plating method though, realized on LB agar filled Petri dishes, here used as a quantification procedure, is the number of colonies that the operator can distinguish as well as the maximum number of colonies that are considered reliable for single Petri dish.

Two plating methods have been used, here referred as spread plate technique or drain drop plate method; in the former 100µl from the sample are poured on the dish and distributed on the whole surface through a disposable spreader. In the latter, a 10µl drop from the sample is poured on the upper part of the dish, which is then inclined to allow the drop to flow vertically and spread along a vertical line; from 4 to 6 drops per dish can be plated, from different samples.

As for the spread plate approach, a colony count comprised between 30 and 300 is considered reliable [54]; as for the drain drop plate method, given the smaller volume plated, at least 3 to 30 colonies can be distinguished reliably [55], up to 100 colonies in the best plating conditions, where the drop was able to cover the whole diameter of the dish.

In order to be able to guarantee that plated concentrations are in the range of reliability as explained above, different dilutions of the same sample are always plated, commonly up to 5 dilutions, but depending on different prediction that can be done on the expected concentration in the sample. Serial dilutions are prepared mixing 20 $\mu$ l from higher concentration dilute on into 180 $\mu$ l PB in an Eppendorf tube in order to obtain serial dilution of 1/10.

After plating procedure, Petri dishes are incubated at 37°C overnight (16h to 18h) with no agitation.

Depending on the experiment, duplicates or triplicates are produced to confirm results.

### 2.2.7. Protocol for cytometric platform

By the moment that the microfluidic device has the aim of constituting a preparative step to produce a labelled and concentrated sample of the target bacteria to be detected into a magnetic cytometric platform, 2 samples have been evaluated in a platform under development at INESC-MN by Soares et al. and results are reported in section 5.2. The protocol followed for the discussed tests is the following.

Prior to sample detection, a blank detection with PB only is performed, at 10 $\mu$ l/min while sensor output is recorder, in order to establish a baseline for the noise detection, used in the post-processing of the signal.

After, 50 $\mu$ l of the sample are injected at a flow rate of 10 $\mu$ l/min and output signal is recorded. Some volume of PB only is flowed to wash the channel for any accumulation of bacteria of beads cluster, making the system ready for the next sample. Used set-up is displayed in Figure 24.

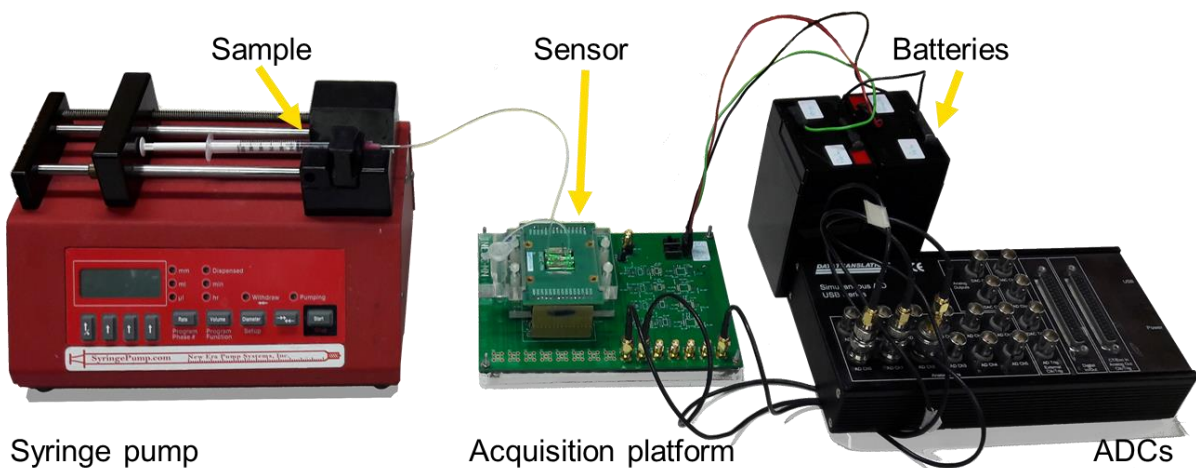


Figure 24- Magnetic cytometric platform set-up [5]



### 3. Theoretical Background

In this section, some of the theoretical aspects beyond the device simulation and realization will be discussed, as well as some background information will be provided.

#### 3.1. Bench-top assay: immobilization of antibodies and bacteria capture

As anticipated in section 1.2.3, different recognition elements can be exploited in order to achieve the capture of target bacteria. As a model element antibodies immobilized on magnetic beads are explored. In fact, as previously presented always in section 1.2.3, antibodies are the gold standard for bacteria recognition, used in different assays (ELISA, paper microfluidics, etc), with the advantage of being a well established technology.

For as said, before moving to the microfluidic platform, a bench protocol for antibodies immobilized on magnetic beads was developed, initially following beads supplier advices, as indicated in the datasheets.

Nonetheless, the use of antibody as a mean of capture has not been as straightforward as it may be predicted, and optimization steps were needed to individualize better conditions.

Two are the most influent steps to be majorly taken into account to ensure a successful capture, a sufficient immobilization efficiency must be achieved, which is, a suitable number of recognition elements need to stably be anchored to the beads, and furtherly such elements must be able to recognise and interact specifically with the target bacteria, with no impediments, involving an advantageous orientation, avoiding degradation of the active site and correct condition of the environment.

The first step, the immobilization, depends on the utilized beads and active element; In the case of antibodies, different methods can be implied, but one with recognized efficiency and simplicity, involving a more direct immobilization chemistry, is represented by the natural affinity between biotin and streptavidin protein.

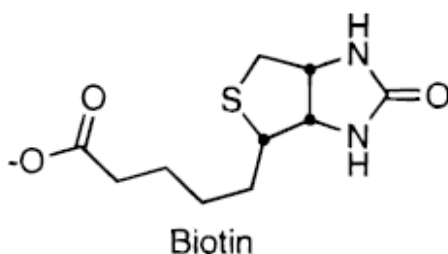


Figure 25 - Biotin structure [56]

These two molecules have the strongest non-covalent interaction in nature, given the very complementary steric fit, with biotin cyclic urea group buried in streptavidin pocket allowing extensive hydrogen bond formation, as well as carbonyl group interaction with Asn-23, Ser-27, and Tyr-43 of Streptavidin [56], as verified by crystal structure of the complex determined in [57].

In order to exploit the explained interaction, streptavidin functionalised beads were acquired from AdemTech (mean diameter 200nm, *see Appendix A: Ademtech beads Datasheet*) while biotin modified antibodies exploited are ab69468 Rb pAb to *Klebsiella spp* (biotin) and ab68539 Rb pAb to *Pseudomonas aeruginosa* (biotin) respectively (AbCam, *see Appendix F: Antibodies AbCam Datasheets*)

Chosen beads are the type of superparamagnetic, with the property, as reported in section 1.2.3, to be magnetically active only when immersed in an external magnetic field, or said in different words, presenting no hysteresis and no remanent magnetization.

The immobilization of antibodies is reached by mixing a solution of the former with one of the latter, at a controlled temperature, agitation and time. One intrinsic limitation of the process is the random orientation that recognition elements can take once fixed on beads surface, given the fact that streptavidin proteins on the particle and biotin molecules on the antibody are located with no specific positioning, thus the interaction of the element and particle can happen at any orientation and location, possibly impeding the active side to be exposed; for such reason, the amount of antibodies willing to be immobilized is high, so that statistically at least some of the active sites are correctly exposed and functional.

The second step, the recognition, is mainly dependent on the property of the antibody itself, selected to be able to specifically recognize the target bacteria.

As target bacteria, efficiency of capture for *Pseudomonas aeruginosa* and *Klebsiella pneumoniae* are explored, with active elements specific for these two bacteria, and for *Escherichia coli*, used as further negative control.

A list of parameters considered as effectively affecting the results on immobilization and capture have been individualized and reported in Table 3

Table 3- Factors involved in bench protocol optimization and their influence

Factor		Influence on
Antibody and beads incubation	Time Temperature Agitation	Immobilization
Beads and bacteria incubation	Time Temperature Agitation	Capture
Blocking step	Time Temperature Agitation	Specificity
	Volume Type	
Beads and antibody ratio		Immobilization
Beads and bacteria ratio		Capture
Bacteria dilution		Capture
Plating technique		Result errors

Such parameters have been tuned to achieve a capture up to ~90%, and a specificity demonstrated by a capture for the negative control of maximum ~8% and generally lower, as reported in section 4.1. The meaning of percentage of capture is explained same section 4.1, Results analysis.

### 3.2. Microfluidic Device Fabrication

In this section, further information on fabrication process are presented and discussed; for relative fabrication protocols the reader can refer to section 2.2.4, while for details on parameters for section 7.5, appendix E

#### 3.2.1. Hard Mask

The realization of the hard mask is the first step to be achieved, so called as it represents the elements that will mask the polymeric substrate, when the mold will be realized, from the UV light in the areas that are supposed to be removed; the concept will be clarified later.

First step involves glass substrate preparation for metal deposition; dimensions of the substrate are limited at its top by the holders for the PR spin coating and the DWL exposure, as well as at its bottom by the dimension of the digital mask. In fact, the glass substrate needs to be at least bigger than the digital mask by 5mm at each side, this is, to avoid patterning the PR or etching the metal at the edge of the substrate, where non-uniformities are found due to the deposition/spin coating process as well as some areas covered by presence of the tape, needed to hold the glass substrate in position during all the processes.

Deposited metal layer at thickness of 3000 Å is generally considered adequate for the role of shielding the mold from UV light, as its height is enough to completely absorb the rays.

After the metal is homogeneously deposited, the substrate is covered with a photoresist (PR). Such polymer has the particular property of being reactive to certain frequencies of electromagnetic waves, usually optimized for a narrow interval. If irradiated at such wavelength, their behaviour is distinguished in two categories (Figure 26), well described by the name of the photoresist class: negative photoresist cross-link as a consequence of irradiation by the proper waves and thus, once developed, maintain a negative of the transferred pattern, while positive photoresist will decrease its ability to cross-link where illuminated, leading to the transfer on the polymer of a copy of the pattern.

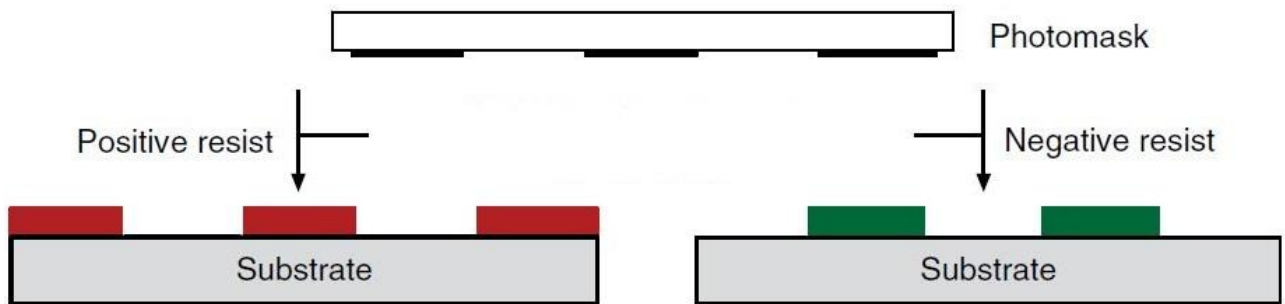


Figure 26- Positive and negative photoresist [58]

The role that a hard mask appears now clearer, as it is able to spatially select the areas of the photoresist to be exposed and so transfer the pattern it contains to the polymeric substrate. But this may sound as a counterintuitive, as it seems that a hard mask is necessary to produce another hard mask. Such puzzle is easily resolved, as a hard mask is an efficient and convenient way to obtain the wanted selectivity in exposure, but not the only possible; so to produce a hard mask, the photoresist used in the process is selectively exposed using a laser beam whose exposure area is moved by moving the substrate below it, in Lasarray DWL 2.0.

The ability of the photoresist to be selectively polymerized allows a differentiation in its removal rate when attacked by specific chemical agents, called developers. When entered in contact with such solutions, the non-polymerized areas are removed while the others are retained on the substrate. Exploiting this difference, a pattern can be impressed in the polymeric layer. In the case of the formation of the hard mask, such pattern is further used to cover selectively areas of the metal deposited on glass, when put in contact with another particular type of chemical, an etchant, tuned to preferentially dissolve the metal while almost not interact with the polymer.

Thanks to this smart chemistry, the following effect can be achieved, summing up the production of the hard mask: a pattern is transferred to the PR through a regulated source of light at the correct wavelength, controlled through software, using the CAD file (as shown in section 4.2) as guide or digital mask. Then the substrate is developed, and after this step, some areas of the metal beneath became exposed. At this point, the substrate is immersed in the etchant, which dissolves the metal in the exposed areas, while the rest is protected by the polymer. Finally, after the etching reaction is

blocked and substrate washed, a solvent for the photoresist is used to remove cross-linked polymer and reveal the pattern now impressed in the metal.

### 3.2.2. SU-8 mold

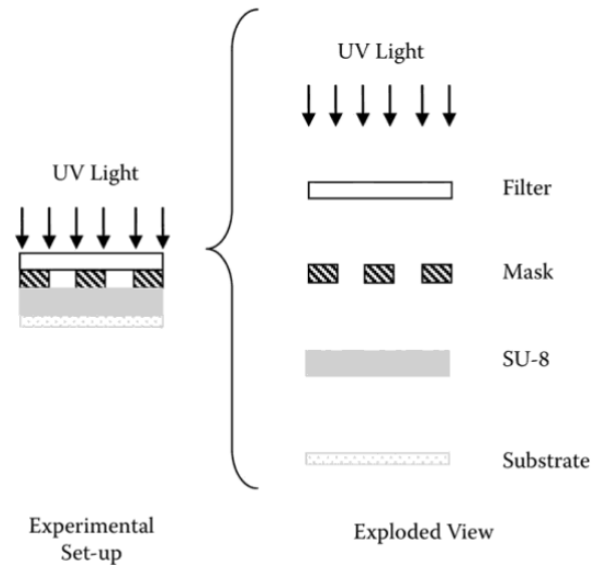


Figure 27 – General scheme for SU-8 mold production [59]

This section discusses the production of the SU-8 mold as a subsequent step in the soft lithography frame. At first, a silicon substrate is cut in the wanted shape and measure. This step is more immediate than compared to glass cutting, as it can easily be achieved by introducing a small defect in the wafer, for example, a scratch produced by a diamond-tip pen and then applying relatively small mechanical stresses at the position of the defect and at its sides, with inverted direction, in order to provoke the rupture of the substrate. The produced crack will move according to the crystalline structure of the silicon, FCC diamond lattice, as the edges of the lattice at {111} plane represent the direction of minimum energy.

The shape of the substrate is typically squared, following the mask shape, and it should be at least 5mm wider each side, once again to limit the impact of the non-uniformities, in this case for an additional reason. While, obviously, less uniform areas of photoresist should be avoided so that the final mold has spatially constant properties, especially as for thickness, it is also important to ensure that mask and mold during the exposition phase are as close as possible, limiting the air gap in between; this because increased distance in the air gap limits the resolution of the process, as shown by the relationship expressed in Equation 13

$$\text{Minimum feature size} = \sqrt{k * \lambda * s}; \tag{13}$$

Equation 13 – diffraction limit in photolithography

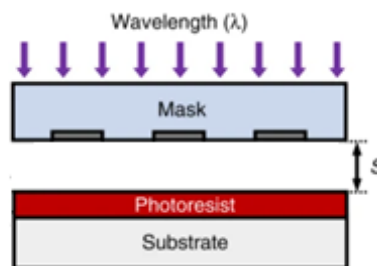


Figure 28- Exposure in photolithography [60]

where  $k$  is a constant depending on the photoresist and the development process,  $\lambda$  is the used wavelength and  $s$  is the gap (also refer to Figure 28).

The bigger dimensions on the substrate compared to the mask guarantee that the mask do not lay on the substrate edges, where spun PR is thicker, forming a rim especially with the used SU-8, precisely the SU-8 50, a negative photoresist characterized by an high viscosity to allow major thicknesses, but inevitably cause of more important edge beads. This phenomenon is caused by drops formations at the edge, where due to surface tension proportional to viscosity, drop can resist the outward spinning force and create a thicker ring at the edges [61].

In order to achieve better adherence of the photoresist to silicon substrate, surface modification is performed. This modification is achieved by exposing the substrate to an oxygen plasma formed in the Plasma Cleaner which is capable of form some radicals that interacts with the silicon surface and promote formation of SiOH groups, as well as interacting with any organic residue still present on the silicon surface and breaking down them to little chains, that then spontaneously evaporate in the low pressurized chamber, thus enhancing substrate cleaning.

Finally, the substrate is heated through the help of a hot plate, at  $110^\circ$ , or above the boiling temperature of water, to ensure any humidity deposited on the surface is removed. Once cooled down, silicon is now ready to be covered with the Photoresist. Cooling down is essential and must be verified as, higher temperature of the substrate would heat up the PR changing its viscosity, which is fundamental for the following step.

A layer of PR with wanted thickness can be achieved by Spin Coating, obtained by pouring a specific volume of the polymeric solution on to the substrate (1ml per inch) and thus rotate the substrate so that centrifugal forces push the solution to the sides, thus spreading it. The thickness that is reached is function of different parameters as: spinning speed, spinning time, spinning acceleration, volume of solution, area of the substrate and viscosity of the solution [61].

The distribution of the PR at wanted thickness is reached in two subsequent steps, where the first is always represented by constant speed, time and acceleration, specifically 500rpm for 10s at 100 rpm/s, and provides an uniform distribution of the polymer along the substrate, while a second step with fix time and acceleration, equal to 30s at 300rpm/s, and variable speed allow to tune the reached thickness, while removing excess PR.

Except for the spinning speed at the second step, during different fabrication tests all other parameters have been maintained constant while speed has varied in order to verify which was more suitable for the wanted thickness, hence  $100\mu\text{m}$ .

Even though the supplier of the PR provides some information on the required speed, time and acceleration needed to reach a target thickness, such parameters are not completely reliable as approximation of different set-ups. This will be greatly evident when the exposure time is discussed, with its great variation respect to the suggested one in order to obtain the wanted definition (see section 4.3.2)

Further steps involved a baking process, called Soft-Bake, to be distinguished with the further heating step performed after the exposition.

Such step allows the solvent in which the PR is dissolved to evaporated and creates a solid layer of polymer; it is essential, though, that the heating is achieved gradually, in order to avoid embrittlement of the polymer with further formation of cracks, due to introduced mechanical stresses.

Now the layer of polymer shows acceptable mechanical properties to be put in contact with the previously produced hard mask; as said the space between the polymer and the mask must be limited at its best, so the metal layer of mask is directly in contact with the PR, to minimize further dispersion of the light through the glass after spatial selection of the metal layer. Once put in contact,

mask and substrate are ready to be exposed. Exposition is achieved in the proprietary set up filtered at a wavelength of 365nm.

Su-8 is formed by a solution of a resin dissolved in an organic solvent (like PGMEA) and added to 10 wt% photoinitiator, sensitive to a specific wavelength; it is a chemically amplified resist where one photon interacting with the photoinitiator produces a photoproduct that causes a chain reaction which changes the solubility of the resin through cross-linking. [59]

The energy to which the PR is exposed is central for the definition of the structures that are wanted to be transferred in the layer. As the power of the lamp is fixed, as well as the distance at which the substrate is placed (which thus sets the power per unit of surface or energy over time per unit of surface), the only variable from which absorbed energy is dependent is exposition time, which is the parameter to be optimized to obtain maximum performance.

The optimization is needed because slight variations of the absorbed energies can imply a distortion in the transferred design; over-exposure of the photoresist could cause also areas that should be shielded to be reached by the UV waves as some lateral diffusion in the polymer is present, which, for longer interval of time, can transfer enough energy to the surrounding to broaden the exposed area. In such case, channels and pillars would be formed at bigger width than planned, while holes would be narrower, and at its extreme, be completely absent. In addition, over-exposure does not cause a uniform widening, thus changing the slope of the wholes and so the shape of structures, as displayed in Figure 29.

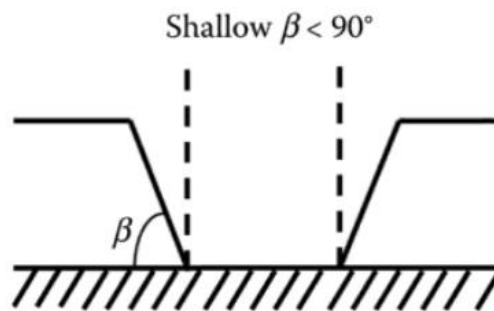


Figure 29-example of non-vertical walls due to high exposure dose [59]

Since the mold represents a negative of the structures of the final device, the obstacles present in the design correspond to holes in the mold and for this reason, over-exposure is vital to be avoided. Also under-exposition brings unwanted effect, as the PR may be not completely exposed up to its base, where the contact with the silicon is present, and thus be affected by undercuts (Figure 30), which may cause the mold to peel out from the silicon substrate during developing or PDMS device peeling.

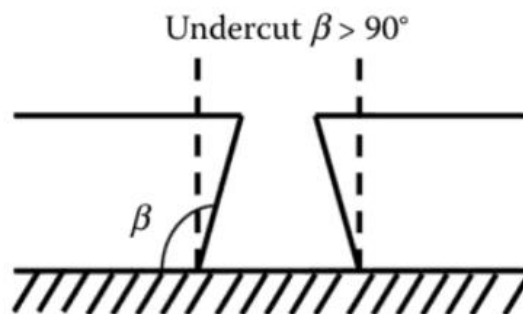


Figure 30-example of undercut in SU-8 due to low exposure dose [59]

Once the exposition is completed, the samples is set to rest for few minutes and then Post-Exposure Bake (PEB) can occur. This second baking process is essential in order to increase the cross-linking of the polymer in the exposed area and stabilize the pattern.

Once the substrate reaches room temperature again, the final step of the mold fabrication can take place; the areas of the polymer not exposed needs to be removed, a process called developing, similarly to the one achieved during hard mask production. The developer (PGMEA) is able to dissolve non-crosslinked photoresist and so reveal the pattern.

Before the use of the newly produced mold , an intermediate step can be added, namely silanization in FDTS, in order to obtain a reduction in the hydrophilicity of the SU-8 on Silicon substrate and help, in the following step, the peeling of the formed PDMS device, as well as a better definition of the smallest structures avoiding air bubble inclusion.

This step, indeed, was finally removed from the production process of the finalized device, as problem with device sealing emerged in late experiments; but it was still maintained when PDMS were produced only to be sacrificed to evaluate the performance in SU-8 mold production, and thus produce the images shown in section 4.3.

### 3.2.3. PDMS production

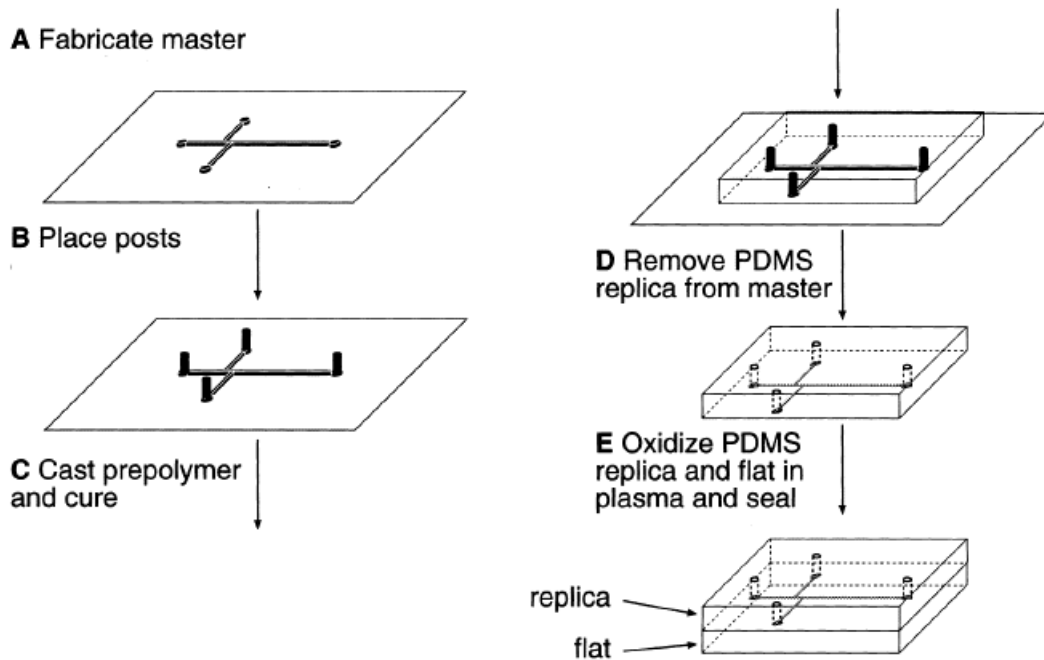


Figure 31 - General schema for PDMS production, adapted from [62]

PDMS fabrication is a straightforward procedure. Most delicate step is represented by device sealing against glass substrate.

To reach a satisfying sealing of the channels, a slab of glass is accurately cleaned and both substrate and PDMS are treated with oxygen plasma. Such treatment, in addition to furtherly remove any organic residue from the surfaces, induces the formation of SiOH groups in the PDMS which can react with other SiOH groups on glass surface and form Si-O-Si covalent bonding, thus forming a strong, irreversible connection between PDMS and substrate and isolate the channels.

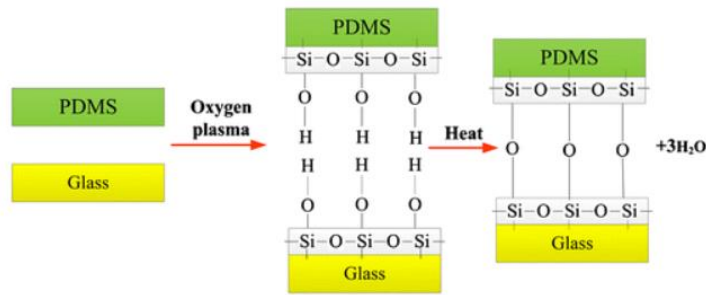


Figure 32- Oxygen plasma treatment for PDMS/glass sealing [63]

### 3.3. Cytometer output signal simulation

While the aim of the microfluidic device is to obtain a sufficient mixing of magnetic nanoparticles and sample containing target bacteria, favouring capture and retaining of the target and consequent elution in a reduced volume, this section addresses final step for the bacterial detection, through simulations of a magnetic cytometric platform output, if eluted volume would be measured. Figure 33 shows an example of detection event in a system with two magnetic sensors and displays the output of the platform.

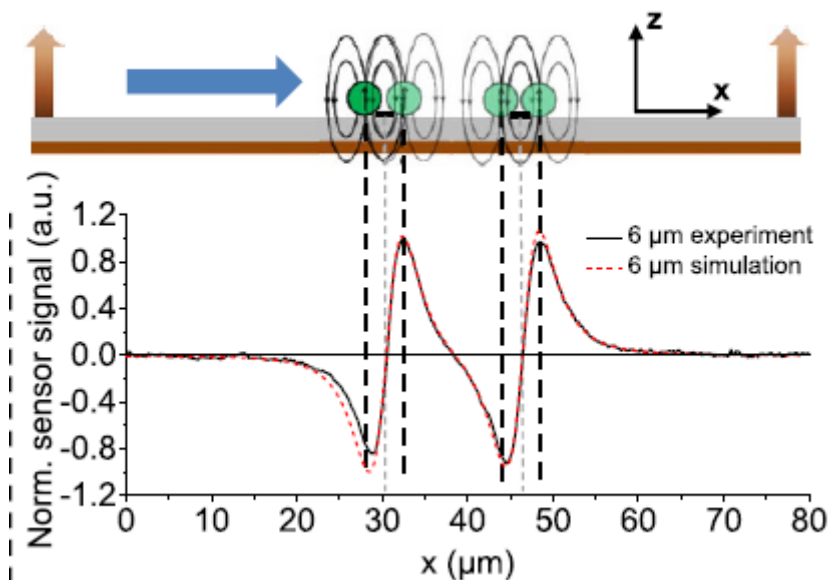


Figure 33-Magnetic fingerprint of a particle detected with sensors half-bridge configuration [28]

The detection, as explained in section 1.2.3, is given by the variation of the direction of the free layer of the magnetoresistive sensor which cause a change in resistance, read as a change in the voltage across the sensor. In order to be able to identify the signal correctly among the noise, and analyse its characteristics, a simulation of the expected sensor output is performed.

Matlab™ represents the optimal platform to develop such model, and so a simple code has been written. The above-mentioned script takes into account different factors, which are hard coded but can also be given as an input by the user:

- Sensor parameters as sensitivity, bias current and geometric factors
- Beads information as magnetic moment
- Beads dimensions and bacteria dimensions for coverage computation, or as an alternative, the already known coverage



- Flow rate of the solution
- Cross section of the channel
- Distance between bacteria centre and sensor surface
- Bacteria shape between spherical, spheroidal and rod-like, in case a tri-dimensional distribution of beads is wanted
- Number of bacteria passing on the sensor
- Alignment of bacteria along pre-defined X, Y or Z axis, if the number is major than one
- Distance between bacteria, if the number is major than one

Given all the parameters, the script will compute and print the graph of the resulting sensor perceived field and sensor output in volts. In addition, if a beads distribution is selected, the code will generate a graph showing such distribution.

Spherical distribution of beads is obtained according to Equation 14 and an example is displayed in Figure 34

$$P(d, \phi, \theta) = \left(\frac{d}{2}\right) * \sin(\phi) * \cos(\theta); \left(\frac{d}{2}\right) * \sin(\phi) * \sin(\theta); \left(\frac{d}{2}\right) * \cos(\phi); \quad (14)$$

Equation 14 - Spherical beads distribution

where  $\frac{180}{\sqrt{Nm+1}} < \phi < 180 - \frac{180}{\sqrt{Nm+1}}$  with a step of  $\frac{180}{\sqrt{Nm+1}}$ ;  $\frac{360}{\sqrt{Nm+1}} < \theta < 360 - \frac{360}{\sqrt{Nm+1}}$  with a step of  $\frac{360}{\sqrt{Nm+1}}$ , d equal to bacteria diameter and Nm to the number of beads.

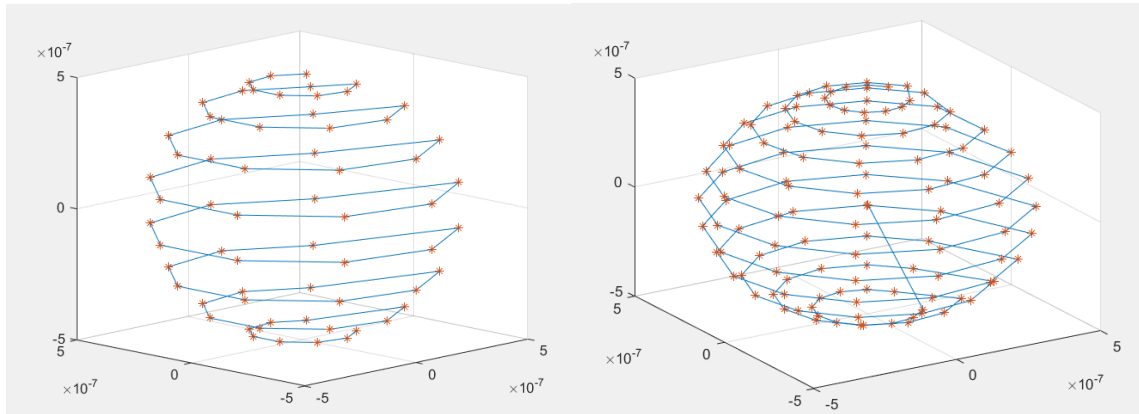


Figure 34- Example of spherical beads distribution: left, 64 beads; right, 128beads

Spheroidal distribution of beads obtained according to Equation 15 and an example is displayed in Figure 35

$$P(C, \phi, \zeta, \varepsilon) = C * \zeta * \varepsilon; C * \sqrt{(\zeta^2 - 1) * (1 - \varepsilon^2)} * \sin(\phi); C * \sqrt{(\zeta^2 - 1) * (1 - \varepsilon^2)} * \cos(\phi); \quad (15)$$

Equation 15 - Spheroidal beads distribution

where  $C = \sqrt{L1^2 - L2^2}$ ,  $\zeta = \cosh(\mu)$ ,  $\varepsilon = \cos(\theta)$ ,  $\frac{180}{\sqrt{Nm+1}} < \theta < 180 - \frac{180}{\sqrt{Nm+1}}$  with a step of  $\frac{180}{\sqrt{Nm+1}}$ ;  $\frac{360}{\sqrt{Nm+1}} < \phi < 360 - \frac{360}{\sqrt{Nm+1}}$  with a step of  $\frac{360}{\sqrt{Nm+1}}$ , L1 is the major semi-axis, L2 is the minor semi-axis,  $\mu$  is equal 1 and Nm is the number of beads.

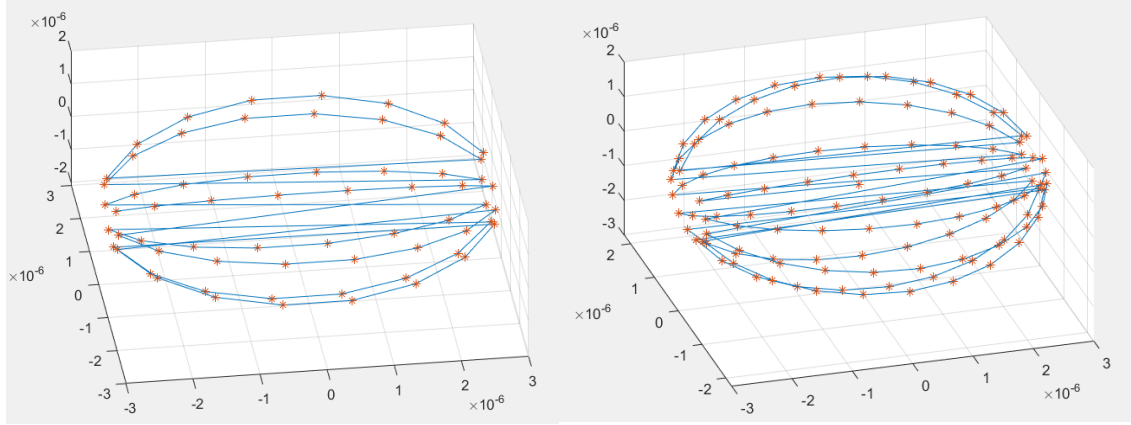


Figure 35 - Example of spheroidal beads distribution: left, 64 beads; right, 128 beads

Rod-like distribution of beads is obtained as a combination of a cylindrical distribution made by half of the beads number and two emi-spherical distribution at the sides, each one accounting for one fourth of the total number of beads.

Here are reported the three equations defining the distributions while an example is displayed in Figure 36

First Emi-sphere in Equation 16

$$P(d, L, \phi, \theta) = \left[ \left( \frac{d}{2} \right) * \sin(\phi) * \cos(\theta); \left( \frac{d}{2} \right) * \sin(\phi) * \sin(\theta) + \frac{L}{2}; \left( \frac{d}{2} \right) * \cos(\phi) \right]; \quad (16)$$

Equation 16 – Rod-like beads distribution, 1<sup>st</sup> emisphere

where  $\frac{180}{\sqrt{\frac{Nm}{4}+1}} < \phi < 180 - \frac{180}{\sqrt{\frac{Nm}{4}+1}}$  with a step of  $\frac{180}{\sqrt{\frac{Nm}{4}+1}}$ ,  $\frac{180}{\sqrt{\frac{Nm}{4}+1}} < \theta < 180 - \frac{180}{\sqrt{\frac{Nm}{4}+1}}$  with a step of  $\frac{180}{\sqrt{\frac{Nm}{4}+1}}$ , L equal to the length of the cylinder and d equal to the diameter of the cylinder

Cylindrical in Equation 17

$$P(d, H, \phi, \theta) = \left[ \left( \frac{d}{2} \right) * \sin(\phi) * \cos(\theta); \left( \frac{d}{2} \right) * \sin(\phi) * \sin(\theta) + H; \left( \frac{d}{2} \right) * \cos(\phi) \right]; \quad (17)$$

Equation 17 – Rod-like beads distribution, cylinder

where  $\theta=0, \frac{L}{2} + \frac{L}{\sqrt{\frac{Nm}{2}+1}} < H < \frac{L}{2} - \frac{L}{\sqrt{\frac{Nm}{2}+1}}$  with step equal to  $\frac{L}{\sqrt{\frac{Nm}{2}+1}}$ ,  $0 < \phi < 360 - \frac{360}{\sqrt{\frac{Nm}{2}+1}}$  with step equal to  $\frac{360}{\sqrt{\frac{Nm}{2}+1}}$ , L equal to the length of the cylinder, d equal to the diameter of the cylinder.

Second Emi-sphere in Equation 18

$$P(d, L, \phi, \theta) = \left[ \left( \frac{d}{2} \right) * \sin(\phi) * \cos(\theta); \left( \frac{d}{2} \right) * \sin(\phi) * \sin(\theta) - \frac{L}{2}; \left( \frac{d}{2} \right) * \cos(\phi) \right]; \quad (18)$$

Equation 18 – Rod-like beads distribution, 2<sup>nd</sup> cylinder

where  $\frac{180}{\sqrt{\frac{Nm}{4}+1}} < \phi < 180 - \frac{180}{\sqrt{\frac{Nm}{4}+1}}$  with a step of  $\frac{180}{\sqrt{\frac{Nm}{4}+1}}$ ,  $180 < \theta < 360 - \frac{180}{\sqrt{\frac{Nm}{4}+1}}$  with a step of  $\frac{180}{\sqrt{\frac{Nm}{4}+1}}$ , L equal to the length of the cylinder and d equal to the diameter of the cylinder

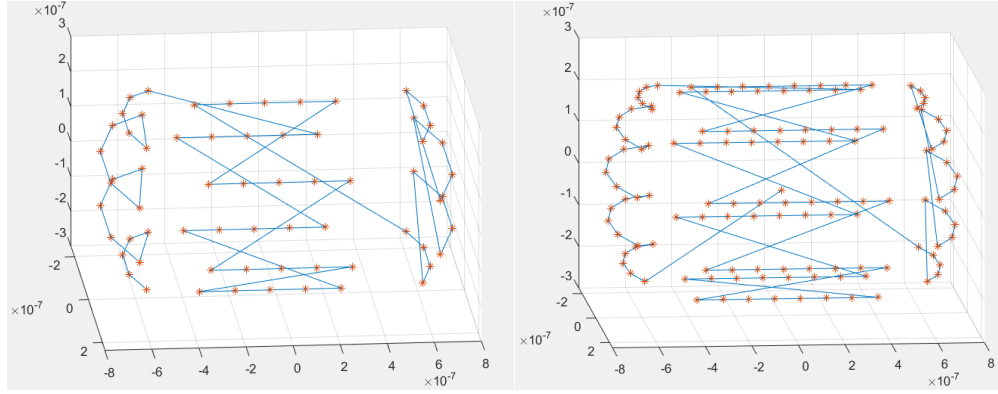


Figure 36 – Example of rod-like beads distribution: left, 64 beads; right:128 beads

The number of beads covering each bacteria, also defined *coverage* (Equation 19), can be supplied to the code directly, or its computed through the dimensions of beads and bacteria as user input; the simple calculation takes into consideration the available bacteria surface respect to the surface occupied by a bead, equal to its larger section, where both are assumed having a spherical shape:

$$Coverage = \frac{(4 * \pi * (R_{bact})^2)}{\pi * (R_{bead})^2}; \quad (19)$$

Equation 19 – Bacteria coverage

This parameter, directly affects the output of the sensor, being directly proportional to the number beads.

The field produced by the superparamagnetic particles is, in fact, regulated by equations Equation 9 and Equation 10 , where beads are assumed being magnetic dipoles of one dimension, as described in section 1.2.3.

Where the first represents the three- dimensional field produced, while the second refers to the sole projection on the sensor axis, the only one that the sensor is sensitive to. The voltage output of the sensor is instead characterized by Equation 11, again in section 1.2.3.

Other parameters like flowrate and microfluidic channel cross-section, are also involved in the computation of the voltage output of the sensor; Through such information, in fact, the mean speed of bacteria covered by beads can be assessed(Equation 20), and so the spatial reference of the signal can be converted into a temporal reference(Equation 21)

$$v = \frac{Q}{S}; \quad (20)$$

Equation 20- Mean velocity of fluid in the channel

where v is the mean speed of the fluid in the channel, equal to the speed of the particles, and Q and S represent respectively the flow rate and the cross section.

$$\Delta t = \frac{\Delta x}{v}; \quad (21)$$

Equation 21- Time to space relationship

where t represents time, x distance and v the speed of the particles

Outputs from the simulation are shown in Figure 37, where inserted parameters are displayed to the user, and in Figure 38 where one example of simulated signal is reported.

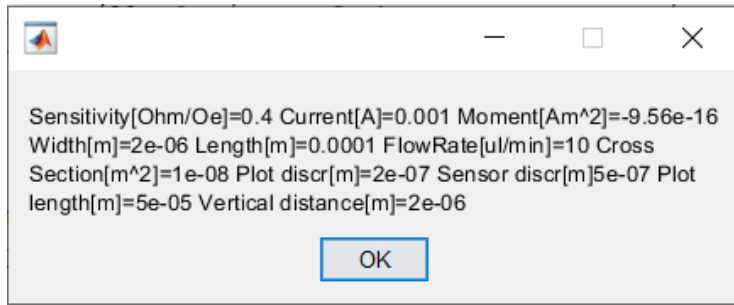


Figure 37 - Matlab output window for set parameters

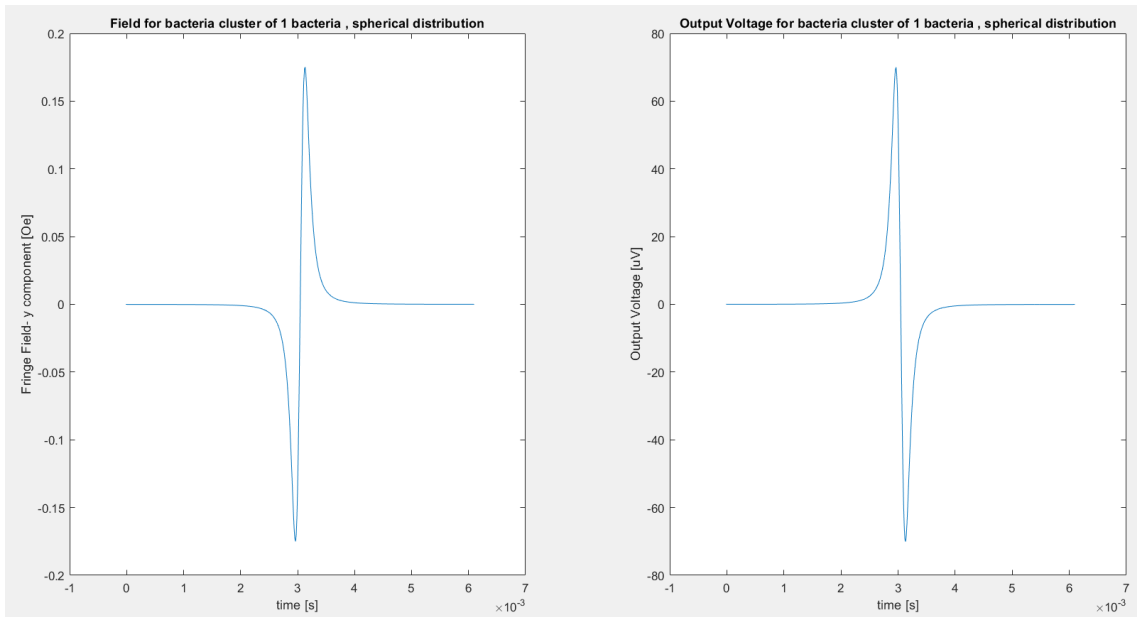


Figure 38 - Fringe field and corresponding sensor output for a spherical distribution of beads on single bacteria with a coverage equal to 64 beads, other parameters as shown in Figure 37

Some parameters are then extracted from the signal (Figure 39) and displayed (Figure 40) Peak-to-peak amplitude is dependent on factors as the number of particles aggregated (around a bacteria or clustered) and the vertical distance of the detected element from the sensor, while peak-to-peak time interval is related to the dimension of the element [4].

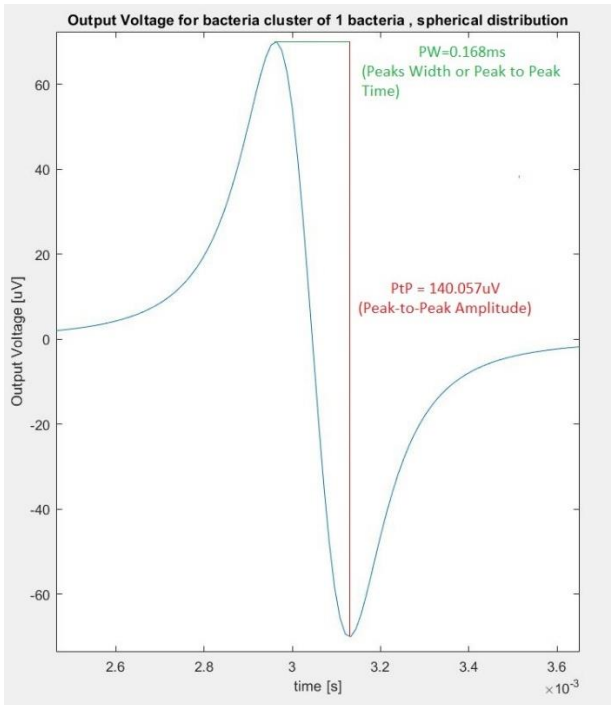


Figure 39- PtP and PW parameters for the example signal presented in Figure 38

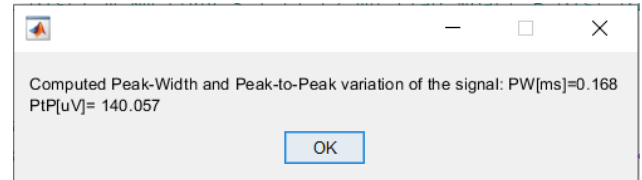


Figure 40-Code output for extracted parameters

### 3.4. Sample detection in a magnetic cytometric platform

This section is to be seen as a reconnection with the statement produced in section 1.1, where the aim of the project where this work is inserted has been discussed. Devices and protocols here developed are in fact preparative to supply a concentrated sample of “magnetized” target bacteria (to be read as bacteria surrounded by magnetic elements) and for this reason some of the parameters were adapted to this aim.

To evaluate if the goal has been reached, few samples treated with the microfluidic device has been evaluated through a magnetic cytometric platform, under development at INESC-MN by Soares et al [4] [5].

The sensing component of the cytometer are several sensors and two of them can be used for a single measurement. The one exploited for the measurement reported in section 5.2 are  $100 \times 2 \mu\text{m}^2$  SV sensors (see section 1.2.3) separated by  $237 \mu\text{m}$  and the dimension of the microfluidic component concerning its cross-section is  $100 \times 10 \mu\text{m}^2$ .

Figure 41 presents a top view of both elements. The protocol applied for the detection is briefly discussed in section 2.2.7.

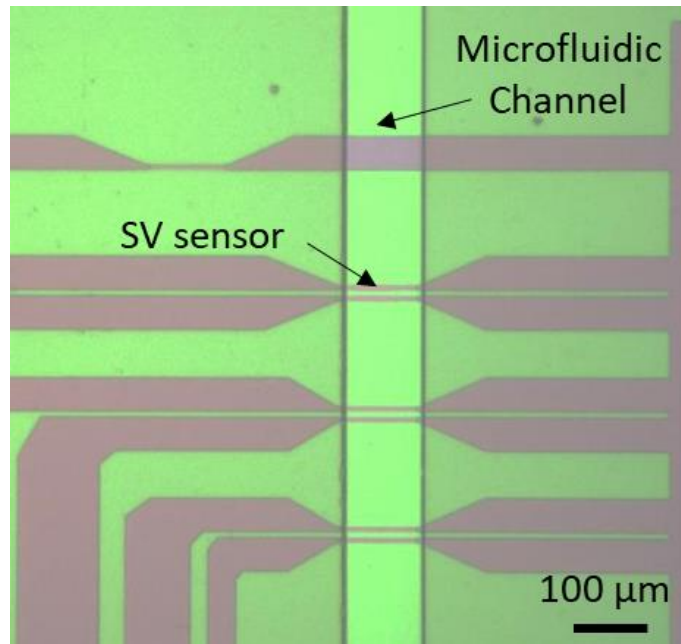


Figure 41- Top view of sensor and microfluidic from cytometric platform [4]

Once the signal from the sensor is recorded, some processing is required; this step includes, but it is not limited to, application of a bandpass filter to reduce noise contribution. After processing, peak detection is performed, in order to identify bipolar peaks that are related to bacteria surrounded by particles. This step is based on the application of two thresholds, one in signal amplitude and one in time interval between peaks detected by the two sensors. Amplitude threshold is imposed depending on the detected signal from blank sample (see section 2.2.7), while time interval threshold is chosen with some considerations on sensors distance and particle speed, dependent on applied flow rate; specifically, an event, defined as a bacteria covered with particles flowing over the sensors, is selected only if peak amplitude is higher than amplitude threshold, and if two events are recorded in the two sensors with a time delay equal to the speed of the particle multiplied by sensor distance. Particle speed is assumed to be in a range of values around the mean flow velocity of the fluid in the channel, equal to imposed flow rate divided by channel cross-section.

Automatically detected events are lately manually evaluated, to discard events that are not in accordance with the expected bipolar shape of the signal provoked by a superparamagnetic particle covered bacteria, as simulated in section 3.3.

Once events are verified, peak-to-peak voltage and peak-to-peak time interval are extracted and stored; these are generally furtherly analysed in the attempt to distinguish between events rising from bacteria covered with magnetic particles and events coming from particles clusters, but this aspect is not covered in this work.

## 4. Results

### 4.1. Benchtop optimization for antibody immobilization and bacteria capture

Numerous experiments have been performed, following protocol discussed in section 2.2.1 and 2.2.3, involving antibodies immobilization on superparamagnetic beads and their exploitation for bacteria capture. Here optimization and results are reported for different parameters, while Figure 42 represents protocol steps.

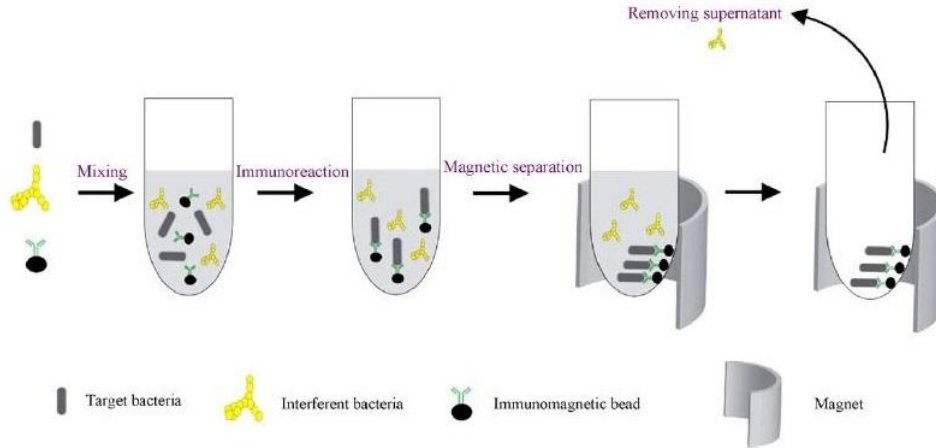


Figure 42- Benchtop protocol schematics, only first washing step is represented, adapted from [64]

#### Ratio between antibodies and beads during antibodies immobilization

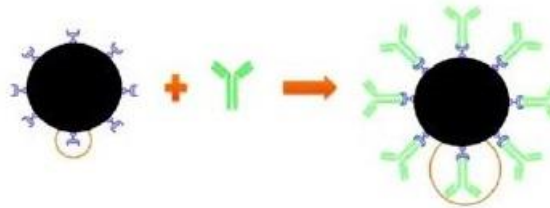


Figure 43- Superparamagnetic beads covered with antibodies, adapted from [64]

First step of the benchtop protocol is immobilization of antibodies on magnetic particles, as shown in the schematics in Figure 43.

As initial approach the ratio antibody:beads was set to 3925:1, which is 3925 antibodies per beads, according to the following calculation:

$$Coverage = \frac{4*\pi*(R_{bead})^2}{[(L_{Ab})^2+(L_{Ab}*H_{Ab})]/2} \approx 3925; \quad (22)$$

Equation 22 – Antibodies to bead ratio based on geometrical parameters

where  $R_{beads}$  is bead radius,  $L_{Ab}$  is antibody length and  $H_{Ab}$  is antibody height. Here beads are treated as spheres of 200nm of diameter while an antibody as a parallelepiped 15 nm long and 5nm wide and assuming two possible configurations in which the antibody can link to the bead, horizontal and vertical, and thus considering the mean of the two possible occupied surfaces in the two configurations. With the aim to increase interactions a number of antibodies 10 times higher than the full coverage was chosen as approximately  $10^4$  antibodies per beads, in order to take into account possible phenomena of aggregation or non-efficient orientation.

This method, though, overestimate the amount of antibodies that can interact with the beads, and after few experiments, in order to consume a minor amount of antibodies and avoid expenses, a different approach have been applied. To evaluate the maximum number of antibodies that a bead

could interact with, the number of active sites is considered. Streptavidin is a protein which presents 4 active site useful for biotin interaction as it is constituted in a tetramer, so 4 biotinylated antibodies per streptavidin may be considered;

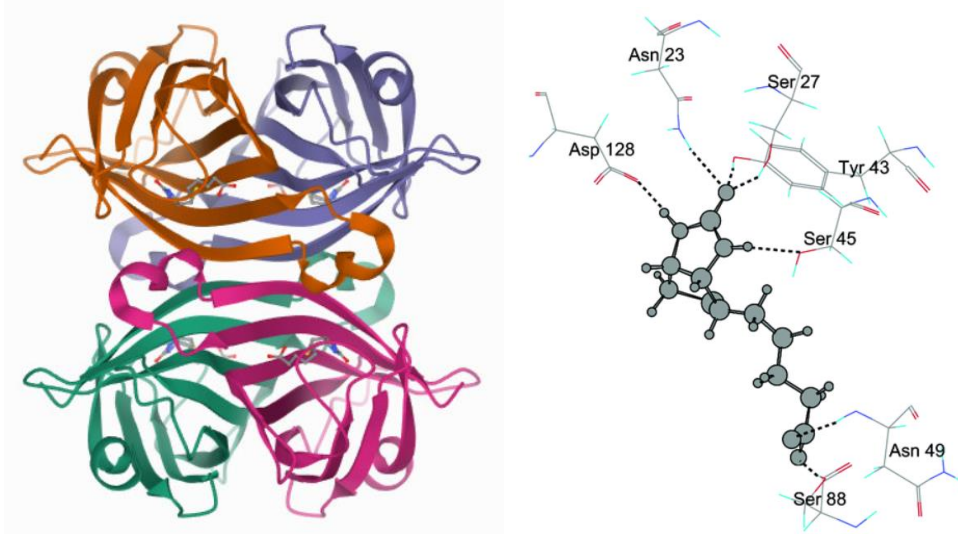


Figure 44 - Streptavidin/Biotin interaction: left, tetrameric streptavidin structure [65]; right, active site and evidenced hydrogen bonds [66]

Nonetheless such active sites are spatially close to each other so it is assumed that when one site is occupied in interaction with one biotin molecule, another site is shielded by antibody presence, not allowing a further biotinylated antibody to interact. For this reason, 2 antibodies per streptavidin molecule are assumed as maximum interacting elements. Knowing from the supplier the average number of streptavidin molecules per beads, the calculation of number of needed antibodies to fully load the binding sites is then straightforward:

$$Coverage = (2 * 500) sites/beads = 1000 Abs/bead; \quad (23)$$

Equation 23 - Antibodies to bead ratio based on number of available interaction sites

where 2 are the available active sites.

Approximatively 4 times the coverage was chosen as acceptable antibodies number, setting 4210:1, or 4210 antibodies per bead, as the optimal ratio, due to rounding useful when choosing the volume of antibodies to use. Table 4 shows how such modified ratio is linked to an increased capture for the positive sample (where antibodies where target specific) from ~9% to >30% depending on the other parameters.



### Ratio between beads and bacteria for bacteria capture

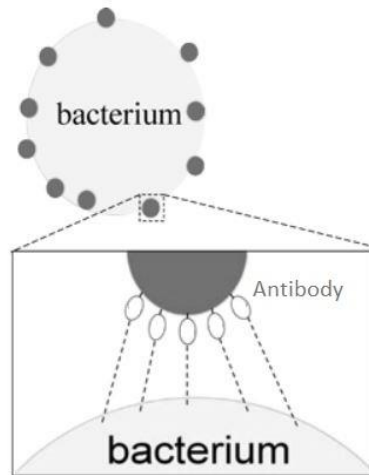


Figure 45- Bacteria surrounded by magnetic beads, adapted from [67]

In the first experiment the ratio between beads and bacteria was set as 4:1, but it appeared that such small amount of particles was not sufficient to retain bacteria efficiently after their recognition from the antibodies, as shown in Table 4 where the capture efficiency obtained is <14% for the positive sample.

It was decided then to compute the amount of beads needed to cover the entire surface of the cell with beads, and maximize magnetic forces acting on them, as well as the global magnetic moment for further magnetic detection; some simplification are used for such computation, considering the bacteria as a sphere of 1 $\mu$ m diameter and beads all equal spheres of 200nm diameter, which leads to a maximum number of beads as indicated by Equation 24

$$Coverage = \frac{(4*\pi*(R_{bact})^2)}{\pi*(R_{bead})^2} \approx 64; \quad (24)$$

Equation 24 – Coverage

where  $R_{bact}$  and  $R_{bead}$  are respectively the radius of the bacteria and the radius of the bead.

To promote interactions and increase coverage avoiding unspecific binding 10 times more beads than the amount calculated to be accommodated have been chosen for the subsequent experiments, as not all beads would be able to enter in contact with bacteria in the right conditions and clusters of beads may also form, assessing the ratio to 640:1 (results not shown for this ratio). After increasing such ratio up to 1900:1 trying evidencing further improvements, the optimal value was established as 950:1; Table 4 shows how 1900:1 ratio achieved capture up to ~62%, but 950:1 ratio reached equal or higher capture efficiencies, up to ~97%, with the further advantage of requiring less particles.

### Negative control

Setting the adequate negative control for an experiment is always a central challenge and a factor that can influence the importance of the results. Regarding bacteria capture with active components immobilized on beads (antibodies in this case), different negative sample have been considered along the experimentation:

- Bare beads: this sample do not represent an optimal negative control as the conditions at which bacteria can interact with them are different if considering covered beads, as for the distance of interaction, for the chemistry of such interaction and the lack of steric impediments. This control was indeed interesting to evaluate the interactions that occur between bacteria and

beads, in absence of antibodies, and so give an idea of the unspecific capture that beads can bring, giving important information on the need of a blocking step in the procedure

- Non-biotinylated antibodies: using non biotinylated antibodies could be useful to evaluate non-specific adsorption of antibodies to the beads. If the antibodies are non-specific for the bacteria, as in the case, they also play the role of a blocking step regarding beads exposed sites. This control has been useful in the first experiments to evaluate how aspecifically adsorbed antibodies interacts with the target
- Biotinylated antibody specific for a different bacteria: one of the efficient negative control is represented by the use of an antibody which is biotinylated, able then to interact efficiently with streptavidin molecules on beads but specific for a bacteria different from the target. In this way, aspecific capture are less connected to interaction with beads or antibody non-active site, and should be very low, outlining a difference with the test sample if capture is correctly achieved.
- Antibody target specific with a different bacteria: another efficient way to verify specificity and so design a proficient negative control is the use of a second bacteria, different from the target, and verify that the antibody specific for the target is not able to recognise it, and thus the related capture should result low.

The last two controls, applied in the experiments shown in Table 4 alternatively, represent the optimal way to perform a negative control and verify specificity of the capture, in the case it occurs in the test sample.

#### Blocking

Blocking evidenced to be a fundamental step to achieve specific capture and guarantee reproducibility of results; even though streptavidin molecules have high affinity with biotin molecules present on used antibodies, not only the active site represent a place where interactions can occur. The remaining structure of the protein as well as the bead surface are both able to interact with bacteria, in an aspecific manner. What is more, even working in condition of high antibody concentration (10 times the computed coverage), some streptavidin molecules are still not covered with antibodies and are prone to interact with bacteria as well. For all this reasons, a standard blocking solution was introduced, namely a 5% (w/v) BSA (Bovine Serum Albumin) in PB. This approach resulted in expected improvements as decreasing aspecific capture, but showed some inconsistency in different experiments, as it can be deduced from Table 4 if comparing capture efficiency in the negative control between experiment 1 (~0.2%) and experiment 2 and 3(~5%). For this reason, a different blocking agent have also been tested, namely SuperBlock™, containing a single purified glycoprotein. The results from the two blocking solutions did not differ consistently, and could be sometime detrimental, as in experiment 4 in Table 4, where capture in negative control reached ~16%; thus the blocking protocol was altered. From a 30 min blocking time, to 1 hours and finally 1 hour blocking at high concentration plus overnight blocking at low concentration, while the volume used was increased from 100µl to 300µl, which resulted in acceptable results, and were set as optimal conditions, together with an agitation of 250rpm, ensuring a low capture in the negative control down to ~1% without affecting positive sample capture efficiency, attested in experiment 7 at ~70%, up to ~96% in experiment 5, as demonstrated in Table 4. Temperature, varied between room temperature and 37° Celsius, did not affect the blocking efficiency; in fact at both temperatures a capture for negative control as low as ~5% was obtained.

#### Parameters during immobilization

Parameters to be taken into account during the immobilization step are: time, temperature and agitation. The time advised by the bead supplier is 30 minutes, which have been increased in later experiments to 2 hours; such time have been demonstrated sufficient for immobilization, and under this condition the highest capture efficiency have been obtained, up to ~97% as shown in Table 4. Both RT and incubation at 37° Celsius have been verified, with no important differences evidenced, as even if in experiment 1 and 4 (T=RT) capture efficiencies are lower than experiment 2 and 3(T=37°C), experiments 5,6 and 7(T=RT) reach higher capture efficiencies, indicating that temperature at 37°C is not a requirement. Agitation at 250rpm is once again introduced, which emerged to not prevent antibody and bead interaction while may decrease the rate of aspecific interactions, interfering in weak interactions.

#### Parameters during capture

Parameters involved in the capture step are: time, temperature and agitation, volume of bacteria and concentration of bacteria. Capture time have been modified from 30 minutes, as advised by beads supplier, to 15 minutes, and given higher capture efficiency (up to ~97%) for positive sample obtained in last experiments described in Table 4, such time is verified as sufficient. Temperature was varied between 37° to room temperature, to avoid bacteria growth during capture, even if experiment 1 in Table 4 show similar capture efficiencies, even though an increase in data dispersion, given by a higher standard deviation, is evidenced for the higher temperature. Agitation was also introduced in latest experiments, at 250rpm, with positive results (see difference between experiment 4 and 5, Table 4). The volume used is chosen to be comparable with predicted to be used in the microfluidic platform, derivative of the volume needed to resuspend on hospital swab, as verified with clinical samples processed in the laboratory. A volume of 100µl has been used, for a directly comparison with the volume chosen in the microfluidic platform for the initial tests. Finally, regarding the concentration of bacterial sample, the parameters is not supposed to undergo optimization as it is fixed by the study, depending on the concentration expected in the swab from clinical samples, discussed in section 4.4. Nonetheless, two concentrations have been tested in the context of preliminary experiments in capture, equal to  $2 \cdot 10^7$  CFU/ml and  $2 \cdot 10^5$  CFU/ml, obtained as 1/10 serial dilution from a  $2 \cdot 10^8$  CFU/ml inoculum, as explained in section 2.2.2.

Table 4-Parameters and results of a series of experiment on antibody immobilization and bacteria capture by bench-top assay. In red: parameters that change compared to previous experiment. Legend below

Experiment	1				2		3		
Sample	P	P	N	N	P	N	P	N	
Bacteria	P.ae	P.ae	Kleb	Kleb	P.ae	Kleb	P.ae	Kleb	
Antibody	P.ae	P.ae	P.ae	P.ae	P.ae	P.ae	P.ae	P.ae	
Beads:bacteria	4:1	4:1	4:1	4:1	1900:1	1900:1	1900:1	1900:1	
Antibodies:beads	39250:1	39250:1	39250:1	39250:1	4210:1	4210:1	4210:1	4210:1	
Antibody immobilization	Time(min)	30	30	30	30	30	30	30	
	Temperature(°C)	RT	RT	RT	RT	37	37	37	
	Agitation(rpm)	250	250	250	250	250	250	250	
Blocking	Type	BSA5%	BSA5%	BSA5%	BSA5%	BSA5%	BSA5%	BSA5%	
	Volume(μl)	100	100	100	100	100	100	100	
	Time(min)	30	30	30	30	30	30	30	
	Temperature(°C)	37	37	37	37	37	37	37	
	Agitation(rpm)	250	250	250	250	250	250	250	
Bacteria capture	Time(min)	30	30	30	30	30	30	30	
	Temperature(°C)	37	RT	37	RT	RT	RT	RT	
	Agitation(rpm)	none	none	none	none	none	none	none	
	Bacterial concentration (CFU/ml)	2*10 <sup>5</sup>	2*10 <sup>5</sup>	2*10 <sup>5</sup>	2*10 <sup>5</sup>	2*10 <sup>7</sup>	2*10 <sup>7</sup>	2*10 <sup>7</sup>	2*10 <sup>7</sup>
	Mean capture %	13.15	7.6	0.23	0.15	37.39	5.77	62.09	5.05
	SD %	10.43	0.94	0.05	0.19	11.4	0.29	0.32	0.54

Experiment	4		5		6		7	
Sample	P	N	P	N	P	N	P	N
Bacteria	P.ae	P.ae	Kleb	Kleb	Kleb	Kleb	Kleb	Kleb
Antibody	P.ae	E.Coli	Kleb	E.Coli	Kleb	E.coli	Kleb	E.coli
Beads:bacteria	950:1	950:1	950:1	950:1	950:1	950:1	950:1	950:1
Antibodies:beads	4210:1	4210:1	4210:1	4210:1	4210:1	4210:1	4210:1	4210:1
Time(min)	120	120	120	120	120	120	120	120

Antibody immobilization	Temperature(°C)	RT		RT	RT	RT	RT	RT	RT	RT							
	Agitation(rpm)	250		250	250	250	250	250	250	250							
Blocking	Type	SB		SB	SB	SB	SB	SB	SB	SB							
	Volume(µl)	100		300+100	300+100	300+100	300+100	300+100	300+100	300+100							
	Time(min)	30		60 + Overnight	60 + Overnight	60 + Overnight	60 + Overnight	60 + Overnight	60 + Overnight	60 + Overnight							
	Temperature(°C)	RT		RT	RT	RT	RT	RT	RT	RT							
	Agitation(rpm)	250		250	250	250	250	250	250	250							
Bacteria capture	Time(min)	15		15	15	15	15	15	15	15							
	Temperature(°C)	RT		RT	RT	RT	RT	RT	RT	RT							
	Agitation(rpm)	none		250	250	250	250	250	250	250							
	Bacterial concentration [CFU/ml]	2*10 <sup>7</sup>	2*10 <sup>5</sup>	2*10 <sup>7</sup>	2*10 <sup>5</sup>	2*10 <sup>7</sup>	2*10 <sup>5</sup>	2*10 <sup>7</sup>	2*10 <sup>5</sup>	2*10 <sup>7</sup>	2*10 <sup>5</sup>	2*10 <sup>7</sup>	2*10 <sup>5</sup>	2*10 <sup>7</sup>	2*10 <sup>5</sup>	2*10 <sup>7</sup>	2*10 <sup>5</sup>
	Mean capture %	19.18	36.66	16.12	15.28	90.43	96.69	2.04	8.17	89.58	85.15	2.72	2.93	52.9	70.97	1.02	1.6
	SD %	2.41	20.76	0.87	1.01	2.1	1.24	0.27	0.26	0.79	2.87	0.57	1.55	1.84	4.32	0.39	0.44

Legend:

**P:** Positive sample, combination of a target bacteria and particles covered with antibodies specific for the target

**N:** Negative sample, combination of a bacteria and particles covered with antibodies non-specific for the bacteria

**P.ae:** *Pseudomonas aeruginosa*

**Kleb:** *Klebsiella pneumoniae*

**BSA5%:** 5% v/v BS solution in DI water

**SB:** SuperBlock™

### Target bacteria

As for the concentration of bacteria used, also the bacteria target chosen is not supposed to be a factor that can be optimized as it is a requirement of the project. Nonetheless, since the aim of the study is to prove capture of gram negative bacteria, due to limitation in the method to verify capture results, namely Colony Counts, some bacteria results as better samples than others. In fact *Klebsiella pneumoniae* produced colonies that are more easily counted, producing a lower dispersion in the data due to error counting; thus in last experiments it became preferable operating on such bacteria, compared to *Pseudomonas aeruginosa* colonies.

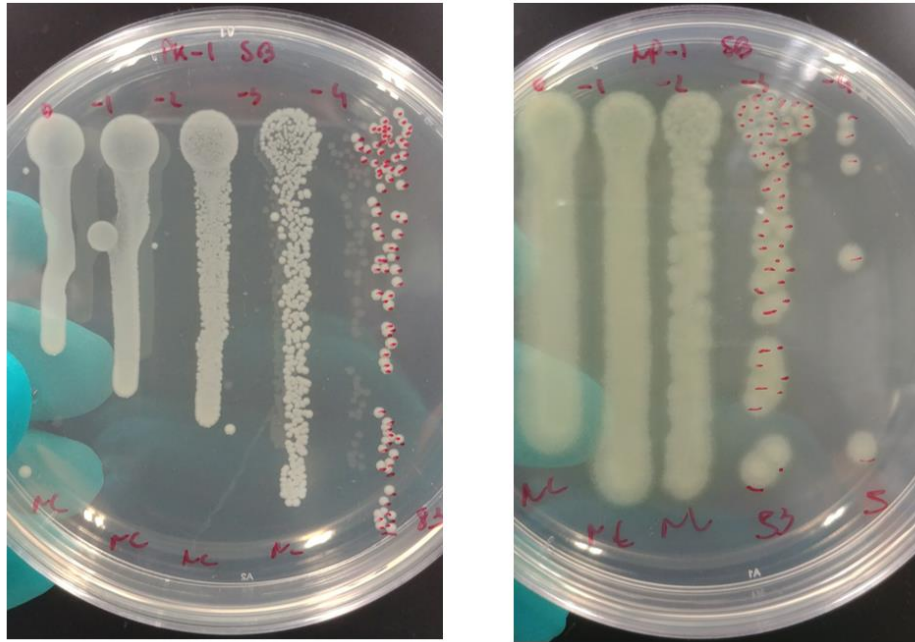


Figure 46- Example of bacteria CFU counting: left, *Klebsiella pneumoniae*; right: *Pseudomonas aeruginosa*

Optimal parameters thus resulted to be:

Table 5- Optimized bench parameters for bacteria capture (on samples of 100µl); o/n refers to overnight.

Parameter	Optimized values		
Beads:bacteria ratio	>950:1		
Antibodies:bead ratio	4210:1		
Immobilization	2h	250rpm	RT
Blocking	300µl for 1h	250 rpm	RT
	100µl o/n		
Capture(100µl)	15min	250rpm	RT

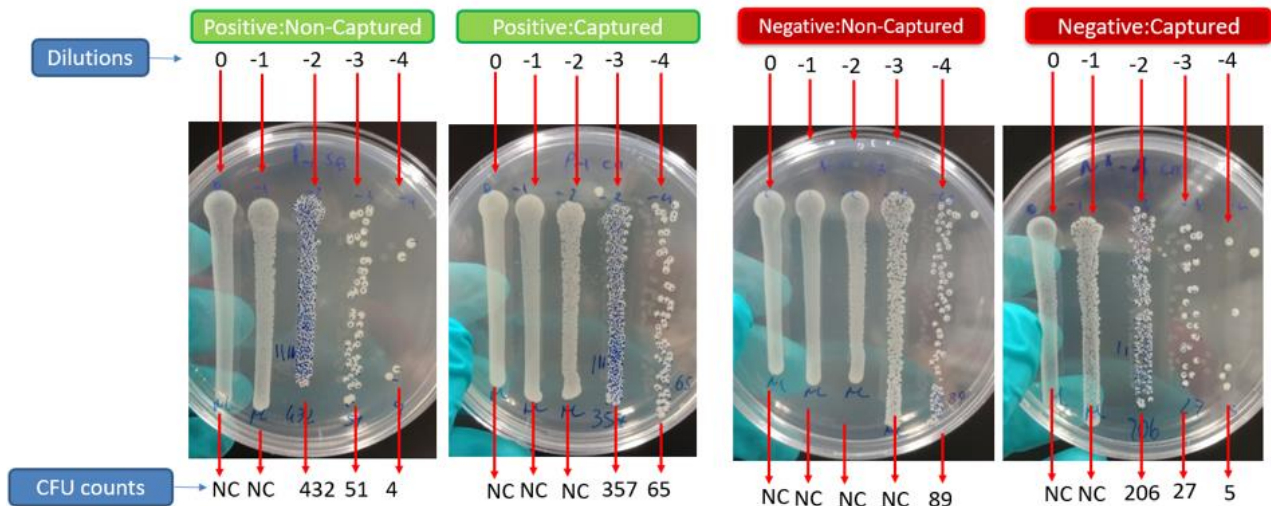


Figure 47 - Example of bench protocol optimized: comparison between specific (positive) and aspecific (negative) antibody for *Klebsiella pneumoniae* capture at -1 dilution ( $10^7$  CFU/ml); NC refers to Non Countable.

### Results analysis

Results are represented by Colonies Counts of different supernatants, called SB, WI and WII respectively indicating the first, second and third supernatants during washes, and the resuspended pellet, called CM. Such values are processed through an Excel spreadsheet, and displayed in a column graph.

#### Individualization and exclusion of outliers

Independent and dependent replicas are produced during the experiments.

Independent replicas refer to results of different experiments while dependent replicas are of two kind:

- Triplicates or duplicates in plating supernatants or resuspend pellet solution
- Different dilutions of the supernatants or resuspended pellet solution

Where triplicates were available, dependent replicas within a single experiment are evaluated with the aim to identify outliers, which are then discarded from the computation of capture efficiency as non representative of the result.

In between different methods for outliers identification, the interquartile one have been chosen. The first quartile of a set of ascending ordered data is represented by the data below which 25% of data are present; if the number of data is odd, the arithmetic mean of the two closest number is made. By extension, the third quartile is the data below which 75% of data are present, with the application of the arithmetic mean once again in the case of an odd number of data.

With the interquartile method, the difference between the third and first quartile is computed, multiplied by 1.5 (for mild outliers) and by 3.0 (for extreme outliers) and finally added to the 3<sup>rd</sup> quartile and subtracted by the 1<sup>st</sup> quartile; this generates two intervals, out of which mild or extreme outliers are identified. Table 6 reports an example of the process.

After outliers are identified, if any, and discarded, capture efficiency is computed with average of remaining dependent replicas.

Efficiencies between independent replicas are then averaged and standard deviation is computed.

Table 6- Example of identification of outliers with quartile method: data on Wash I (WI) sample from -3 dilution *Klebsiella pneumoniae* specific capture

Measurements	Ordered measurements	Quartiles	Mild outlier	Extreme outlier
5.40E+03	4.90E+03	<b>1st quartile =</b> 5.00E+03	NO	NO
7.00E+03	4.90E+03	<b>3rd quartile =</b> 1.00E+04	NO	NO
1.00E+04	5.00E+03	<b>Interquartile =</b> 5.00E+03	NO	NO
1.00E+05	5.40E+03	<b>Interquartile*1.5=</b> 7.50E+03	NO	NO
4.90E+03	6.00E+03	<b>Interquartile*1.5=</b> -2.50E+03 <b>&lt; Range mild outliers &lt;</b> 1.75E+04	NO	NO
5.00E+03	7.00E+03	<b>Interquartile*3=</b> 1.50E+04	NO	NO
4.90E+03	1.00E+04	<b>Interquartile*3=</b> -1.00E+04 <b>&lt; Range extreme outliers &lt;</b> 2.50E+04	NO	NO
6.00E+03	2.00E+04		YES	NO
2.00E+04	1.00E+05		YES	NO

#### Calculation of capture efficiencies

Considering the method used to collect results of the capture, different computation of the capture efficiency can be evaluated. The supernatants collected during the washing steps are named SB, WI and WII respectively, the resuspended final pellet it is named CM while the initial amount of bacteria plated from the diluted second inoculum are referred as *Initial* (refer to section 2.2.3 for the protocol)

Two approaches are based on considering the initial amount of bacteria present before the capture. This is obtained by plating the inoculum and its dilutions, from which the sample of bacteria



for the capture is taken, assuming the experiment last shortly enough so that the concentration of bacteria in that samples do not vary consistently, considering a working temperature which is Room Temperature and so close to 25°C and far from 37°C which is the optimal growing condition for bacteria.

Knowing the number of initial bacteria, then, two computation are possible: it can be computed the ratio between the bacteria in the resuspended pellet and the initial concentration (Equation 25); this approach is limited by the fact that the bacteria in the resuspended beads are surrounded by magnetic beads, used to separate them, and so influenced by it. It must be considered that the Colony Counting method is based on the ability of the bacteria to replicate in a limited area and if the presence of magnetic beads limit this aspect, the number of captured bacteria may be under evaluated.

$$Capture(\%) = \frac{CM}{Initial} * 100; \quad (25)$$

*Equation 25 – Percentage of capture, first method*

where CM is resuspended pellet and *Initial* is plated from diluted second inoculum.

Alternatively, it can be computed as the difference of colonies in all supernatants and colonies in the *Initial* divided by colonies in the *Initial* (Equation 26). In this way, it is assumed that all the bacteria that is missing in the supernatant must be present in the pellet. The limitation of this approach is represented by the step of summing the counts of different supernatants, thus amplifying the counting errors.

$$Capture(\%) = \frac{(Initial - SB + WI + WII)}{Initial} * 100; \quad (26)$$

*Equation 26 – Percentage of capture, second method*

where SB, WI and WII are supernatants from sequential washing step respectively and *Initial* is plated from diluted second inoculum.

Both these methods are anyway limited by the non correct evaluation of the initial amount of bacteria. The assumption of non-growth during experiment (or equal growth as in the other samples) is not precise and provokes errors in the evaluation of the initial concentration. This is outlined by experiments in which the amount of bacteria captured appeared higher than the initial amount due to a wrong evaluation of initial amount (results not shown).

A third method of evaluation of capture consists in a different evaluation of the initial amount of bacteria, as applied by Skjerve et al. [68]; such concentration is in fact evaluated as the sum of all supernatants and of the resuspended pellet counts. The efficiency in capture is then computed as colonies in the resuspended pellet divided by such alternative initial concentration (Equation 27).

$$Capture(\%) = \frac{CM}{SB + WI + WII + CM} * 100; \quad (27)$$

*Equation 27 – Percentage of capture, third method*

where CM is the resuspended pellet and SB, WI and WII are supernatants from sequential washing steps respectively.

Table 7- Mean results from bench experiments, refer to appendix 7.2 for complete results

Sample	Dilution	Concentration[CFU/ml]	Mean %	SD %
Positive	-1 dil	$2 \cdot 10^7$	65.85	21.01
	-3 dil	$2 \cdot 10^5$	85.66	10.23
Negative	-1 dil	$2 \cdot 10^7$	1.65	0.74
	-3 dil	$2 \cdot 10^5$	4.03	2.59

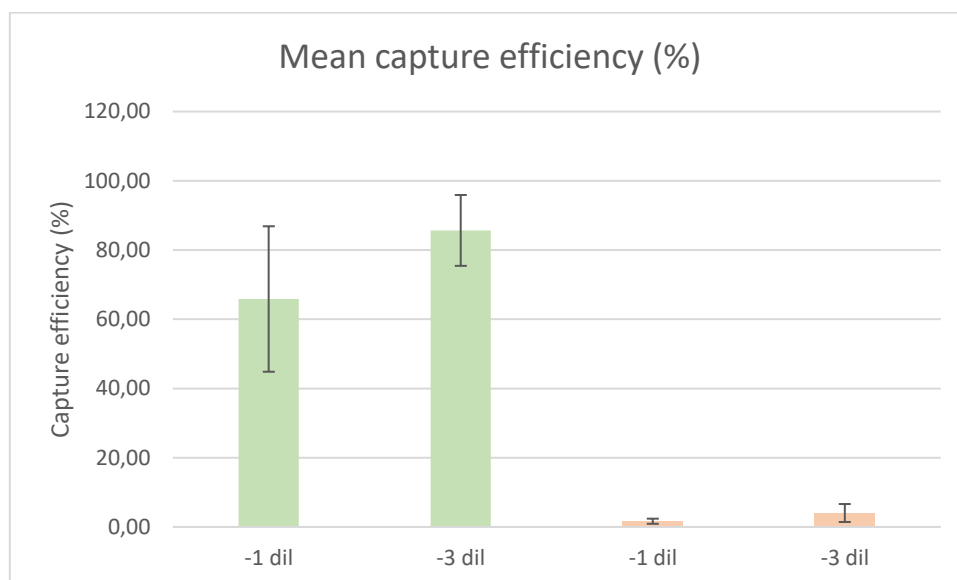


Figure 48 - Graph representing mean results from bench experiments, data from Table 7

Table 7 and Figure 48 summarize the results of the experiments produced on bench-top after the one displayed in Table 4, where only valid experimental results are reported, which is only experiments with optimized parameters as indicated in Table 5.

Through these results it is shown the efficacy of the protocol to achieve an average capture in positive sample (with specific antibody)  $\sim 86\% \pm 10.23\%$  for a concentration of  $2 \cdot 10^5$  CFU/ml while reducing a-specificity, as indicated by average capture in negative control (aspecific antibody) as low as  $4.03\% \pm 2.59\%$  for same concentration.

#### 4.2. Fluidic simulations and design

As a bridge between the presentation of results for the optimized bench-top assay protocol for antibodies immobilization and capture, and the developed microfluidic device, as an automatic alternative for mixing, capture and concentration, this section will cover the preliminary step necessary to determine the properties of the device that is wanted to be produced.

In section 1.2.1, different approached to passive mixing are collected and revised, with one emerging for its conceptual simplicity, proved efficacy and relatively easy implementation in a device, which do not require multiple layers, avoiding the cumbersome process of manual alignment. Implementing obstacles in a chamber result being an applicable method for the objective of this work. Remains to be assessed which kind of obstacles better suits the purpose. One useful tool in order to select most prominent designs is represented by computer-aided simulation, specifically in the area of CFD software, among which COMSOL Multiphysics™ was chosen.

Simulation on the beads and bacteria mixing level in a water-like fluid are performed for different type of obstacles, namely circular pillars at the center of the channel and differently shaped obstacles

at the wall of the channel, and compared with an equivalent channel in absence of any obstacle or structure.

Simulations are based on a simplified structure respect to the design that the devices will acquire; in fact only two inlet channels disposed in a Y configuration with a 90° angle, and a serpentine composed of 20 turns is studied, while obstacles occupies 3 or 4 turns only. These simplifications are due to the high computational power required which applies some limitations; for the same reason a coarse mesh discretization have been applied to the models. Table 8 reports major parameters involved in the simulation.

Figure 49 represents the distribution of magnetic particles(red) and of bacteria(green) at the outlet of the simulated microfluidic device. In Figure 49.A a complete segregation of the two elements resulted; Figure 49.B, C and D all show an higher grade of dispersion with major red and green dots overlapping, with better result obtained in B. In Figure 50 distribution of the particles along the channel width in the area of obstacle concentration is represented; Figure 50.A and C are characterized by particle segregation and their respective side of the channel, while an interesting effect, as predicted by Bhagat et al. [15], is verified in B and D, where obstacles modifies particles trajectories and deviates their flow to the center of the channel, thus increasing the chance of interaction between the two specie; in both two configurations, though, this tendency of concentrating at the center of the channel is not maintained along the serpentine and as visualized in Figure 49 particles are still dispersed at the outlet.

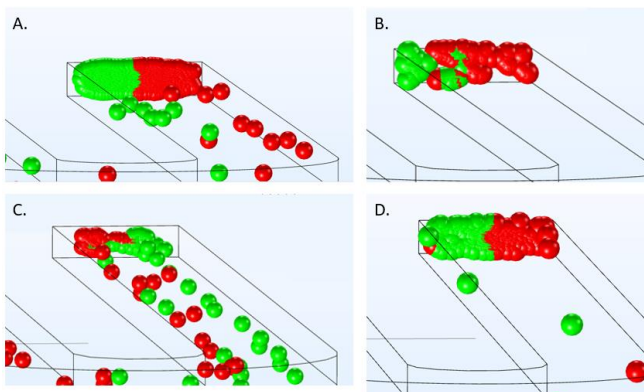


Figure 49- Distribution of beads(red) and bacteria(green) at the outlet. (A) No obstacles (B) Alternated cylindrical pillars (C) Triangular obstacles at the channel walls (D) Rectangular obstacles at the channel walls with curved end

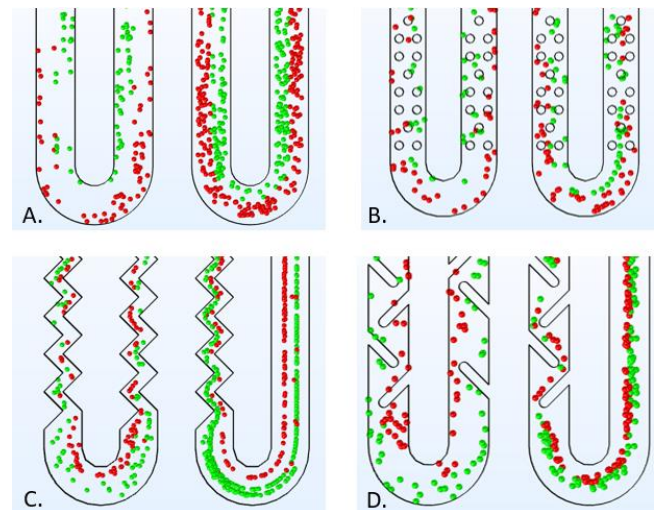


Figure 50- Distribution of beads(red) and bacteria(green) along channel width when close to obstacles (A) No obstacles (B) Alternated cylindrical pillars (C) Triangular obstacles at the channel walls (D) Rectangular obstacles at the channel walls with curved end

This behaviour is amplified in the configuration shown in Figure 51, where the effect of the modified shape of the obstacle, with triangular edges substituted to curved one, in order to avoid Coanda effect, is to force particle convergence to the center of the channel and reach the outlet in this configuration. This configuration could be efficient in increasing interaction events between the magnetic beads and the bacteria, thus promoting recognition and labelling.

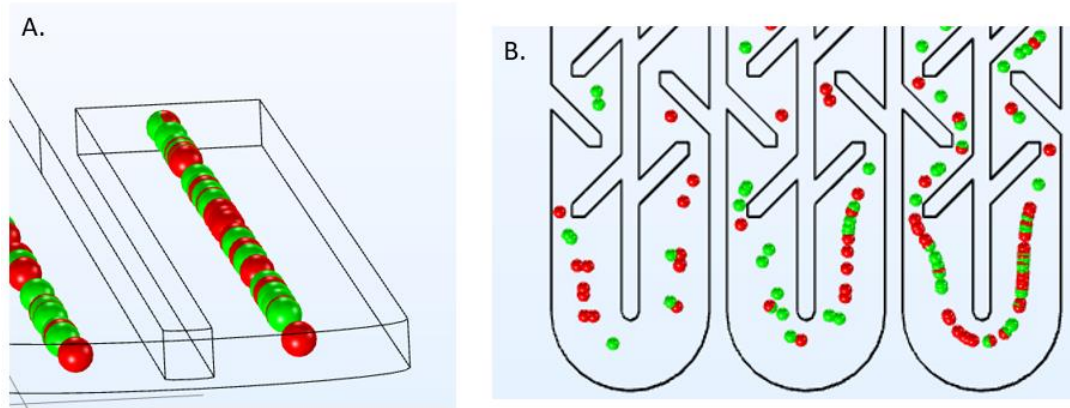


Figure 51- Distribution of beads(red) and bacteria(green) for rectangular obstacles at the channel walls with triangular end (A)at outlet (B)along channel width when close to obstacles

Table 8- Main parameters for simulated models

<b>Q</b>	10[ $\mu\text{l}/\text{min}$ ]	Inlet Flow Rate
<b>S</b>	1E-8 m <sup>2</sup>	Cross section
<b>Vavar</b>	Q/S	Average flow velocity
<b>Dbeads</b>	200[nm]	Diameter of beads
<b>Dbact</b>	1[ $\mu\text{m}$ ]	Diameter of Bacteria
<b>Nbeads</b>	1000	Number of beads
<b>NBact</b>	1000	Number of Bacteria
<b>Rhobeads</b>	2000[kg/m <sup>3</sup> ]	Density of beads
<b>Rhobact</b>	1116.6[kg/m <sup>3</sup> ]	Density of Bacteria
<b>Mesh</b>	Coarse	Accuracy of the discretization
<b>Rhofluid</b>	1000[kg/m <sup>3</sup> ]	Density of the fluid

According to what discussed in the simulation and the information provided by previous studies found in literature [15] [24] [23], two designs are chosen to be verified by experimental tests.



Figure 52- CAD file of the first design of the microfluidic device produced, on the right zoom on channel and obstacles. (all measures are in  $\mu\text{m}$  if not differently specified)

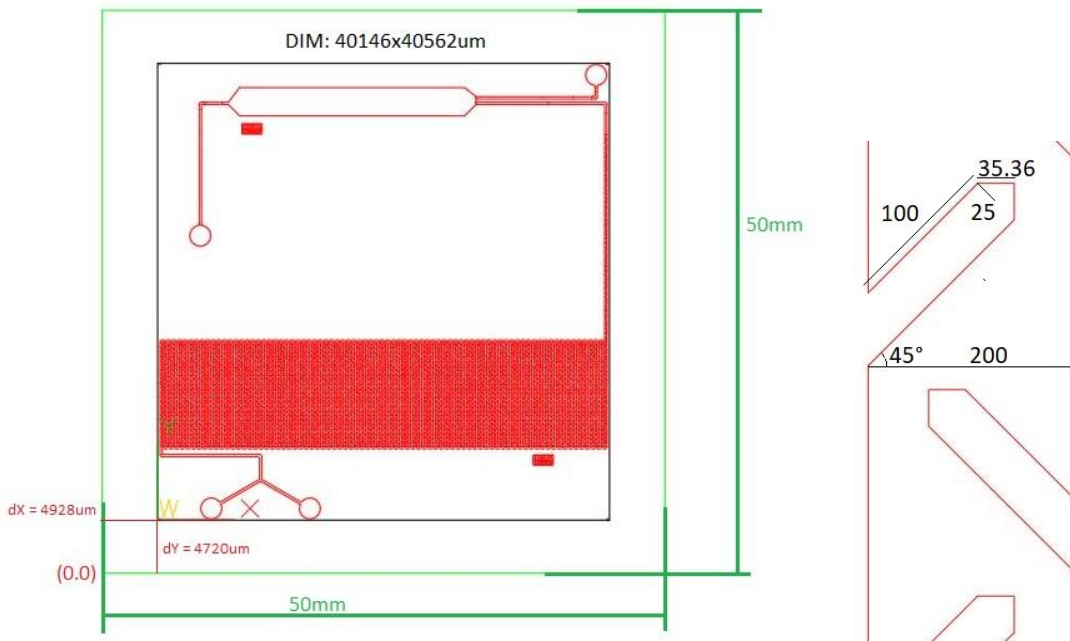


Figure 53- CAD file of the second design of the microfluidic device produced, on the right zoom on channel and obstacles. (all measures are in  $\mu\text{m}$  if not differently specified)

Figure 52 and Figure 53 represent the final result of a process of modification and readaptation, among which some intermediate design have been fabricated but their CAD file are not shown for brevity; as example though, in section 4.3.1, hard masks produced with a different design, with chamber closer to the serpentine, are also shown.

The length of the serpentine is set in order to guarantee the period of time needed for the particles-antibody conjugates to interact with bacteria and specifically attach. From a device realized by Guan et al. [69] for capturing bacteria with antibodies covered microbeads, given the used flow rate and dimensions, a capture with efficiency of 90% was obtained for a contact time of bacteria and

particle between 5s and 20s; thus the upper limit of the range was considered when designing the device.

For the first design the serpentine is composed of 50 turns, each one connecting 2 channels 12000 $\mu\text{m}$  long and so generating a path long 1.2\*10<sup>6</sup> $\mu\text{m}$ . Given a total flow-rate of 20  $\mu\text{l}/\text{min}$  (10  $\mu\text{l}/\text{min}$  at each inlet) and a cross section of 240\*100 $\mu\text{m}^2$  the mean velocity of the fluid in the channel is equal to  $v_{\text{mean}} = Q/A = 13.9 \cdot 10^{-3} \text{m/s}$ . With a serpentine with total length of 1.2\*10<sup>6</sup> $\mu\text{m}$ , fluid and particles take  $t_{\text{contact}} = L/v_{\text{mean}} \cong 86\text{s}$ .

For the second design the serpentine is composed of 79 turns, each one connecting 2 channels 9245 $\mu\text{m}$  long and so generating a path long 1.46\*10<sup>6</sup> $\mu\text{m}$ . Given a total flow-rate of 20  $\mu\text{l}/\text{min}$  (10 $\mu\text{l}/\text{min}$  at each inlet) and a cross section of 200\*100 $\mu\text{m}^2$  the mean velocity of the fluid in the channel is equal to  $v_{\text{mean}} = Q/A = 16.7 \cdot 10^{-3} \text{m/s}$ . With a serpentine with total length of 1.46\*10<sup>6</sup> $\mu\text{m}$ , fluid and particles take  $t_{\text{contact}} = L/v_{\text{mean}} \cong 87\text{s}$ .

As for the chamber, different size and shape were considered, and it was decided to verify the most convenient experimentally, by attributing one of the two main design to each serpentine design. For this reason, in first design, the chamber is preferentially oriented along the flow direction, with a width equal to approximately three times the width of the channel. Instead, for the second design, the chamber is wider, around twelve time the channel width, and longer (refer to Figure 54).

The predicted advantages are different, a wider chamber allows the beads to be well separated by the area of the flow with higher speed, which is the center of the channel, and for this reason it is easier for the beads, once captured, to be retained. Nonetheless, this can lead to a more difficult elution, as well as, given the increased available lateral space in the chamber, beads tend to accumulate in a smaller surface, being more prone to interact within them, cluster, and once again decrease elution efficiency.

From the dimensions displayed in Figure 54 volumes of the chamber can be computed, respectively 1.27 $\mu\text{l}$  for first design and 5 $\mu\text{l}$ . Considering that 3.8\*10<sup>9</sup> magnetic particles of 200nm diameter are used, summing together all their volume, it would be equivalent to 0.016 $\mu\text{l}$ . Even taking into account empty volume between clustered particles, the volume of the chamber is yet orders of magnitude higher and thus enough to contain them all.

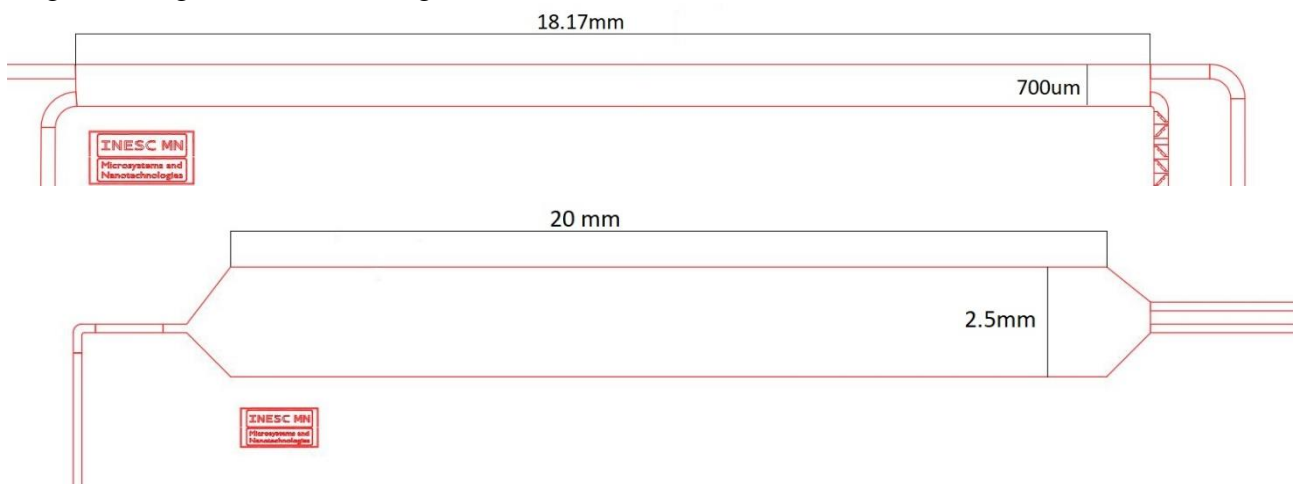


Figure 54- Chambers and relative measures. Upper: first design; lower: second design

To conclude, the design includes two mixing inlets, one eluting inlet and one or two outlets (Figure 52 and Figure 53). Elution inlet is different from mixing inlet because elution buffer is not wanted to flow through the whole serpentine just to reach the chamber as it would require longer time and eventually collected any waste that deposited in the serpentine.

The additional outlet in the first design (Figure 53) has been inserted in the case the first outlet would be blocked by clustered and deposited particles, but tests performed never required the use of the second one as deposition have never been so detrimental.

### 4.3. Microfluidic device fabrication

In this section results relative to the fabrication process will be revealed, regarding both of the designs as presented in the previous section 4.2.

#### 4.3.1. Hard Mask

The production of the hard mask did not involve any particular optimization of the process as already well characterized, and results were satisfying, as shown in Figure 55 and Figure 56, referring to first design

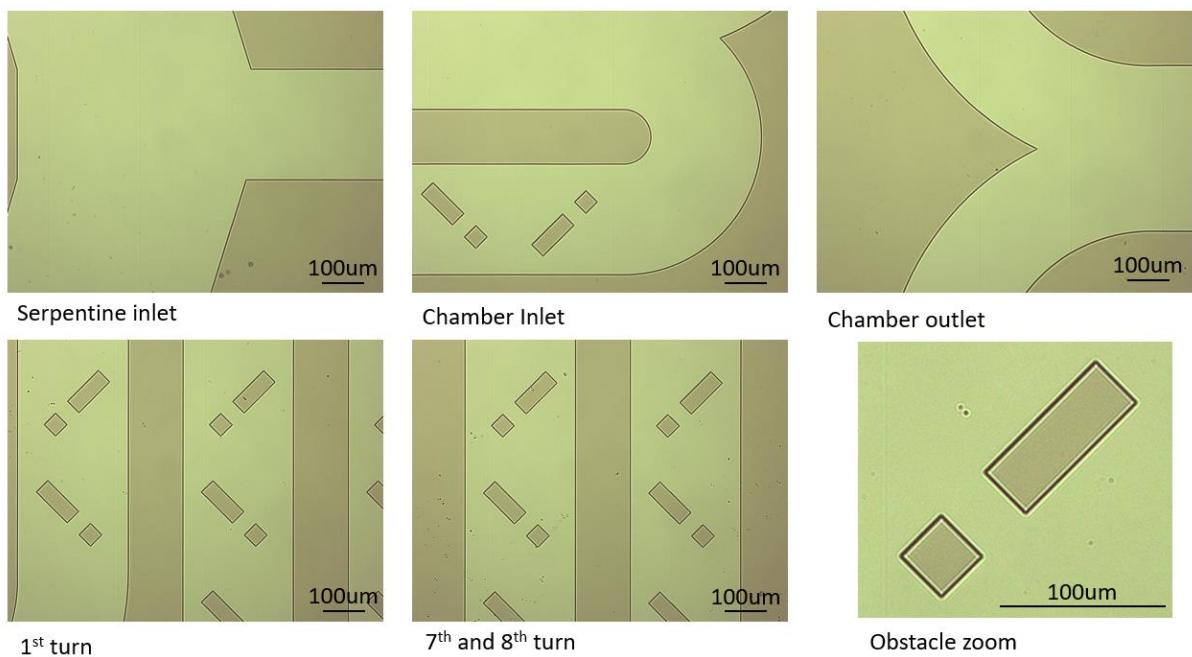


Figure 55-Microscope picture of hard mask of first design, first version

Smaller size elements, represented by the  $36*36\mu\text{m}^2$  squares are well defined and aluminium is correctly removed in the area of the channel. Also junctions aspect is as expected with no defects to be outlined.

A second version of the hard mask was produced in order to accomplish a better capture, as shown as follows in Figure 57, with the chamber further from the serpentine avoiding magnetic particles to be retained at the level of the latter.

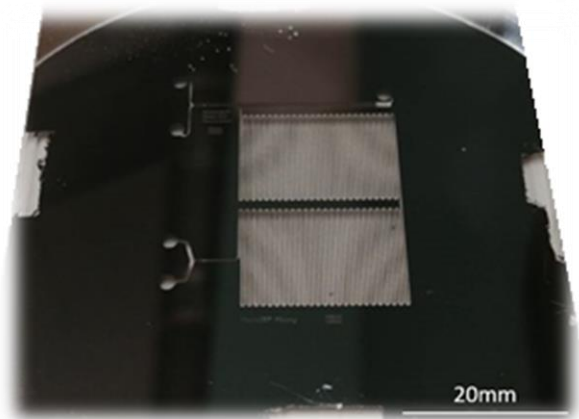


Figure 56-Picture of the hard mask of first design, first version

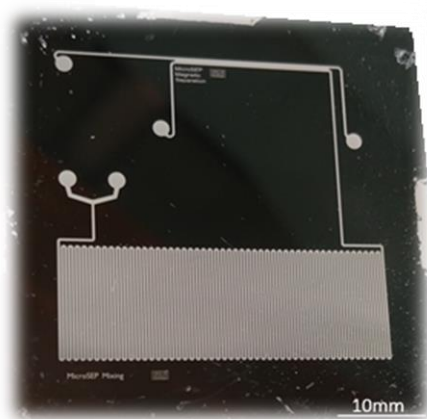


Figure 57- Picture of the hard mask of first design, second version

Regarding the second design, similar results have been obtained, with no major obstacles faced in this step of the production process, as shown below

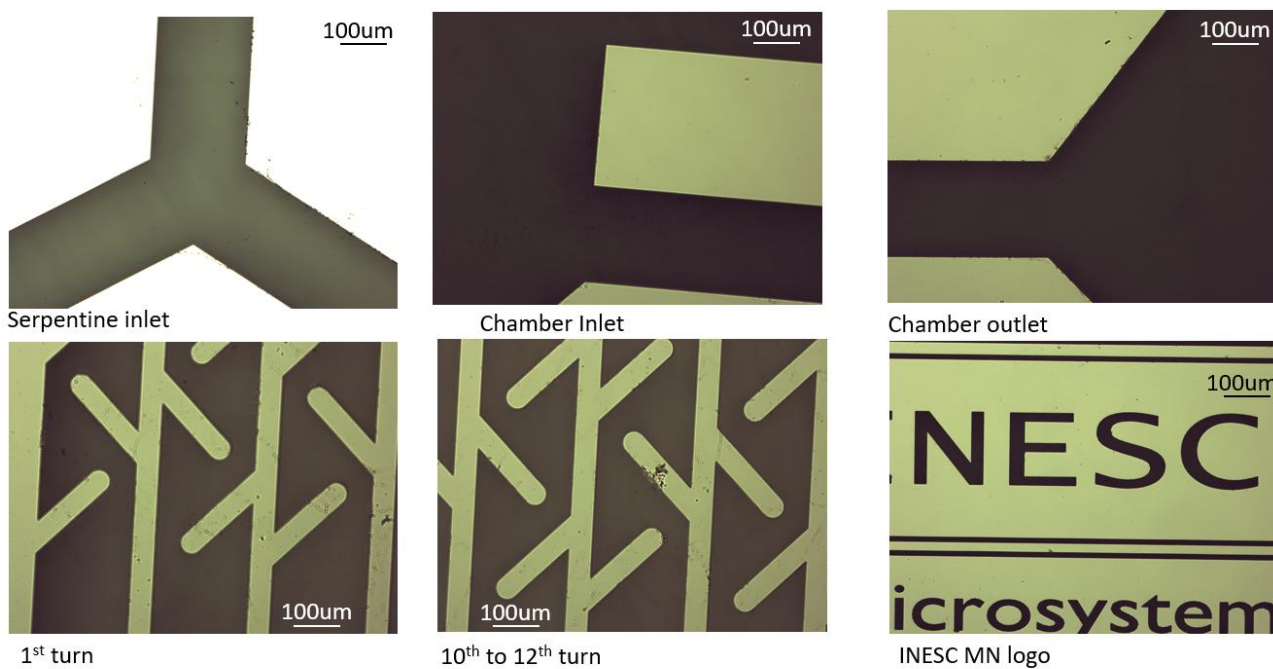


Figure 58-Microscope picture of hard mask of second design, first version



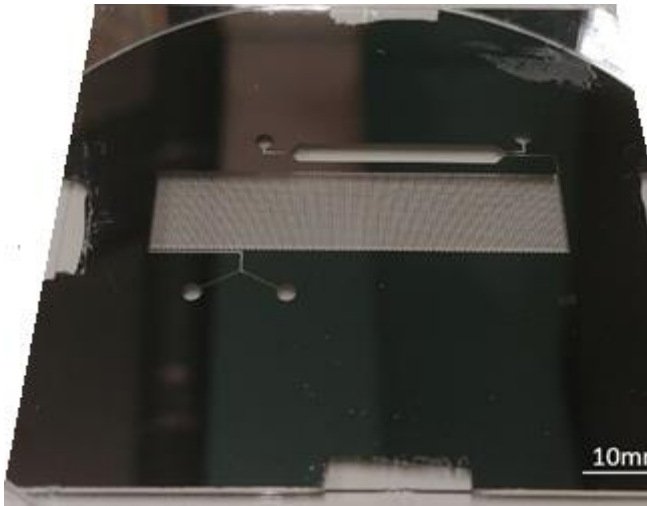


Figure 59- Picture of the hard mask of second design, first version

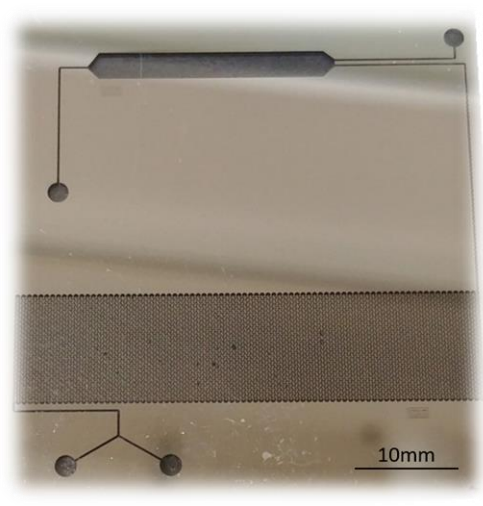


Figure 60- Picture of the hard mask of second design, second version

Small defects are inevitable in such a delicate production process, when the etching of the metal layer can be disturbed by any contaminant and its geometrical characteristics depends on the sacrificial photoresist layer but the shown masks did not present any major defect that could prevent well-functioning in the derived device, and thus the process is considered successful.

#### 4.3.2. SU-8 mold

The production of the SU-8 mold revealed being less direct and in need of some parameter tuning. Simply following the advices of the polymer supplier results were not sufficient, and some optimization has been performed, first establishing the correct parameters to obtain the aimed thickness for the microfluidic channels, later to set the optimal exposition dose for the feature definition, given the fact that the latter property, which is exposition dose, is dependent on the thickness.

##### *Experiments for thickness exploration*

As shown by Figure 61 and Table 9 part of the supplier datasheet, advised spin speed for the second step of the spin coating process of the photoresist on the silicon substrate, as explained in section 3.2.2, is between 1000rpm and 1250rpm, for a wanted thickness of 100 $\mu$ m with SU-8 50 photoresist.

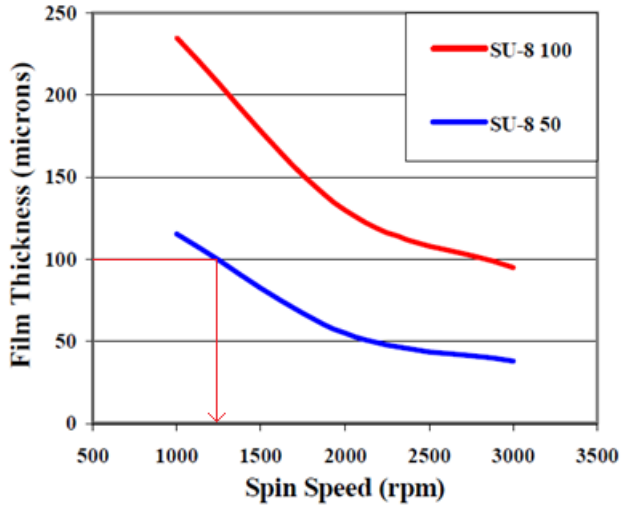


Figure 61-Graph showing relation between spin speed during coating and obtained thickness, from section 7.4, annex D

Table 9- Relation between spin speed and thickness of the polymeric substrate during spin coating, from section 7.4, annex D

Product	Viscosity** est @ 25°C	Thickness µm	Spin Speed rpm
SU-8 50	12250	40	3000
		50	2000
		100	1000
SU-8 100	51500	100	3000
		150	2000
		250	1000

Table 10-Measured values of thickness at different spin speed

Spin speed (rpm)	Thickness (µm)
1000	74.141
1000	68.57
1000	68.99
1000	82.81
1000	73.53
1000	73.13
1000	137
950	108
900	115
900	125
900	99
850	168
700	200

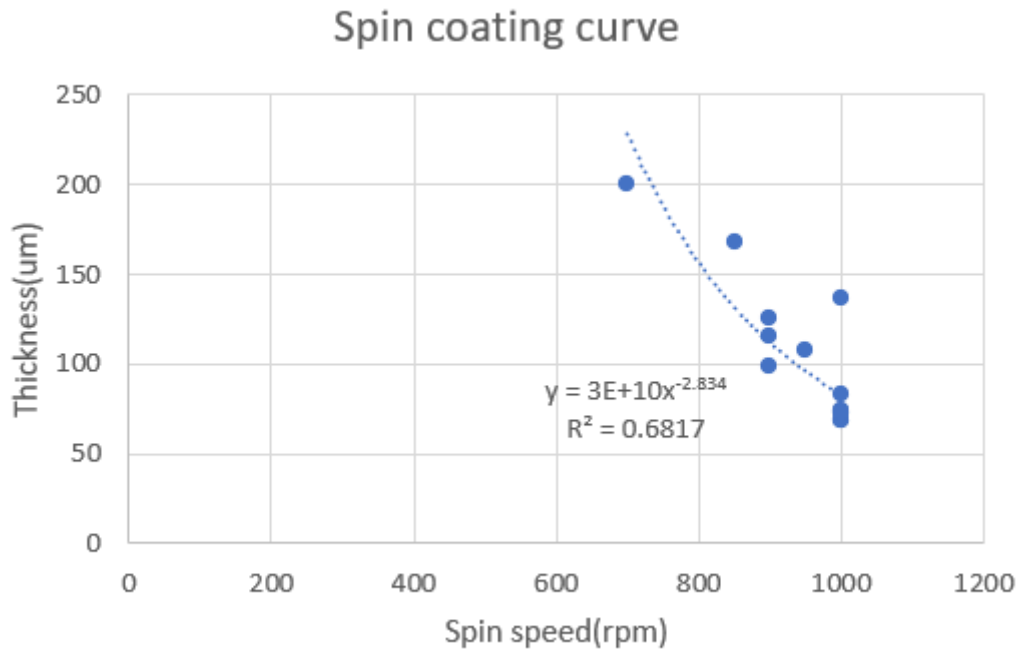


Figure 62-Experimental spin coating curve

Given the values in Table 10, it appears clear as the advised spin speed do not guarantee a final thickness above 100µm and thus it is not the optimal value. A spin speed of 900rpm instead, is more reasonable and closer to the aimed optimal value and for this reason it is chosen as the speed to be applied in the production of the final devices.

*Experiments for exposure dose exploration*

As previously mentioned, another parameter essential in the production of the SU-8 mold is represented by the exposure dose that the photoresist is made to absorb, which is also dependent on the photoresist thickness. Thus, once fixed the spin speed able to provide the wanted thickness of the final device, a suitable exposition dose is researched, with the aim to guarantee correct definition of the features of the final device, where the obstacles represent the smaller features and so a good method to verify the quality of the exposition. As also mentioned in section 3.2.2, overexposure and underexposure must be avoided and verticality of the walls must be verified. The starting point of the exploration process is represented by the advised supplier dose, reported in Table 11

Table 11-Relation between thickness and needed exposure dose, from section 7.4 , annex D

Product	Thickness µm	Expose Dose mJ/cm <sup>2</sup>
SU-8 50	40	250-300
	50	400-500
	100	500-650
SU-8 100	100	500-650
	150	600-675
	250	625-700



Knowing the energy per unit of area per unit of time that the UV lamp can deliver at a given distance, the time correspondent to the wanted dose is computed, according to Equation 28

$$E = \frac{t}{P}; \quad (28)$$

Equation 28 – Relation between exposition time and absorbed dose

where E is the exposure energy in mJ/cm<sup>2</sup>, P is the lamp power in mW/cm<sup>2</sup> and t is the exposure time in s

Table 12-Results on different exposition dose applied, first design

Spin speed(μm)	Exposure dose (mJ/cm <sup>2</sup> )	Visual result	
		Space between turns	Obstacles
1000	588.3	Not defined	Not defined
1000	666	Not defined	Not defined
1000	638.25	Not defined	Not defined
1000	610.5	Not defined	Not defined
1000	588.3	Not defined	Not defined
1000	571.65	Not defined	Not defined
1000	555	Not defined	Not defined
1000	527.25	Not defined	Not defined
1000	588.3	Not defined	Not defined
1000	527.25	Not defined	Not defined
950	571.65	Not defined	Not defined
900	527.5	Not defined	Not defined
900	555	Not defined	Not defined
900	588.3	Not defined	Not defined
900	407.16	Defined	Not defined
900	249.75	Defined	Not defined
900	194.25	Defined	Defined
900	166.5	Defined	Defined
850	499.5	Not defined	Not defined
700	588.12	Not defined	Not defined

Various exposition doses are tested, and results are defined qualitatively by visualization of the PDMS device obtained from the produced mold.

A visual explanation of the results reported in Table 12 can be obtained in Table 13, where microscope picture for some the experimented dose is shown.

The information extracted by such exploration imposes the maximum dose able to provided a sufficient definition of both, the space between the turns of the serpentine and the obstacles inside the channels, to lay between  $194.25\text{mJ}/\text{cm}^2$  and  $249.75\text{mJ}/\text{cm}^2$ . Nevertheless, even if such dose ensures that an good amount of obstacles are well-defined in the subsequent PDMS device produced by the SU-8 mold, as shown in the last line, 4<sup>th</sup> column of Table 13, some phenomena of overexposition is present in some area of the device, as discussed in section 4.3.3.

Table 13-Microscope picture of molds at different exposure dose

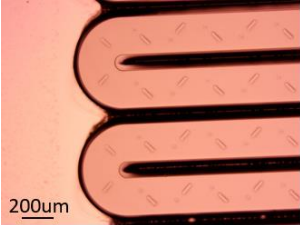
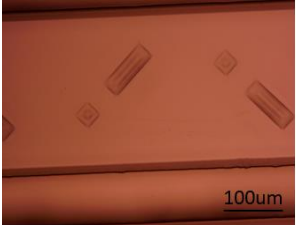
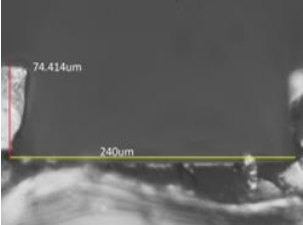
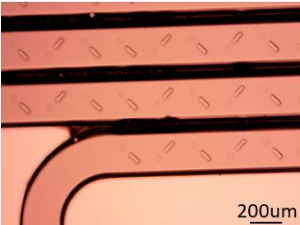

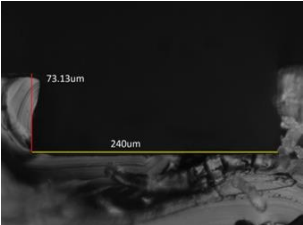
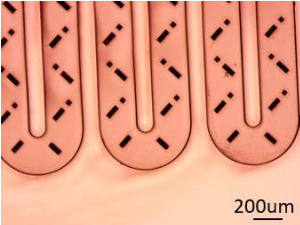
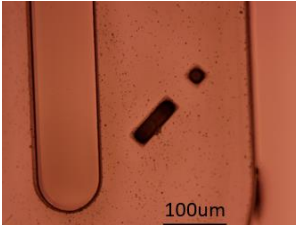
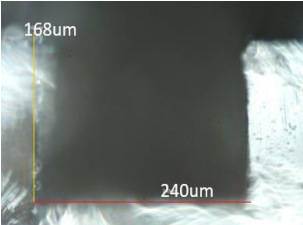
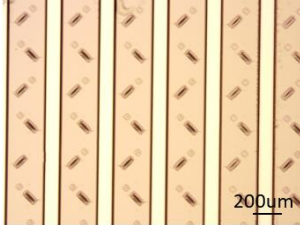
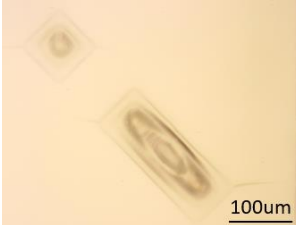
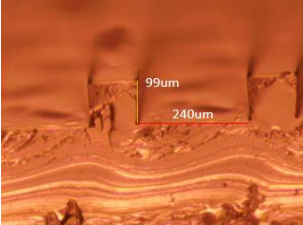
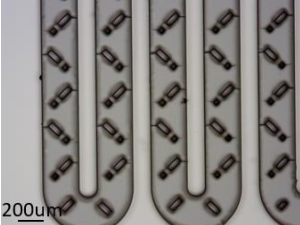
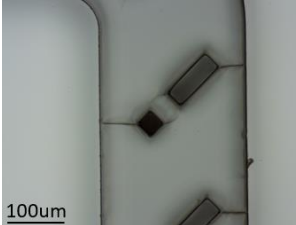
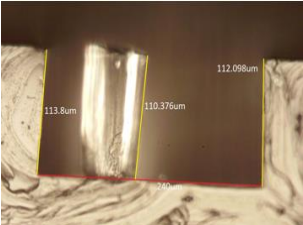
Exposition dose mJ/cm <sup>2</sup>	Serpentine turns	Obstacles	PDMS
666			
527.25			
499.5			
249.75			
194.25			

Table 14-Results on different exposition dose applied, second design

Spin speed( $\mu\text{m}$ )	Exposition dose( $\text{mJ}/\text{cm}^2$ )	Visual result	
		Space between turns	Obstacles
1000	588.3	Not defined	Not defined
900	333	Defined	Defined
900	277.5	Defined	Defined
900	166.5	Defined	Defined

Selected values for the explored parameters are after applied to produce a similar mold for the second design, as shown in Table 14

*Final device and optimal parameters*

In conclusion, here are reported the values for all the parameters involved in the production of the mold with ensured the best results, as concern this study, displayed in Table 15

Table 15-Parameters of the final device

Substrate dimensions	Oxygen plasma	Dehydration Bake	SU-8 50 volume	Spin coating 1 <sup>st</sup> step
50x50mm <sup>2</sup>	1 min, RF 11W, 800mTorr	5 min @ 110°C	2ml	500rpm @ 100rpm/s for 10s
Spin coating 2 <sup>nd</sup> step	Soft Bake	Exposure Dose	Post exposure bake	Development time
900rpm @ 300rpm/s for 30s	65° for 10 min @2°C/min 95° for 30 min @2°C/min	166.5mJ/cm <sup>2</sup>	65° for 1 min @2°C/min 95° for 10 min @2°C/min	15min

leading to the production of molds, shown in Figure 63, lately applied to fabricate the correspondent PDMS device

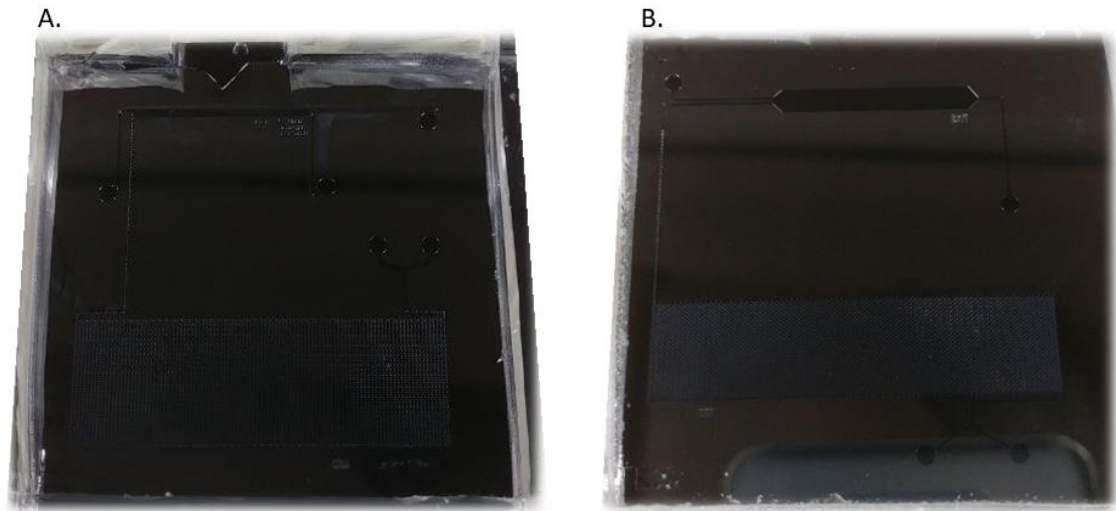


Figure 63- A. First design SU-8 mold; B. Second design SU-8 mold

#### 4.3.3. PDMS Device

In conclusion to the fabrication process of the microfluidic device, once the mold have been produced with satisfying features, the PDMS element is formed.

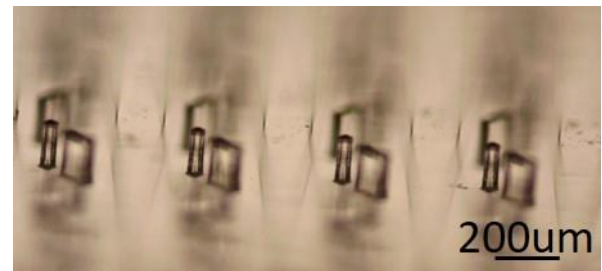
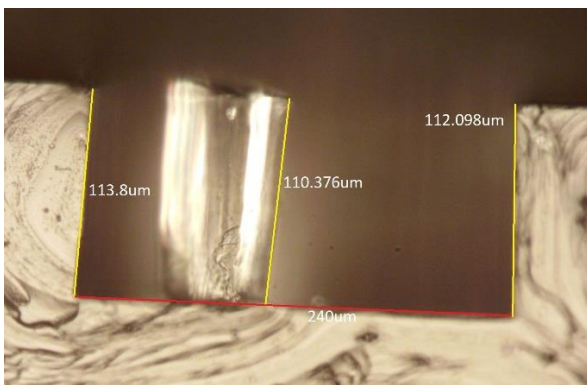
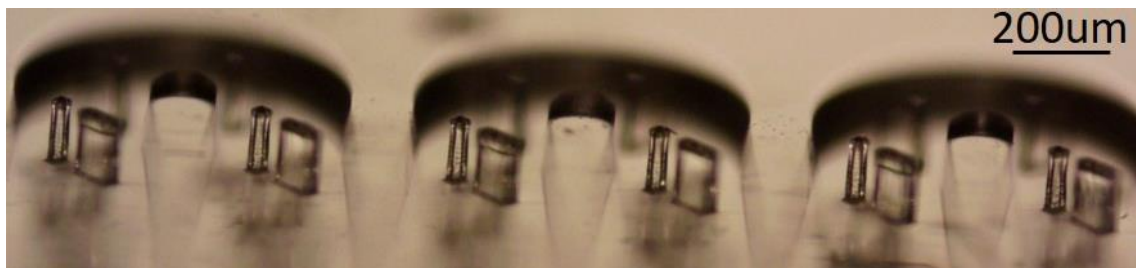


Figure 64- Microscope images of PDMS device for the first design, sectioned transversally: left, inclined at 90deg respect to line of sight; right, inclined >90deg respect to line of sight





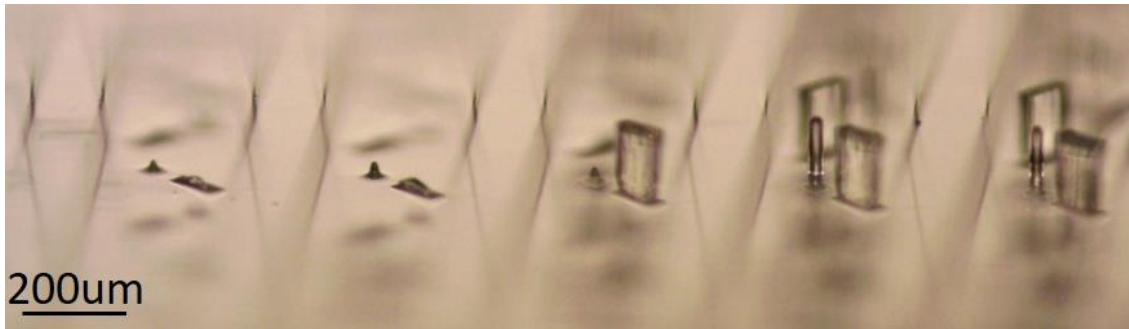


Figure 65- Microscope images of PDMS device for the first design, sectioned transversally: upper, edge of the serpentine; lower: area of the serpentine with obstacles low definition

Figure 64 and Figure 65 reports microscope images of the final device, evidencing the presence of the obstacles. As mentioned before, these represents the most delicate aspect of the device, due to reduced dimensions and high aspect ratio, equal to 2.78, as defined by Equation 29

$$aspect\ ratio = H/W; \quad (29)$$

Equation 29 – Aspect ratio of an element

where H and W are respectively the height and width of the element. This factor makes intuitively more difficult to produce the element as it increases, since a successful result gets more and more dependent on the exposure dose; in other words, when the aspect ratio increases, tolerance in under or overexposure decreases, as well as the probability of rupture of the structure during peeling from the mold increases.

Figure 64 shows an example of an obstacle with nearly perfect features; its height is comparable to the height of channel walls, ensuring that, once the PDMS is sealing against glass, no stream can flow above the obstacle and thus decrease its mixing efficiency.

Quality of the obstacles is generally good along the serpentine, with exception of some areas that present damaged or almost absent obstacles, as demonstrated in Figure 65. Such problematic can be effect of two aspects, or a combination of both, either a non perfectly uniform exposition of the mold which caused local over-exposition and so reduced dimensions of the holes (hosting the obstacles during PDMS fabrication) or rupture of the elements during the peeling phase. Nevertheless, the amount of obstacles present in good conditions and the mixing obtained by other effects is considered to be sufficient for the aim of the device, so an optimization in this sense is not craved, and eventually left to further developments.

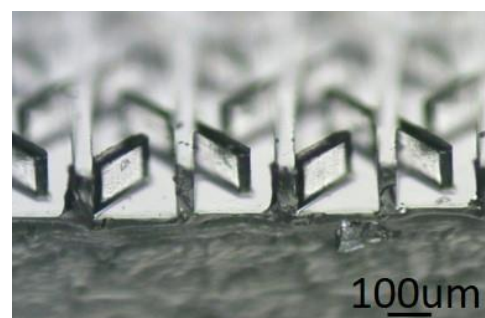
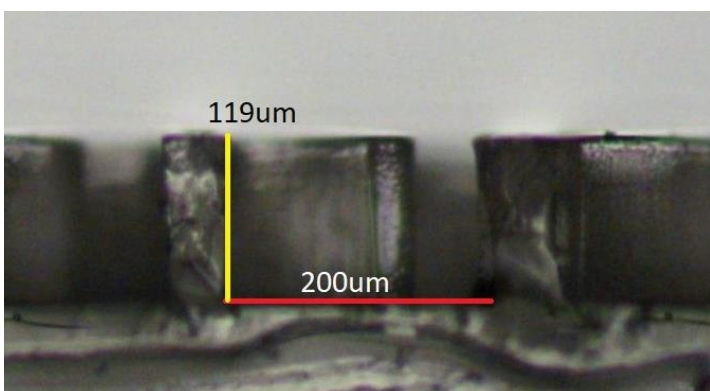


Figure 66- Microscope images of PDMS device for the second design, sectioned transversally: left, inclined at 90deg respect to line of sight; right, inclined >90deg respect to line of sight

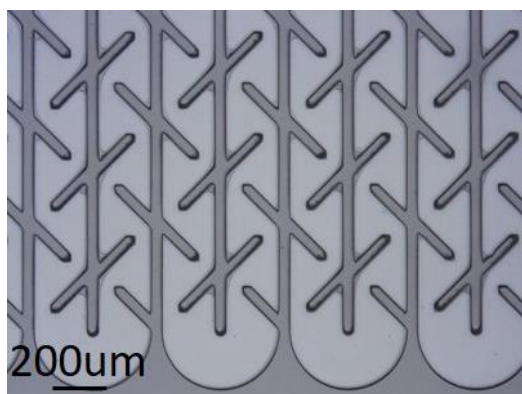


Figure 67-Microscope image of PDMS device for the second design, top view

Similar results are obtained for the second design, as reported in Figure 66 and Figure 67. Obstacles' height is in the expected range and comparable with wall height, and along the whole serpentine they are always sufficiently well defined, with no major defects, also thanks to their lower aspect ratio and generally greater dimensions.

#### 4.4. Microfluidic testing

As presented in the previous sections, the aim of the microfluidic device was meant to substitute and automatize, as well as increase efficiency among other advantages, one step of the process developed to recognise bacterial presence in the sample, precisely the mixing and capture stage.

After the optimization of the bench-top process in bench, described in section 4.1, the optimal parameters are applied and introduced to form a protocol able to verify the efficiency of the microfluidic device.

In order to evaluate the efficiency of the device, it was initially tested parallelly to bench capture, on solutions of *K.pneumoniae* bacteria, using same covered beads stock in order to exclude a priori differences in beads coverage that could be obtained based on a day to day variability.

It is clear from how the protocol is established that the Non-Retained volume is compared with the supernatant obtained in bench-top capture method, where a magnetic column was applied. Similarly, the Retained volume consists of all retained beads and so is to be compared with the magnetic capture sample obtained in bench.

Table 16- Summarized results from comparison in capture efficiency of *K.pneumoniae* solution for bench and 2 microfluidic design devices, refer to appendix 7.3 for complete results. HBC is equal to  $3.8 \cdot 10^{10}$  beads/ml, and LBC is equal to  $1.9 \cdot 10^{10}$  beads/ml

			Mean (%)	SD(%)
Bench		Positive (specific)-HBC	86.12	9.46
		Negative(Aspecific)-HBC	4.49	2.62
Microfluidics	Design 1	Positive (specific)-HBC	100.00	0.00
		Negative(Aspecific)-HBC	20.28	12.29
	Design 2	Positive (specific)-LBC	65.48	14.84
		Negative(Aspecific)-LBC	1.08	0.49
	Design 2	Positive (specific)-HBC	98.57	1.27
		Negative(Aspecific)-HBC	4.91	2.23

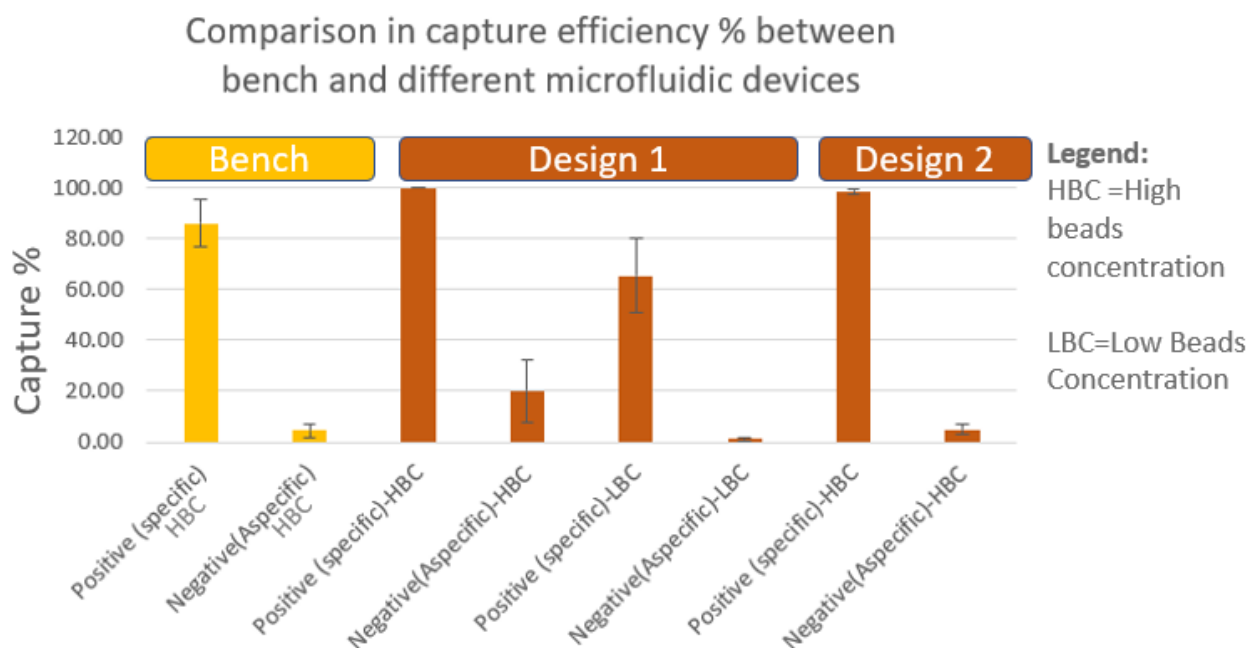


Figure 68 - Graph representing mean results for capture efficiency of *K.pneumoniae* solution comparing different methods, data presented in Table 16.

HBC is equal to  $3.8 \cdot 10^{10}$  beads/ml, and LBC is equal to  $1.9 \cdot 10^{10}$  beads/ml

In order to compute capture efficiency, same approach as for bench evaluation (see section 4.1) was applied. In case of microfluidic evaluation, though, another factor must be taken into account, which is the tendency of any biological species to adhere and interact with channel walls. For this reason, a simple experiment allowed to verify if the blocking step was efficient and thus all bacteria could pass through the device and be collected at the outlet without loss. To assess it, the device has been washed with 100µl PB after one test with a positive sample and the outcome was plated showing no colonies and thus confirming that very few or no bacteria were trapped in the device.

Results from 3 independent experiments with 2 dependent replicas each verify that capture reached in the microfluidics is comparable, if not superior, to results in bench-top capture in bench.

Mean values can in fact been compared with average capture value from bench capture as showed in Table 16, reporting  $86\% \pm 9\%$  for positive samples and  $4\% \pm 3\%$  for negative samples, compared to  $100\% \pm 0\%$  and  $99\% \pm 1\%$  for positive samples and  $20\% \pm 12\%$  and  $5\% \pm 2\%$  for negative samples obtained in the microfluidic device.

This series of experiments confirms the possibility to replace the bench-top assay for mixing and capture with the automatic one allowed by the microfluidic device successfully.

#### Evaluation of Limit of Detection (LoD)

After established the efficiency of the device at a concentration of bacteria in solution equal to  $2 \cdot 10^5$  CFU/ml, the possibility to detect low concentrated samples is verified, as concentration in an clinical sample can vary between different order of magnitude, as discussed in the following section.

Concentrations as low as 20 CFU/ml have been tested for the first design of the microfluidic device, in a volume always equal to 100µl, which guarantees in the lowest concentration samples the presence of 20 bacterial cells in average.

As regarding the protocol of the experiment, it was maintained equal to the one presented in the previous section.

Table 17-Results for capture of bacteria *Klebsiella pneumoniae* at different dilutions with specific antibody

Positive/specific					
Experiment	Bacteria conc. nominal (CFU/ml)	Bacteria conc. measured (CFU/ml)	Capture %		Beads concentration (beads/ml)
			1 <sup>st</sup> replica	2 <sup>nd</sup> replica	
1 <sup>st</sup>	2*10 <sup>5</sup>	1.11*10 <sup>5</sup>	100.00%	100.00%	3.8*10 <sup>10</sup>
	2*10 <sup>4</sup>	1.11*10 <sup>4</sup>	100.00%	100.00%	
	2*10 <sup>3</sup>	1.11*10 <sup>3</sup>	0.00%	100.00%	
	2*10 <sup>2</sup>	1.11*10 <sup>2</sup>	0.00%	0.00%	
2 <sup>nd</sup>	2*10 <sup>5</sup>	6.99*10 <sup>5</sup>	82.85%	62.94%	1.9*10 <sup>10</sup>
	2*10 <sup>4</sup>	6.99*10 <sup>4</sup>	43.23%	37.56%	
	2*10 <sup>3</sup>	6.99*10 <sup>3</sup>	54.43%	54.43%	
	2*10 <sup>2</sup>	6.99*10 <sup>2</sup>	38.24%	38.24%	
3 <sup>rd</sup>	2*10 <sup>5</sup>	1.13*10 <sup>5</sup>	69.05%	47.06%	1.9*10 <sup>10</sup>
	2*10 <sup>4</sup>	1.13*10 <sup>4</sup>	81.19%	60.76%	
	2*10 <sup>3</sup>	1.13*10 <sup>3</sup>	59.62%	59.62%	
	2*10 <sup>2</sup>	1.13*10 <sup>2</sup>	0.00%	0.00%	

Table 18- Results for capture of bacteria *Klebsiella pneumoniae* at different dilutions with non-specific antibody

Negative/aspecific					
Experiment	Bacteria conc. nominal (CFU/ml)	Bacteria conc. measured (CFU/ml)	Capture %		Beads concentration (beads/ml)
			1 <sup>st</sup> replica	2 <sup>nd</sup> replica	
1 <sup>st</sup>	2*10 <sup>5</sup>	1.11*10 <sup>5</sup>	28.97%	11.59%	3.8*10 <sup>10</sup>
	2*10 <sup>3</sup>	1.11*10 <sup>3</sup>	0.00%	0.00%	
2 <sup>nd</sup>	2*10 <sup>5</sup>	6.99*10 <sup>5</sup>	0.65%	0.72%	1.9*10 <sup>10</sup>
	2*10 <sup>3</sup>	6.99*10 <sup>3</sup>	3.15%	3.15%	
3 <sup>rd</sup>	2*10 <sup>5</sup>	1.13*10 <sup>5</sup>	1.67%	1.26%	1.9*10 <sup>10</sup>
	2*10 <sup>3</sup>	1.13*10 <sup>3</sup>	1.44%	2.14%	

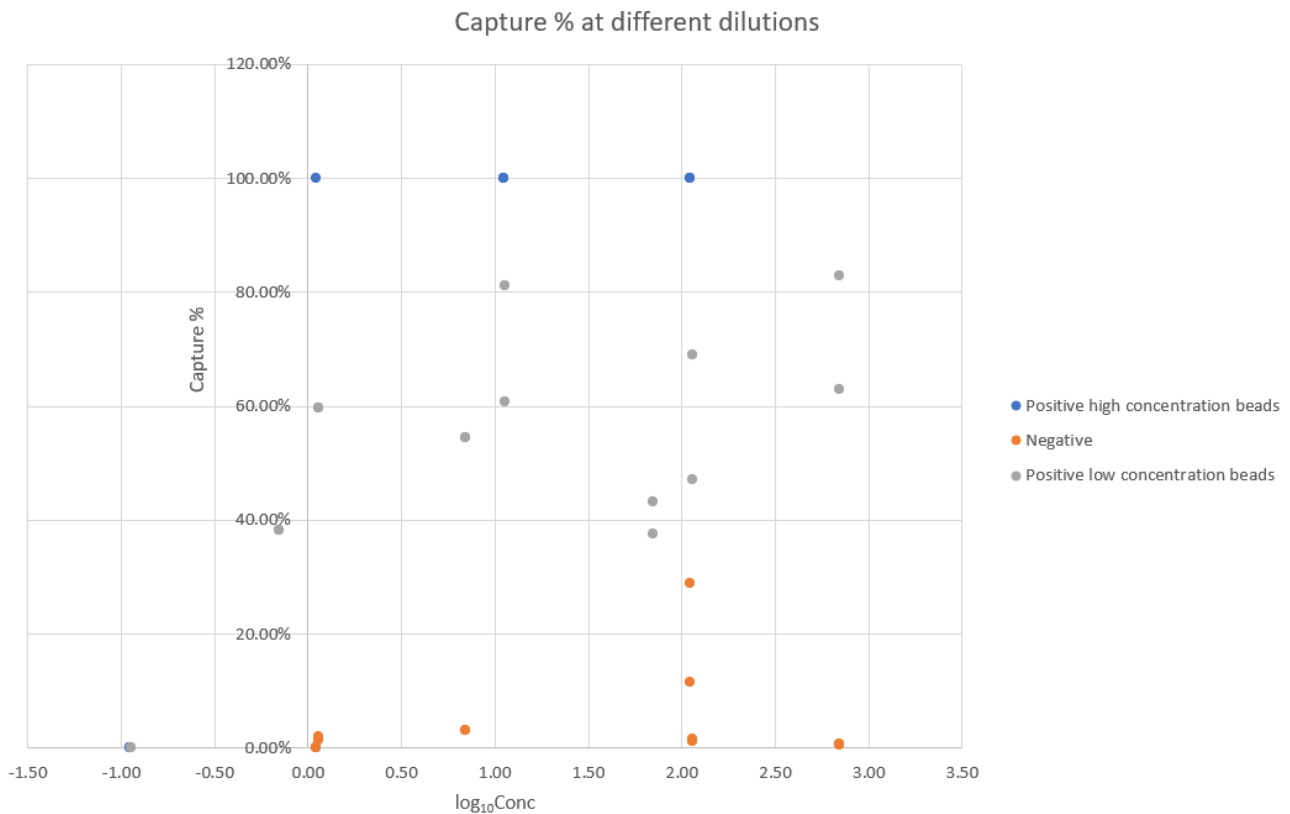


Figure 69- Graph on results for capture of bacteria *Klebsiella pneumoniae* at different dilutions; Concentration as CFU/ $\mu$ l.

As shown in Figure 69, which graphically reports results shown in Table 17 and Table 18, capture efficiency decreases as the concentration of the sample decrease, behaviour expected as the reduced number of bacterial cells increases the probabilities that such few cells do not enters in contact with enough particles or for a long enough time, as well as the possibility that the few cells, even if surrounded by magnetic particles, are not retained by the magnet and escape the magnetic field imposed. In addition, even if limited, some loss of bacteria cell in the channel occurs, and when dealing with such reduced number, the probability that the few cells present do not reach the outlet is high.

Even if at very low concentration as 200 CFU/ml capture is not efficacy, concentrations as low as  $2 \cdot 10^3$  CFU/ml shows, at least at samples constituted of a simple bacteria solution in a buffer, allows an appreciable capture, roughly quantified as above 50%. Such capture efficiency is present only when antibodies specific for the bacteria are immobilized on the beads, demonstrating specificity in the capture, where negative/aspecific samples shows consistently reduced capture efficiency.

#### Clinical samples

Results up to this point shows the ability of the microfluidic device to deal with simple samples, formed by a solution of one bacteria strain in buffer, namely PB, which represent a good model to quantify capture efficiency. On the other hand, such sample does not reflect the complexity that a rectal or nasal swab media brings with it; as for the former, bacteria distribution in such sample is quite vast and  $\sim 7\%$  of the microbiota, for the sample tested in [70], belongs the family of Enterobacteriaceae of which *Klebsiella pneumoniae* is part; some of these bacteria have similar morphology when plated thus making CFU based detection method more complex. In addition,

intestinal residues and highly viscous transport media contributes to rise the challenge in processing such sample.

With the aim to evaluate the effect of the complex matrix and so deal with a sample that could represent all of the difficulties in real sample treatment, 5 rectal swabs have been tested and the ability to retain target bacteria evaluated, once again taking as model a device based on the first design.

Before discussing the results of such tests, some considerations are given. Firstly, the method to verify capture result is discussed, as plating device outcomes in LB-agar filled Petri dishes, as done so far, demonstrates unpractical, given the big amount of non-target bacteria present. In fact, even if the role of the particles is to interact, surround and retain only target bacteria, inevitability other bacteria interact with the particles and are dragged and retain all together, and then evidenced in the plating. While it is not a limiting factor for further analysis in the magnetic cytometric platform, as the device is intended to, it has a strong impact in evaluating results through plating method, as non-target bacteria would tend to cover target bacteria while growing, practically limiting the ability of the operator to count the colonies, as well as resembling target bacteria in morphology, with the possibility to induce a miscounting.

To overcome such limitation, specific Petri dishes filled with selective media are used; tested clinical sample are characterized by its content of a specific type of *Klebsiella pneumoniae*, namely a variation which is Carbapenem resistant, a class of highly effective antibiotic agents exploited for high risk bacteria treatment.

Given this resistance, only bacteria that possess such resistance are able to grow in the correspondent selective media, which is, a media containing mentioned antibiotic. In such way, it is possible to focus the evaluation of the capture efficiency of the microfluidic device only considering this specific bacteria, since used antibodies are equally able to interact with resistant and non-resistant bacteria. As a consequence, it is true that, if non-resistant *Klebsiella pneumoniae* are present in the sample, its contribution in capture cannot be quantified, yet, tested clinical samples are verified positive for the resistant strain and so its presence is confirmed.

Secondly, in order to be consistent to experiment held with previous spiked samples, only an aliquot of 100µl of the 500µl in which swab is resuspend are tested, with the assumption that the solution is homogeneous enough and concentration do not vary significantly in the volume; this assumption can be intuitively considered valid only above a certain concentration, which is not established clearly but which suggests as results gets less reliable as concentration decreases. First sample to be tested has been a spiked sample; a positive clinical sample have been verified through plating method to assess the presence of resistant *Klebsiella pneumoniae*, as expected, and eventually quantify it. Unfortunately, possibly due to long storage time, no resistant bacteria were evidenced, while a consistent amount of other bacteria were found when plated in LB agar media Petri dishes, as shown in Figure 70

Table 19-Parameters and result of spiked clinical sample capture

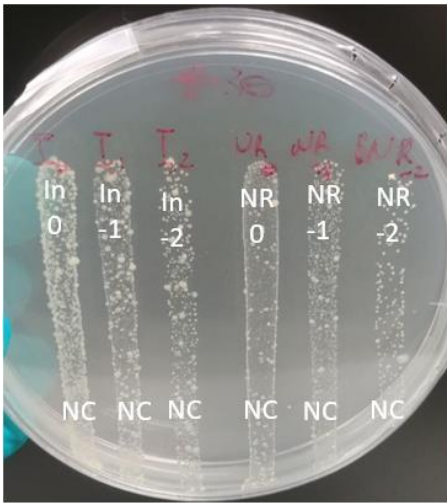


Figure 70-First clinical sample plated in Lb agar media Petri dish ,see legend Figure 71

Initial concentration(CFU/ml)	$1.41 \times 10^9$
CFU in 100 $\mu$ l	$1.41 \times 10^8$
Non-Retained(CFU/ml)	$7.9 \times 10^8$
Retained(CFU/ml)	$6.85 \times 10^6$
Capture %	0.86
Beads concentration(beads/ml)	$3.8 \times 10^{11}$
Beads in 10 $\mu$ l	$3.8 \times 10^9$
Ratio beads:bacteria	26

Since the resuspended swab, even if lacking resistant bacteria to be targeted, represented a realistic sample as for physical properties, equivalent to any other positive clinical sample, it was decided to spike it with one colony of resistant *Klebsiella pneumoniae* cultivated in a different dish filled with selective media, result of a previous experiment. In this way, the presence of resistant bacteria was ensured, and its concentration set at a high, even if unknown, value. Such sample was tested in the microfluidic device following the protocol reported in section 2.2.5.

Results of the experiment are shown in Table 19 and Figure 71.

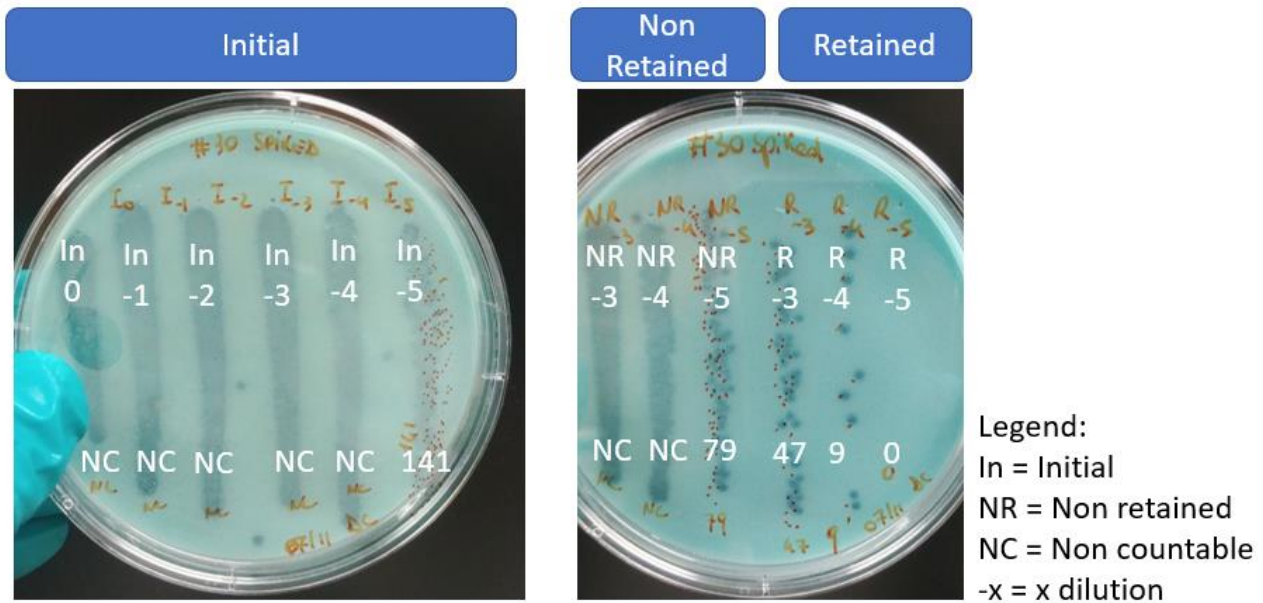


Figure 71-Spiked clinical sample with initial sample (resuspended swab with added colony) compared with retained and non-retained collected volume

As presented, the obtained capture efficiency is very low. One explanation for this result can be given by the very high concentration of resistant bacteria in the sample, equal to  $1.41 \cdot 10^9$  CFU/ml; from the previous section, in Table 16 and Table 17, highest capture efficiencies are obtained for high concentration of particle solution, with beads to bacteria ratio in the order of  $10^5$  or more. In addition, in section 4.1 is discussed as during the optimization of the bench-top assay, a minimum ratio of 950 beads per bacteria was needed to ensure sufficient capture.

Differently, considering the concentration of bacteria in the initial sample and concentration of particles reported in Table 19, the ratio computed is equal to 26, inferior of different orders of magnitude. In fact, considering the concentration of bacteria captured, compared with particle concentration, the ratio is equal to 5547, closer to the order of magnitude discussed; this may imply that only the amount of bacteria that could efficiently interact with the particles have been captured, and thus that a sample with lower concentration could result in better capture percentage. This reasoning is supported by the fact that a concentration of  $1.41 \cdot 10^9$  CFU/ml is not in the expected range from positive clinical sample, and thus expecting better performance in one of them, where concentration is lower, is reasonable.

Lately four more clinical samples covered the role of stabilizing the range of possible concentration to be expected; this demonstrated to be highly dispersed, as shown by Table 20

Table 20-Results from four clinical sample testing, as shown in Figure 72 and Figure 73

Sample	Measured initial concentration (CFU/ml)	Captured	Initial – Non Retained
1 <sup>st</sup>	$2.3 \cdot 10^7$	Impossible to quantify	77%
2 <sup>nd</sup>	$7 \cdot 10^2$	None	71%
3 <sup>rd</sup>	0	None	0%
4 <sup>th</sup>	0	None	0%



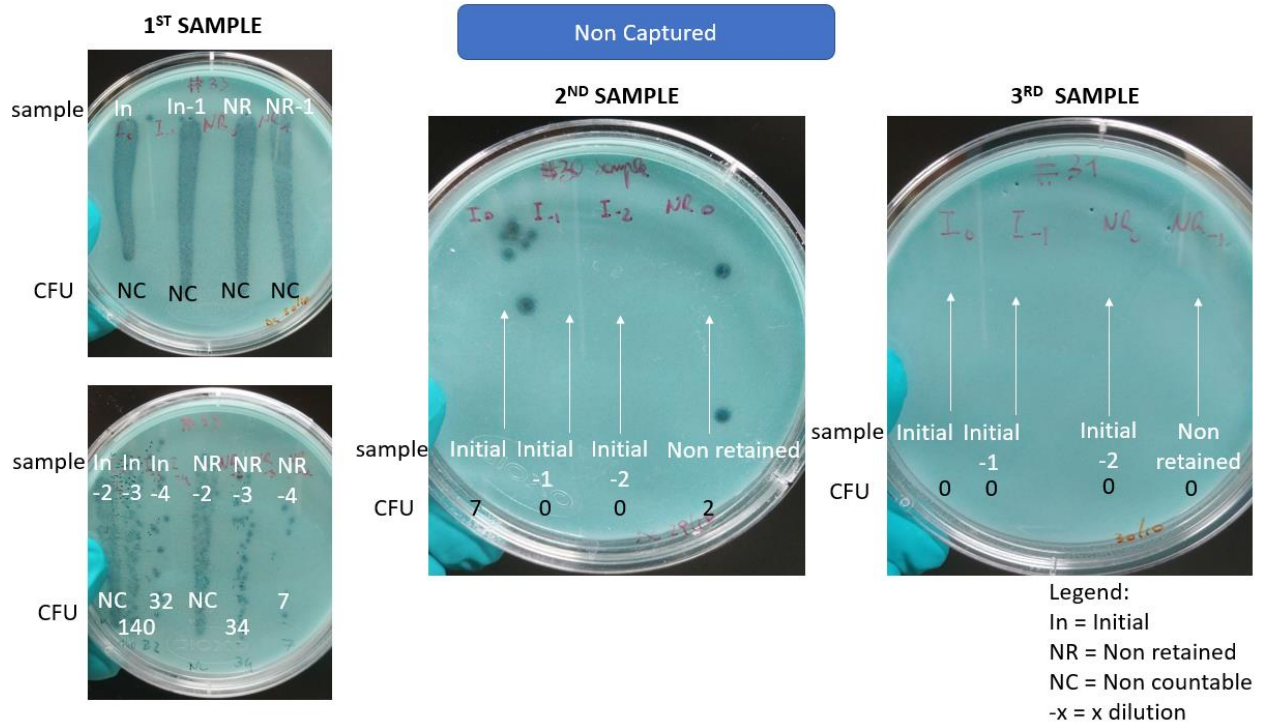


Figure 72-Result of plating sample aliquot and microfluidic non-retained outcome from three of the four clinical sample testing

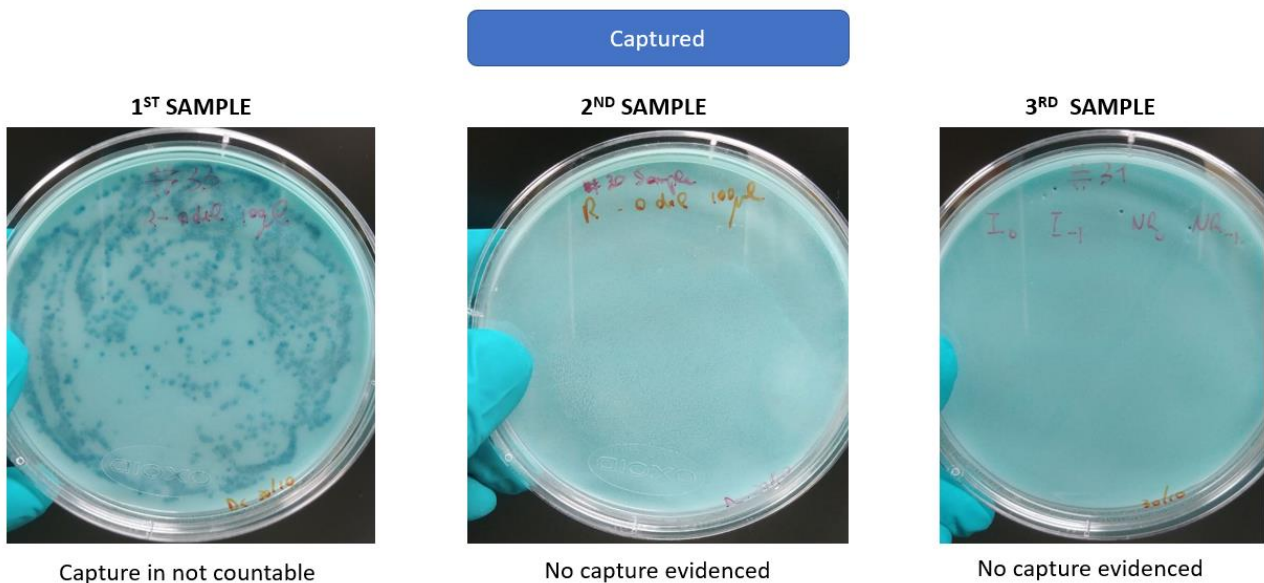


Figure 73- Result of plating microfluidic retained outcome from three of the four clinical sample testing

Given the different concentrations, unexpected in such a wide range, testing was not quantitatively efficient in identifying the results, but gave important qualitative information; approach on quantifying the results for new samples needs to evaluate a wider range of dilutions to cover all possible concentration. In addition, further tests can be promising, as the 1st sample showed capture at some level. In such sample, approximately 77% of cells are computed as difference between a plated aliquot of the original sample (initial) and aliquot from non-retained, and at the same time an unquantifiable number of cells are captured. The two amounts are necessary not equal, considering also how this computation was already discussed to be not reliable in evaluating the capture

percentage (section 4.1), but it suggests at least that capture was efficient at a certain rate, and would thus justify further testing, that are not part of this study.

## 5. Conclusions and Discussion

### 5.1. Importance of results

The realization and testing of a microfluidic device for sample preparation in the role of bacteria labelling and concentration have been discussed, and results compared with a previously optimized bench-top assay. It was demonstrated that the device can proficiently substitute the bench-top protocol as comparable, when not superior, capture efficiencies have been verified.

When tested with clinical samples, with the need to process a complex matrix and a high concentration of non-target bacteria, even if limited, results are shown promising, with capture obtained at expected concentration range, even though a quantitative analysis resulted impossible and further tests are required.

Coupling with a magnetic cytometer results, with the outcome of the device injected into the platform, is still not verified and preliminary results are briefly presented in section 5.2.

A further step has been made in the path of optimizing a platform formed by a sample pre-treatment device coupled with a magnetic cytometer, representing a suitable tool to achieve the aim of a rapid and efficient bacteria detection for hospital infections.

### 5.2. Future optimization of the studied platform: modification, improvements and integration in an automatic system

As discussed since the introduction of this work, the original purpose for the microfluidic device here produced and tested is pre-processing of an clinical sample for bacteria labelling and capture, to allow detection in a magnetic cytometer. Nevertheless, even if some features are designed with the attempt to address this goal, the device represent a general and adaptive tool from sample processing, involving a target bacteria solution of different kind and a magnetic particle solution, covered with any desired recognition element. The detection is not necessarily limited to magnetic sensors, as fluorescence or colorimetry, just to name some examples, could be implemented as well. Anyway, an attempt to verify successful bacteria labelling through magnetic cytometric detection is produced, as an early step on a discussion on optimization and improvements that are not part of this work and are left for future research.

Thus, 2 samples (bacteria suspensions in PB) prepared in the microfluidic device (second design) were assayed in the magnetic flow cytometer. The samples tested refers to non-retained (NR\_P) and retained(R\_P) volume from a positive sample (antibody specific for the target). Events, or peaks, have been selected according to the process discussed in section 3.4 and showed in Figure 74.

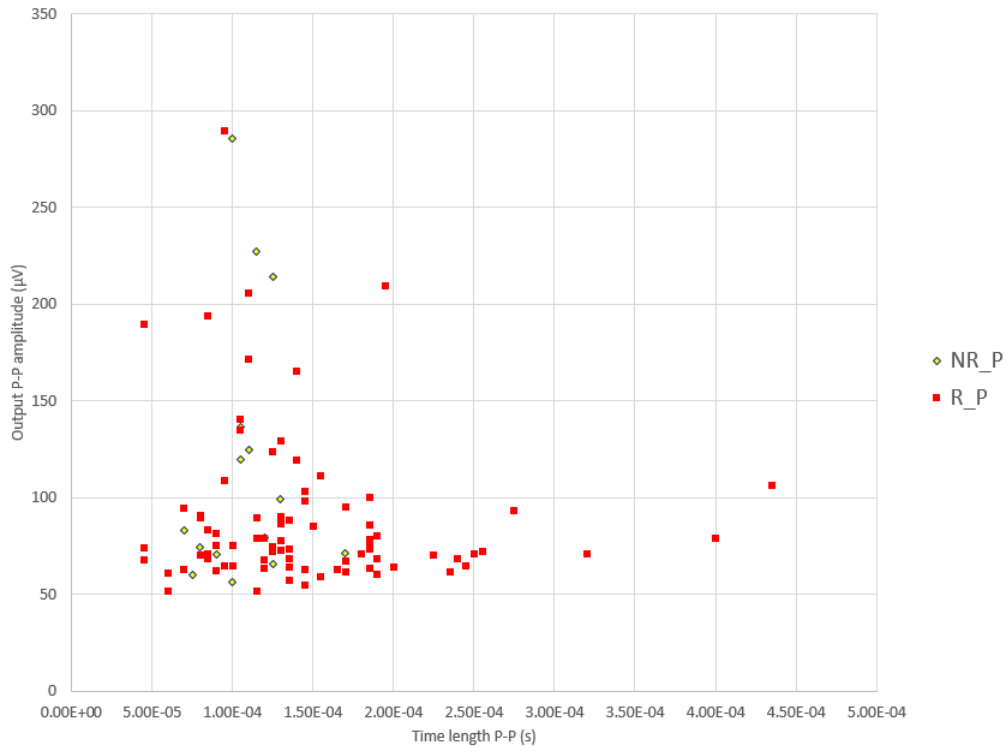


Figure 74-Analysis of output from first sensor as correlation between peak to peak time interval and peak to peak amplitude of the bipolar signal

The graph shows the detection of different peaks and the correlation between the peak-to-peak time interval and the peak-to-peak amplitude. It can be seen that an higher amount of peaks are detected for the retained volume, compared to the non-retained; this is in accordance with the results from colonies count obtained from plating method (refer to Appendix C: table with microfluidic and bench results comparison, 01/10/20, replica #2) where a capture of ~97% was measured. These results are a preliminary confirmation that cell labelling occurred. The presence of peaks in the non-retained volume can be due to cells that escaped the magnetic force produced by the magnet and thus were not captured by the system. In the context of a qualitative device, where the infection is wanted to be detected, but the amount of bacteria cells not necessary quantified, non-retained cells, if in small amount, are not detrimental. This factor becomes more important for samples with lower concentration, as even few bacteria cells not retained may be decisive for the downstream measure, depending also on detection method sensitivity.

Such limitations can be assessed by optimizing magnet position, dimension and field, as well as chamber geometry or applied flow rate, in order to maximise effective interactions of particles with the magnetic field and reduce phenomena of particle release prior to elution.

Nevertheless, it is important to outline that as reported by Soares et al. [4] [5] clusters of magnetic particles can form and can be detected by the cytometer. In order to distinguish between labelled cells and clusters, a classification of the detected peaks is needed, which is ahead the aim of this work and requires to be assessed separately.

A way to tackle such problem may be represented by the insertion of array of obstacles, similar to the one used in the serpentine, at the chamber outlet. The hypothesis here made is that such obstacles would promote further mixing between the eluting buffer and beads, and in such way reduce the dimensions of the formed cluster promoting homogenization. This step could help reducing the detection of bigger clusters and its interpretation as labelled cells.

Another aspect to deal with in a future perspective is the conversion of the device to complete automation. As presented in this work, the microfluidic device is not prone to be directly included in

a LoC PoC-oriented device, as external components and operator interventions are part of its functioning. All these elements, though, can be implemented as internal to the device so that the only required action is sample insertion in a specific well.

A solution of magnetic particles already functionalised with recognition elements, and elution buffers, can be stored in reservoirs and be injected in the serpentine, or in the chamber respectively, by a system of micropumps and microvalves electrically actuated. Such approach can eliminate untrained personal handling of connections and external pumps while standardizing the conditions of the detection, imposing more stable flows; as an example, implementation of thermo-actuated pneumatic micropump can be achieved as proposed by Chia [71], where heating of air sealed in a chamber can cause its dilation and consequential volume change cause diaphragm deformation that can push fluid toward the channel. Same peristaltic effect and PDMS deformability may also be exploited to design valves and direct flow [3].

The permanent magnet can be substituted by an electromagnet or eventually mechanically separated from the chamber during particle elution; the presence of an electromagnet though brings some limitations as the generally minor field intensity able to generate and the heat management necessary to deal with joule effect derived heat formation, possibly detrimental for biological samples. In conclusion, outlet processed by the device could be stored for a short period of time or directly coupled with a detection method, eventually a magnetic cytometer integrated on the same board.

## 6. References

- [1] De Mello, A. J., & Beard, N. (2003). Dealing with real samples: sample pre-treatment in microfluidic systems., *Lab Chip*, 3(1). <https://doi.org/10.1039/b301019h>.
- [2] Tang, R. H., Yang, H., Choi, J. R., Gong, Y., Feng, S. S., Pingguan-Murphy, B., ... Xu, F. (2017). Advances in paper-based sample pretreatment for point-of-care testing., *Critical Reviews in Biotechnology*, 37(4), 411–428. <https://doi.org/10.3109/07388551.2016.1164664>.
- [3] Lei, K. F. (2012). Microfluidic systems for diagnostic applications: A review., *Journal of Laboratory Automation*, 17(5), 330–347. <https://doi.org/10.1177/2211068212454853>.
- [4] Soares, A. R., Afonso, R., Caetano, D. M., Martins, V. C., Piedade, M., & Cardoso, S. (2019). Analytical strategy for magnetic flow cytometry signals classification., 6th IEEE Portuguese Meeting on Bioengineering, ENBENG 2019 - Proceedings, 2–5. <https://doi.org/10.1109/ENBENG.2019.8692507>.
- [5] Soares, A. R., Afonso, R., Lampreia, J., Joao, J., Martins, V. C., Piedade, M., & Cardoso, S. (2019). Automatic System to Count and Classify Bacteria Based on Magnetic Cytometry., *IEEE Magnetics Letters*, 10(June), 24–27. <https://doi.org/10.1109/LMAG.2019.2953865>.
- [6] Yang, P., Chen, Y., Jiang, S., Shen, P., Lu, X., & Xiao, Y. (2020). Association between the rate of fluoroquinolones-resistant gram-negative bacteria and antibiotic consumption from China based on 145 tertiary hospitals data in 2014., *BMC Infectious Diseases*, 20(1), 1–7. <https://doi.org/10.1186/s12879-020-04981-0>.
- [7] European Centre for Disease Prevention and Control. Antimicrobial resistance in the EU/EEA (EARS-Net), Annual Epidemiological Report 2019. Stockholm: ECDC; 2020..
- [8] Bohara, R. A., & Pawar, S. H. (2015). Innovative Developments in Bacterial Detection with Magnetic Nanoparticles., *Applied Biochemistry and Biotechnology*, 176(4), 1044–1058. <https://doi.org/10.1007/s12010-015-1628-9>.
- [9] Worthington, R. J., & Melander, C. (2013). Combination approaches to combat multidrug-resistant bacteria., *Trends in Biotechnology*, 31(3), 179–186. <https://doi.org/10.1016/j.tibtech.2012.12.006>.
- [1 Cassini, A., Högberg, L. D., Plachouras, D., Quattrocchi, A., Hoxha, A., Simonsen, G. S., Colomb-Cotinat, 0] M., Kretzschmar, M. E., Devleeschauwer, B., Cecchini, M., Ouakrim, D. A., Oliveira, T. C., Struelens, M. J., Suetens, C., Monnet, D. L., Strauss, R., *The Lancet Infectious Diseases*, 19(1), 56–66. [https://doi.org/10.1016/S1473-3099\(18\)30605-4](https://doi.org/10.1016/S1473-3099(18)30605-4).
- [1 Sonker, M., Sahore, V., & Woolley, A. T. (2017). Recent advances in microfluidic sample preparation 1] and separation techniques for molecular biomarker analysis: A critical review., *Analytica Chimica Acta*, 986, 1–11. <https://doi.org/10.1016/j.aca.2017.07.043>.
- [1 Nguyen, N. T., & Wu, Z. (2005). Micromixers - A review., *Journal of Micromechanics and 2] Microengineering*, 15(2), 1–16. <https://doi.org/10.1088/0960-1317/15/2/R01>.

- [1 Bhagat, A. A. S., Peterson, E. T. K., & Papautsky, I. (2007). A passive planar micromixer with  
3] obstructions for mixing at low Reynolds numbers., *Journal of Micromechanics and Microengineering*, 17(5), 1017–1024. <https://doi.org/10.1088/0960-1317/17/5/023.122>.
- [1 Lee, C., Wang, W., Liu, C., & Fu, L. (2016). Passive mixers in microfluidic systems : A review., *Chemical  
4] Engineering Journal*, 288, 146–160. <https://doi.org/10.1016/j.cej.2015.10.122>.
- [1 Bhagat, A. A. S., & Papautsky, I. (2008). Enhancing particle dispersion in a passive planar micromixer  
5] using rectangular obstacles., *Journal of Micromechanics and Microengineering*, 18(8).  
<https://doi.org/10.1088/0960-1317/18/8/085005>.
- [1 Tofteberg, T., Skolimowski, M., Andreassen, E., & Geschke, O. (2010). A novel passive micromixer:  
6] Lamination in a planar channel system., *Microfluidics and Nanofluidics*, 8(2), 209–215.  
<https://doi.org/10.1007/s10404-009-0456-z>.
- [1 Roudgar, M., Brunazzi, E., Galletti, C., & Mauri, R. (2012). Numerical Study of Split T-Micromixers.,  
7] *Chemical Engineering and Technology*, 35(7), 1291–1299. <https://doi.org/10.1002/ceat.201100611>.
- [1 Li, J., Xia, G., & Li, Y. (2013). Numerical and experimental analyses of planar asymmetric split-and-  
8] recombine micromixer with dislocation sub-channels., *Journal of Chemical Technology and  
Biotechnology*, 88(9), 1757–1765. <https://doi.org/10.1002/jctb.4044>.
- [1 Xia, H. M., Wang, Z. P., Koh, Y. X., & May, K. T. (2010). A microfluidic mixer with self-excited  
9] “turbulent” fluid motion for wide viscosity ratio applications., *Lab on a Chip*, 10(13), 1712–1716.  
<https://doi.org/10.1039/b925025e>.
- [2 Cortes-quiros, C. A., Azarbadegan, A., Zangeneh, M., & Goto, A. (2010). Analysis and multi-criteria  
0] design optimization of geometric characteristics of grooved micromixer., *Chemical Engineering  
Journal*, 160(3), 852–864. <https://doi.org/10.1016/j.cej.2010.02.029>.
- [2 Du, Y., Zhang, Z., Yim, C. H., Lin, M., & Cao, X. (2010). Evaluation of floor-grooved micromixers using  
1] concentration-channel length profiles., *Micromachines*, 1(1), 19–33.  
<https://doi.org/10.3390/mi1010019>.
- [2 Loferer-Krößbacher, M., Klima, J., & Psenner, R. (1998). Determination of bacterial cell dry mass by  
2] transmission electron microscopy and densitometric image analysis., *Applied and Environmental  
Microbiology*, 64(2), 688–694. <https://doi.org/10.1128/aem.64.2.688-694.1998>.
- [2 Wong, S. H., Bryant, P., Ward, M., & Wharton, C. (2003). Investigation of mixing in a cross-shaped  
3] micromixer with static mixing elements for reaction kinetics studies., *Sensors and Actuators, B:  
Chemical*, 95(1–3), 414–424. [https://doi.org/10.1016/S0925-4005\(03\)00447-7](https://doi.org/10.1016/S0925-4005(03)00447-7).
- [2 Fang, Y., Ye, Y., Shen, R., Zhu, P., Guo, R., Hu, Y., & Wu, L. (2012). Mixing enhancement by simple  
4] periodic geometric features in microchannels., *Chemical Engineering Journal*, 187, 306–310.  
<https://doi.org/10.1016/j.cej.2012.01.130>.
- [2 Fernandes, A. C., Duarte, C. M., Cardoso, F. A., Bexiga, R., Cardoso, S., & Freitas, P. P. (2014). Lab-on-  
5] chip cytometry based on magnetoresistive sensors for bacteria detection in milk., *Sensors  
(Switzerland)*, 14(8), 15496–15524. <https://doi.org/10.3390/s140815496>.

- [2 Loureiro, J., Fermon, C., Pannetier-Lecoeur, M., Arrias, G., Ferreira, R., Cardoso, S., & Freitas, P. P. 6] (2009). Magnetoresistive detection of magnetic beads flowing at high speed in microfluidic channels., *IEEE Transactions on Magnetics*, 45(10), 4873–4876. <https://doi.org/10.1109/TMAG.2009.2026287>.
- [2 Duarte, C., Costa, T., Carneiro, C., Soares, R., Jitariu, A., Cardoso, S., Piedade, M., Bexiga, R., & Freitas, 7] P. (2016). Semi-quantitative method for streptococci magnetic detection in raw milk., *Biosensors*, 6(2), 1–14. <https://doi.org/10.3390/bios6020019>.
- [2 Reisbeck, M., Helou, M. J., Richter, L., Kappes, B., Friedrich, O., & Hayden, O. (2016). Magnetic 8] fingerprints of rolling cells for quantitative flow cytometry in whole blood., *Scientific Reports*, 6, 1–11. <https://doi.org/10.1038/srep32838>.
- [2 Issadore, D., Chung, H. J., Chung, J., Budin, G., Weissleder, R., & Lee, H. (2013).  $\mu$ Hall chip for sensitive 9] detection of bacteria., *Advanced Healthcare Materials*, 2(9), 1224–1228. <https://doi.org/10.1002/adhm.201200380>.
- [3 Shen, W., Liu, X., Mazumdar, D., & Xiao, G. (2005). In situ detection of single micron-sized magnetic 0] beads using magnetic tunnel junction sensors., *Applied Physics Letters*, 86(25), 1–3. <https://doi.org/10.1063/1.1952582>.
- [3 Huang, L., Yuan, Z. H., Tao, B. S., Wan, C. H., Guo, P., Zhang, Q. T., Yin, L., Feng, J. F., Nakano, T., 1] Naganuma, H., Liu, H. F., Yan, Y., & Han, X. F. (2017)., Noise suppression and sensitivity manipulation of magnetic tunnel junction sensors with soft magnetic Co<sub>70.5</sub>Fe<sub>4.5</sub>Si<sub>15</sub>B<sub>10</sub> layer. *Journal of Applied Physics*, 122(11). <https://doi.org/10.1063/1.4990478>.
- [3 Dwivedi, H. P., & Jaykus, L. (2011). Detection of pathogens in foods : the current state- of-the-art and 2] future directions., *Critical Reviews in microbiology*.37(1):40-63. <https://doi.org/10.3109/1040841X.2010.506430>.
- [3 Bohaychuk, V. M., Gensler, G. E., King, R. K., Wu, J. T., & McMullen, L. M. (2005). Evaluation of 3] detection methods for screening meat and poultry products for the presence of foodborne pathogens., *Journal of Food Protection*, 68(12), 2637–2647. <https://doi.org/10.4315/0362-028X-68.12.2637>.
- [3 Oliveira, T. C. R. M., Barbut, S., & Griffiths, M. W. (2005). Detection of *Campylobacter jejuni* in naturally 4] contaminated chicken skin by melting peak analysis of amplicons in real-time PCR., *International Journal of Food Microbiology*, 104(1), 105–111. <https://doi.org/10.1016/j.ijfoodmicro.2005.02.008>.
- [3 Hsu, C. F., Tsai, T. Y., & Pan, T. M. (2005). Use of the duplex TaqMan PCR system for detection of Shiga- 5] like toxin-producing *Escherichia coli* O157., *Journal of Clinical Microbiology*, 43(6), 2668–2673. <https://doi.org/10.1128/JCM.43.6.2668-2673.2005>.
- [3 Hadjinicolaou, A. V., Demetriou, V. L., Emmanuel, M. A., Kakoyiannis, C. K., & Kostrikis, L. G. (2009)., 6] Molecular beacon-based real-time PCR detection of primary isolates of *salmonella typhimurium* and *salmonella enteritidis* in environmental and clinical samples. *BMC Microbiology*, 9, 1–14. <https://doi.org/10.1186/1471-2180-9-97>.
- [3 Cheng J, Sheldon EL, Wu L, Uribe A, Gerrue LO, Carrino J, Heller MJ,, *Nat Biotechnol* 16 (6), 541– 7] 6.<https://doi.org/10.1038/nbt0698-541>.



- [3 Hudson, J. A., Lake, R. J., Savill, M. G., Scholes, P., & McCormick, R. E. (2001). Rapid detection of *Listeria* monocytogenes in ham samples using immunomagnetic separation followed by polymerase chain reaction., *Journal of Applied Microbiology*, 90(4), 614–621. <https://doi.org/10.1046/j.1365-2672.2001.01287.x>.
- [3 Tully, E., Hearty, S., Leonard, P., & O’Kennedy, R. (2006). The development of rapid fluorescence-based immunoassays, using quantum dot-labelled antibodies for the detection of *Listeria monocytogenes* cell surface proteins., *International Journal of Biological Macromolecules*, 39(1–3), 127–134. <https://doi.org/10.1016/j.ijbiomac.2006.02.023>.
- [4 McClelland, R. G., & Pinder, A. C. (1994). Detection of *Salmonella typhimurium* in dairy products with flow cytometry and monoclonal antibodies., *Applied and Environmental Microbiology*, 60(12), 4255–4262. <https://doi.org/10.1128/aem.60.12.4255-4262.1994>.
- [4 Sakamoto, C., Yamaguchi, N., & Nasu, M. (2005). Rapid and simple quantification of bacterial cells by using a microfluidic device., *Applied and Environmental Microbiology*, 71(2), 1117–1121. <https://doi.org/10.1128/AEM.71.2.1117-1121.2005>.
- [4 Tanji, Y., Furukawa, C., Na, S. H., Hijikata, T., Miyanaga, K., & Unno, H. (2004). *Escherichia coli* detection by GFP-labeled lysozyme-inactivated T4 bacteriophage., *Journal of Biotechnology*, 114(1–2), 11–20. <https://doi.org/10.1016/j.jbiotec.2004.05.011>.
- [4 Jassim, S. A. A., & Griffiths, M. W. (2007). Evaluation of a rapid microbial detection method via phage lytic amplification assay coupled with Live/Dead fluorochromic stains., *Letters in Applied Microbiology*, 44(6), 673–678. <https://doi.org/10.1111/j.1472-765X.2007.02115.x>.
- [4 Guan J, Chan M, Allain B, Mandeville R, Brooks BW. (2006). Detection of multiple antibiotic-resistant *Salmonella enterica* serovar Typhimurium DT104 by phage replication-competitive enzymelinked immunosorbent assay., *J Food Prot* 69 (4), 739–42. <https://doi.org/10.4315/0362-028x-69.4.739>.
- [4 Joshi, R., Janagama, H., Dwivedi, H. P., Senthil Kumar, T. M. A., Jaykus, L. A., Schefers, J., & Sreevatsan, S. (2009). Selection, characterization, and application of DNA aptamers for the capture and detection of *Salmonella enterica* serovars., *Molecular and Cellular Probes*, 23(1), 20–28. <https://doi.org/10.1016/j.mcp.2008.10.006>.
- [4 Soares, R., Martins, V. C., Macedo, R., Cardoso, F. A., Martins, S. A. M., Caetano, D. M., Fonseca, P. H., Silvério, V., Cardoso, S., & Freitas, P. P. (2019). Go with the flow: advances and trends in magnetic flow cytometry., *Analytical and Bioanalytical Chemistry*, 411(9), 1839–1862. <https://doi.org/10.1007/s00216-019-01593-9>.
- [4 Murali, P., Niknejad, A. M., & Boser, B. E. (2017). CMOS Microflow Cytometer for Magnetic Label Detection and Classification., *IEEE Journal of Solid-State Circuits*, 52(2), 543–555. <https://doi.org/10.1109/JSSC.2016.2621036>.
- [4 Cubells-Beltrán, M. D., Reig, C., Madrenas, J., De Marcellis, A., Santos, J., Cardoso, S., & Freitas, P. P. (2016). Integration of GMR sensors with different technologies., *Sensors (Switzerland)*, 16(6), 1–21. <https://doi.org/10.3390/s16060939>.

- [4 Shen, W., Schrag, B. D., Carter, M. J., Xie, J., Xu, C., Sun, S., & Xiao, G. (2008). Detection of DNA labeled  
9] with magnetic nanoparticles using MgO-based magnetic tunnel junction sensors., *Journal of Applied Physics*, 103(7), 14–17. <https://doi.org/10.1063/1.2832880>.
- [5 Freitas P., Cardoso F., Martins V.C., Martins S. AM., Loureiro J., Amaral J., Chaves R. C., Cardoso S.,  
0] Fonseca L. P., Sebastião A. M., Pannetier-Lecoeur M., Fermon C.,(2012). Spintronic platforms for  
biomedical applications., *Lab on a Chip*, 546–557. <https://doi.org/10.1039/c1lc20791a>.
- [5 Plouffe, B. D., Murthy, S. K., & Lewis, L. H. (2015). Fundamentals and application of magnetic particles  
1] in cell isolation and enrichment: A review., *Reports on Progress in Physics*, 78(1).  
<https://doi.org/10.1088/0034-4885/78/1/016601>.
- [5 Hagens, S., & Loessner, M. J. (2007). Application of bacteriophages for detection and control of  
2] foodborne pathogens., *Applied Microbiology and Biotechnology*, 76(3), 513–519.  
<https://doi.org/10.1007/s00253-007-1031-8>.
- [5 Xuan, X., Zhu, J., & Church, C. (2010). Particle focusing in microfluidic devices. *Microfluidics and*  
3] *Nanofluidics*, 9(1), 1–16. <https://doi.org/10.1007/s10404-010-0602-7>.
- [5 Sieuwerts, S., De Bok, F. A. M., Mols, E., De Vos, W. M., & Van Hylckama Vlieg, J. E. T. (2008). A simple  
4] and fast method for determining colony forming units., *Letters in Applied Microbiology*, 47(4), 275–  
278. <https://doi.org/10.1111/j.1472-765X.2008.02417.x>.
- [5 Naghili, H., Tajik, H., Mardani, K., Razavi Rouhani, S. M., Ehsani, A., & Zare, P. (2013). Validation of drop  
5] plate technique for bacterial enumeration by parametric and nonparametric tests., *Veterinary  
Research Forum : An International Quarterly Journal*, 4(3), 179–183.  
<http://www.ncbi.nlm.nih.gov/pubmed/25653794>  
<http://www.pubmedcentral.nih.gov/articlerender.fcgi?artid=PMC4312378>.
- [5 Babine, R. E., & Bender, S. L. (1997). Molecular recognition of protein-ligand complexes: Applications  
6] to drug design., *Chemical Reviews*, 97(5), 1359–1472. <https://doi.org/10.1021/cr960370z>.
- [5 Weber PC, Ohlendorf DH, Wendoloski JJ, Salemme FR.(1989). Structural origins of high-affinity biotin  
7] binding to streptavidin., *Science*. Jan 6;243(4887):85-8. doi: 10.1126/science.2911722..
- [5 Qin, D., Xia, Y., & Whitesides, G. M. (2010). Soft lithography for micro- and nanoscale patterning.,  
8] *Nature Protocols*, 5(3), 491–502. <https://doi.org/10.1038/nprot.2009.234>.
- [5 Sushanta K. Mitra, Suman Chakraborty, (2011), *Microfluidics and Nanofluidics Handbook*, CRC Press, p  
9] 252.
- [6 Paik, S., Kim, G., Chang, S., Lee, S., Jin, D., Jeong, K. Y., Lee, I. S., ... Shim, W. (2020). Near-field sub-  
0] diffraction photolithography with an elastomeric photomask., *Nature Communications*, 11(1), 1–13.  
<https://doi.org/10.1038/s41467-020-14439-1>.
- [6 Sahu, N., Parija, B., & Panigrahi, S. (2009). Fundamental understanding and modeling of spin coating  
1] process: A review., *Indian Journal of Physics*, 83(4), 493–502. <https://doi.org/10.1007/s12648-009-0009-z>.

- [6 Duffy, D. C., McDonald, J. C., Schueller, O. J. A., & Whitesides, G. M. (1998). Rapid prototyping of  
2] microfluidic systems in poly(dimethylsiloxane)., *Analytical Chemistry*, 70(23), 4974–4984.  
<https://doi.org/10.1021/ac980656z>.
- [6 Xiong, L., Chen, P., & Zhou, Q. (2014). Adhesion promotion between PDMS and glass by oxygen plasma  
3] pre-treatment., *Journal of Adhesion Science and Technology*, 28(11), 1046–1054.  
<https://doi.org/10.1080/01694243.2014.883774>.
- [6 Qiu, J., Zhou, Y., Chen, H., & Lin, J. M. (2009). Immunomagnetic separation and rapid detection of  
4] bacteria using bioluminescence and microfluidics., *Talanta*, 79(3), 787–795.  
<https://doi.org/10.1016/j.talanta.2009.05.003> .
- [6 Three dimensional structure from RCSB Protein DataBank (PDB), <https://www.rcsb.org/structure/1stp>.  
5]
- [6 Zhang, D. W., Xiang, Y., & Zhang, J. Z. H. (2003). New advance in computational chemistry: Full  
6] quantum mechanical ab initio computation of streptavidin - Biotin interaction energy., *Journal of  
Physical Chemistry B*, 107(44), 12039–12041. <https://doi.org/10.1021/jp0359081>.
- [6 Lin, Y. S., Tsai, P. J., Weng, M. F., & Chen, Y. C. (2005). Affinity capture using vancomycin-bound  
7] magnetic nanoparticles for the MALDI-MS analysis of bacteria., *Analytical Chemistry*, 77(6), 1753–  
1760. <https://doi.org/10.1021/ac048990k>.
- [6 Skjerve E., Rorvik L.M., Olsvik O. (1990). Detection of *Listeria monocytogenes* in foods by  
8] Immunmagnetic Separation, *Applied and Environmental Microbiology*, p.3478-3481. doi:  
10.1128/AEM.56.11.3478-3481.1990.
- [6 Guan, X., Zhang, H., Bi, Y., & Zhang, L. (2010). Rapid detection of pathogens using antibody-coated  
9] microbeads with bioluminescence in microfluidic chips., 683–691. <https://doi.org/10.1007/s10544-010-9421-6>.
- [7 Biehl, L. M., Garzetti, D., Farowski, F., Ring, D., Koepfel, M. B., Rohde, H., Schafhausen, P., Stecher, B.,  
0] & Vehreschild, M. J. G. T. (2019). Usability of rectal swabs for microbiome sampling in a cohort study of  
hematological and oncological patients., *PLoS ONE*, 14(4).  
<https://doi.org/10.1371/journal.pone.0215428>.
- [7 Chia, B. T., Liao, H. H., & Yang, Y. J. (2011). A novel thermo-pneumatic peristaltic micropump with low  
1] temperature elevation on working fluid., *Sensors and Actuators, A: Physical*, 165(1), 86–93.  
<https://doi.org/10.1016/j.sna.2010.02.018>.
- [7 Magiorakos, A.-P., Srinivasan, A., Carey, R.B., Carmeli, Y., Falagas, M.E., Giske, C.G., Harbarth, S.,  
2] Hindler, J.F., Kahlmeter, G., Olsson-Liljequist, B., Paterson, D.L., Rice, L.B., Stelling, J., Struelens, M.J.,  
Vatopoulos, A., Weber, J.T. and Monnet,, Multidrug-resistant, extensively drug-resistant and pandrug-  
resistant bacteria: an international expert proposal for interim standard definitions for acquired  
resistance. *Clinical Microbiology and Infection*, 18: 268-281. doi:10.1111/j.1469-0691.2011.03570.
- [7 Kee, S. P., & Gavriilidis, A. (2008). Design and characterisation of the staggered herringbone mixer.,  
3] *Chemical Engineering Journal*, 142(1), 109–121. <https://doi.org/10.1016/j.cej.2008.02.001>.
- [7 Issadore, D., Chung, J., Shao, H., Liong, M., Ghazani, A. A., Castro, C. M., Weissleder, R., & Lee, H.  
4] (2012). Ultrasensitive clinical enumeration of rare cells ex vivo using a micro-hall detector.[1] D.

Issadore, J. Chung, H. Shao, et al., "Ultrasensitive clinical enumeration of rare cells ex vivo using a micro-hall detector," *Sci. Transl. Med.*, vol. 4, no. 141, Science Translational Medicine, 4(141), 141ra92. <https://doi.org/10.1126/scitranslmed.3003747>.

[7 Freitas, P. P., Ferreira, R., Cardoso, S., & Cardoso, F. (2007). Magnetoresistive sensors., *Journal of Physics Condensed Matter*, 19(16). <https://doi.org/10.1088/0953-8984/19/16/165221>.

[7 Chícharo, A., Martins, M., Barnsley, L. C., Taouallah, A., Fernandes, J., Silva, B. F. B., Cardoso, S.,  
6] Diéguez, L., Espiña, B., & Freitas, P. P. (2018). Enhanced magnetic microcytometer with 3D flow focusing for cell enumeration., *Lab on a Chip*, 18(17), 2593–2603. <https://doi.org/10.1039/c8lc00486b>.

[7 Rifai, D., Abdalla, A. N., Ali, K., & Razali, R. (2016). Giant magnetoresistance sensors: A review on  
7] structures and non-destructive eddy current testing applications., *Sensors (Switzerland)*, 16(3). <https://doi.org/10.3390/s16030298>.

## 7. Appendix

### 7.1. Appendix A: Ademtech beads Datasheet



#### Bio-Adembeads Streptavidin plus 0322

For research use only

#### PRODUCT DESCRIPTION

Bio-Adembeads Streptavidin plus are monodispersed and superparamagnetic particles coated with streptavidin. They are produced under aseptic conditions and are supplied in an aqueous suspension containing 0.05% Proclin 300.

#### Physical characteristics

Diameter : 200 nm (CV max 20%)  
Density : approx. 2.0 g/cm<sup>3</sup>  
Magnetisation at saturation : approx. 40 emu/g  
Specific surface area : 15 m<sup>2</sup>/g  
Iron oxide content : approx. 70%  
Solid content : 5 mg/ml

#### Streptavidin

Streptavidin is a protein produced by *Streptomyces avidinii* and isolated from fermentation filtrates. The protein is composed of four identical subunits. Each one can bind a molecule of biotin with a high affinity ( $K_D = 10^{-15} M^{-1}$ ). Specific activity is >14.0 U/mg protein.

#### Binding Capacity

Bio-Adembeads plus bind more than 1600 moles of biotin per mg.

#### PRINCIPLE

Bio-Adembeads Streptavidin plus are used for binding biotinylated ligands such as oligonucleotides, nucleic acids or proteins. Their high iron oxide content associated with the powerful streptavidin-biotin interaction, make Bio-Adembeads Streptavidin plus a very efficient tool for separation assays.

Version 1.2

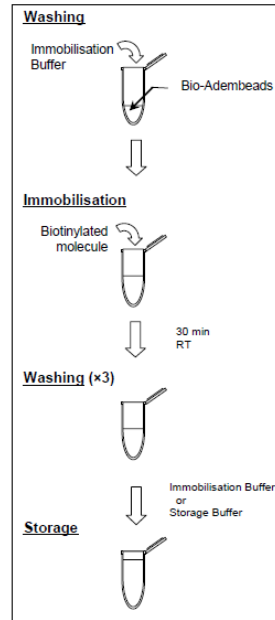
#### INSTRUCTION FOR USE

##### A) Washing procedure

1. Resuspend the Bio-Adembeads Streptavidin plus by pipetting and vortexing. Avoid foaming.
2. Pipette the volume to be used into the desired test tube.
3. Place the tube in a magnet (see Related Products) for 1min.
4. Pipette off the supernatant carefully, leaving beads undisturbed.
5. Remove the test tube from the magnet (see Related Products) and resuspend the beads carefully in the original sample volume with adequate buffer (Immobilisation Buffer recommended, see Related Products).

##### B) Immobilisation of biotinylated molecules

1. Wash the Bio-Adembeads Streptavidin plus twice with Immobilisation Buffer pH 7.
2. Resuspend the beads in Immobilisation Buffer to a final concentration of 5mg/mL.
3. Add the biotinylated molecule, and incubate at room temperature 30min under gentle rotation.
4. Place the tube in a magnet for 1-2min.
5. Pipette off the supernatant carefully, leaving beads undisturbed.
6. Wash 3 times with Immobilisation Buffer for an immediate use (or with the storage Buffer), and resuspend to the desired concentration.



#### ADDITIONAL MATERIAL REQUIRED

- Magnetic device
- Rotation device
- Test tubes
- Related products: [Buffers solutions](#)
  - Storage Buffer (#10201)
  - Immobilisation Buffer (#10301)[Magnetic Devices](#)
  - Adem-Mag SV, 1.5 ml (#20101)
  - Adem-Mag MV, 15 ml (#20102)
  - Adem-Mag HV, 50 ml (#20103)

#### STORAGE/STABILITY

When stored in unopened vials at 2-8°C, Bio-Adembeads are stable until expiration date printed on the label. The Bio-Adembeads must be maintained in liquid during storage and all handling steps. Drying will result in reduced performance. Do not freeze the product.

#### PRECAUTIONS

Precautions should be taken to prevent bacterial contamination of protein-coated Adembeads. If cytotoxic preservatives are added these must be carefully removed before use by washing.

#### WARNINGS AND LIMITATIONS

For *in vitro* research only. Not for use in human diagnostic or therapeutic procedures.

Proclin 300 is toxic if ingested. Avoid pipetting by mouth.

#### WARRANTY

The products are warranted to the original purchaser only to conform to the quality and contents stated on the vial and outer labels for duration of the stated shelf life. Ademtech's obligation and the purchaser's exclusive remedy under this warranty is limited either to replacement, at Ademtech's expense, of any products which shall be defective in manufacture, and which shall be returned to Ademtech, transportation prepaid, or at Ademtech's option, refund of the purchase price.

Claims for merchandise damaged in transit must be submitted to the carrier.

Ademtech SA – Bioparc BioGallien - 27, allée Charles Darwin - 33600 PESSAC - FRANCE  
[www.ademtech.com](http://www.ademtech.com)

7.2. Appendix B: table with summarized bench results

Date	Sample	Target Bacteria	Capture %
01_10_20	Positive(specific) #1	Klebsiella dilution - 3	96.39
	Positive(specific) #2	Klebsiella dilution - 3	96.05
	Negative(aspecific) #1	Klebsiella dilution - 3	1.38
	Negative(aspecific) #2	Klebsiella dilution - 3	2.97
27_09_20	Positive(specific) #1	Klebsiella dilution - 3	77.83
	Positive(specific) #2	Klebsiella dilution - 3	88.77
	Negative(aspecific) #1	Klebsiella dilution - 3	2.36
	Negative(aspecific) #2	Klebsiella dilution - 3	7.79
23_09_20	Positive(specific) #1	Klebsiella dilution - 3	73.27
	Positive(specific) #2	Klebsiella dilution - 3	84.42
	Negative(aspecific) #1	Klebsiella dilution - 3	6.92
	Negative(aspecific) #2	Klebsiella dilution - 3	5.50
15_09_20	Positive(specific) #1	Klebsiella dilution - 3	99.29
	Positive(specific) #2	Klebsiella dilution - 3	99.38

	Negative(aspecific) #1	Klebsiella dilution - 3	3.07
	Negative(aspecific) #2	Klebsiella dilution - 3	3.38

Date	Sample	Target Bacteria	Capture %
02_09_20	Positive(specific) #1	Klebsiella dilution -1	47.69
	Positive(specific) #2	Klebsiella dilution -1	48.15
	Positive(specific) #3	Klebsiella dilution -1	43.92
	Negative(aspecific) #1	Klebsiella dilution -1	1.23
	Negative(aspecific) #2	Klebsiella dilution -1	1.23
	Negative(aspecific) #3	Klebsiella dilution -1	1.44
	Positive(specific) #1	Klebsiella dilution -3	83.56
	Positive(specific) #2	Klebsiella dilution -3	84.05
	Positive(specific) #3	Klebsiella dilution -3	82.22
04_08_20	Positive(specific) #1	Klebsiella dilution -1	53.92
	Positive(specific) #2	Klebsiella dilution -1	54.00
	Positive(specific) #3	Klebsiella dilution -1	50.77
	Negative(aspecific) #1	Klebsiella dilution -1	0.58
	Negative(aspecific) #2	Klebsiella dilution -1	1.18
	Negative(aspecific) #3	Klebsiella dilution -1	1.31
	Positive(specific) #1	Klebsiella dilution -3	67.03
	Positive(specific) #2	Klebsiella dilution -3	75.59
	Positive(specific) #3	Klebsiella dilution -3	70.30
	Negative(aspecific) #1	Klebsiella dilution -3	1.12
	Negative(aspecific) #2	Klebsiella dilution -3	1.70
	Negative(aspecific) #3	Klebsiella dilution -3	1.99

Date	Sample	Target Bacteria	Capture %
28_07_20	Positive(specific) #1	Klebsiella dilution -1	90.14
	Positive(specific) #2	Klebsiella dilution -1	89.02
	Negative(asepecific) #1	Klebsiella dilution -1	3.12
	Negative(asepecific) #2	Klebsiella dilution -1	2.32
	Positive(specific) #1	Klebsiella dilution -3	83.12
	Positive(specific) #2	Klebsiella dilution -3	87.18
	Negative(asepecific) #1	Klebsiella dilution -3	1.83
	Negative(asepecific) #2	Klebsiella dilution -3	4.03
26_07_20	Positive(specific) #1	Klebsiella dilution -1	88.94
	Positive(specific) #2	Klebsiella dilution -1	91.92
	Negative(asepecific) #1	Klebsiella dilution -1	2.23
	Negative(asepecific) #2	Klebsiella dilution -1	1.85
	Positive(specific) #1	Klebsiella dilution -3	95.81
	Positive(specific) #2	Klebsiella dilution -3	97.56
	Negative(asepecific) #1	Klebsiella dilution -3	7.99
	Negative(asepecific) #2	Klebsiella dilution -3	8.35

Sample	Dilution	Concentration[CFU/ml]	Mean(%)	SD(%)
Positive	-1 dil	$2 \cdot 10^7$	65.85	21.01
	-3 dil	$2 \cdot 10^5$	85.66	10.23
Negative	-1 dil	$2 \cdot 10^7$	1.65	0.74
	-3 dil	$2 \cdot 10^5$	4.03	2.59



7.3. Appendix C: table with microfluidic and bench results comparison

Date	Bench			Microfluidic - Second design		
	Sample	Target Bacteria	Capture %	Sample	Target Bacteria	Capture %
01_10_20	Positive(specific) #1	Klebsiella dilution -3	96.39	Positive(specific) #1	Klebsiella dilution - 3	97.30
	Positive(specific) #2	Klebsiella dilution -3	96.05	Positive(specific) #2	Klebsiella dilution - 3	97.05
	Negative(aspecific) #1	Klebsiella dilution -3	1.38	Negative(aspecific) #1	Klebsiella dilution - 3	6.89
	Negative(aspecific) #2	Klebsiella dilution -3	2.97	Negative(aspecific) #2	Klebsiella dilution - 3	2.61
27_09_20	Positive(specific) #1	Klebsiella dilution -3	77.83	Positive(specific) #1	Klebsiella dilution - 3	100.00
	Positive(specific) #2	Klebsiella dilution -3	88.77	Positive(specific) #2	Klebsiella dilution - 3	100.00
	Negative(aspecific) #1	Klebsiella dilution -3	2.36	Negative(aspecific) #1	Klebsiella dilution - 3	6.71
	Negative(aspecific) #2	Klebsiella dilution -3	7.79	Negative(aspecific) #2	Klebsiella dilution - 3	5.76
23_09_20	Positive(specific) #1	Klebsiella dilution -3	73.27	Positive(specific) #1	Klebsiella dilution - 3	98.67
	Positive(specific) #2	Klebsiella dilution -3	84.42	Positive(specific) #2	Klebsiella dilution - 3	98.43
	Negative(aspecific) #1	Klebsiella dilution -3	6.92	Negative(aspecific) #1	Klebsiella dilution - 3	1.63
	Negative(aspecific) #2	Klebsiella dilution -3	5.50	Negative(aspecific) #2	Klebsiella dilution - 3	5.86

Microfluidic - First design			
Date	Sample	Target Bacteria	Capture %
09_10_20	Positive(specific) #1	Klebsiella dilution -3	100.00%
	Positive(specific) #2	Klebsiella dilution -3	100.00%
	Negative(aspecific) #1	Klebsiella dilution -3	28.97%
	Negative(aspecific) #2	Klebsiella dilution -3	11.59%
10_10_20	Positive(specific) #1	Klebsiella dilution -3	82.85%
	Positive(specific) #2	Klebsiella dilution -3	62.94%
	Negative(aspecific) #1	Klebsiella dilution -3	0.65%
	Negative(aspecific) #2	Klebsiella dilution -3	0.72%
11_10_20	Positive(specific) #1	Klebsiella dilution -3	69.05%
	Positive(specific) #2	Klebsiella dilution -3	47.06%
	Negative(aspecific) #1	Klebsiella dilution -3	1.67%
	Negative(aspecific) #2	Klebsiella dilution -3	1.26%

7.4. Appendix D: Su-8 Datasheet



**NANO™ SU-8**  
**Negative Tone**  
**Photoresists**  
**Formulations 50 & 100**

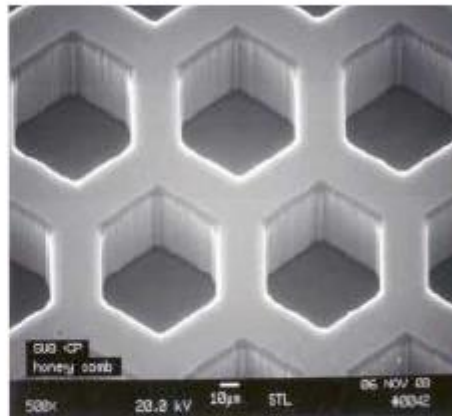
- High aspect ratio imaging with near vertical side walls
- Near UV (350-400nm) processing
- Film thicknesses from 1 to >200µm with single spin coat processes
- Superb chemical and temperature resistance

SU-8 is a chemically amplified, high contrast, epoxy based photoresist designed for micromachining and other micro-electronic applications. SU-8 is a negative tone photoresist. The exposed and subsequently cross-linked portions of the film are rendered insoluble to liquid developers. SU-8 has very high optical transparency, which makes it ideally suited for imaging near vertical sidewalls in very thick films. SU-8 is best suited for permanent applications where it is imaged, cured and left in place.

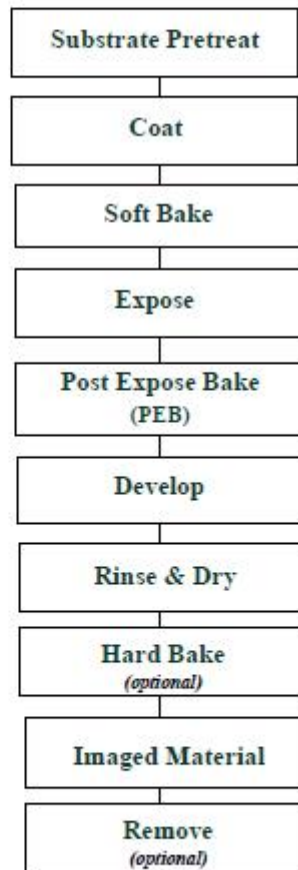
**Process Guidelines**

SU-8 is most commonly processed with conventional near UV (300-400nm) radiation, although it may be imaged with e-beam or x-ray. i-line(365nm) is recommended. Upon exposure, cross-linking proceeds in two-steps (1) formation of a strong acid during the exposure process, followed by (2) acid-initiated, thermally driven epoxy cross-linking during the post exposure bake (PEB) step.

A normal process is: spin coat, soft bake, expose, post expose bake (PEB) and develop. A controlled hard bake is recommended to further cross-link the imaged SU-8 structures when they it will remain as part of the device. The entire process should be optimized for the specific application. A baseline process is given here to be used as a starting point.



*Honey comb structure in thick SU-8 resist*



### Substrate Pretreatment

To obtain maximum process reliability, substrates should be clean and dry prior to applying the SU-8 resist. Start with a solvent cleaning, or a rinse with dilute acid, followed by a DI water rinse. Piranha Etch of the substrates is highly recommended. To dehydrate the surface, bake at 200 °C for 5 minutes on a contact hot plate or 30 minutes in a convection oven. Adhesion promoters are typically not required.

### Coat

SU-8 resists are designed to produce low defect coatings over a very broad range of film thickness using a variety of spin coat conditions. The film thickness versus spin speed data and plots displayed in Table 1. and Figure 1. provide the information required to select the appropriate SU-8 resist and spin conditions, based upon the desired film thickness.

#### Recommended spin coat conditions:

- (1) Dispense approximately 1ml of resist per inch of substrate diameter.
- (2) Spread Cycle: Ramp to 500 rpm at 100rpm/second acceleration and hold for a total of 10 seconds. That is, 5 seconds getting to 500 rpm plus another 5 seconds at 500 rpm. This is necessary since the viscosity of the material is so high.
- (3) Spin Cycle: Ramp to final spin speed, based on film thickness desired, at an acceleration of 300 rpm/sec and hold for a total of 30 seconds.

Product	Viscosity** cst @ 25°C	Thickness µm	Spin Speed rpm
SU-8 50		40	3000
		50	2000
		100	1000
SU-8 100		100	3000
		150	2000
		250	1000

Table 1. Thickness vs. spin speed data for selected SU-8 resists

\*\* Approximate

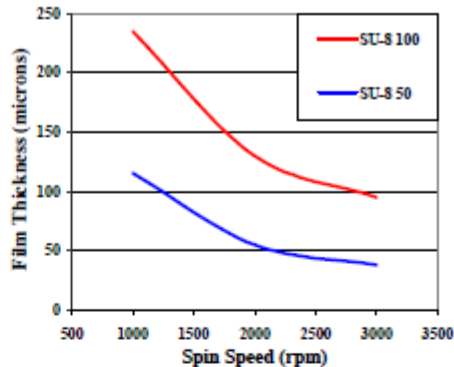


Figure 1. Film thickness vs. spin speed.

### Soft Bake

After the resist has been applied to the substrate, it must be soft baked to evaporate the solvent and densify the film. SU-8 is normally baked on a hot plate, although convection ovens may be used. The following bake times are based on contact hot plate processes. Bake times should be optimized for proximity and convection oven bake processes since solvent evaporation rate is influenced by rate of heat transfer and ventilation.

For best results, ramping or stepping the soft bake temperature is recommended. Lower initial bake temperatures allow the solvent to evaporate out of the film at a more controlled rate, which results in better coating fidelity, reduced edge beads and better resist to substrate adhesion. Refer to Table 2. for recommendations for TWO STEP contact hot plate processes

Product	Thickness µm	Soft Bake Time (minutes)	
		STEP 1 65°C	STEP 2 95°C
SU-8 50	40	5	15
	50	6	20
	100	10	30
SU-8 100	100	10	30
	150	20	50
	250	30	90

Table 2. Recommended soft bake processes.

### Expose

SU-8 is optimized for near UV (350-400nm) exposure. It is virtually transparent and insensitive above 400nm and is highly absorbent and reactive to energy below 350nm. This can be seen in Figure 2. Excessive dose below 350nm may result in over exposure of the top portion of the resist film, resulting in exaggerated negative sidewall profiles or T-topping. The optimal exposure dose will depend on film thickness (thicker films require higher dosage) and process parameters. The exposure dose range recommendations in Table 3. are based on exposure source intensity measurements taken with an i-line (365nm) radiometer and probe.

**Expose tip:** When using a broad spectral output source, for best imaging results, i.e. straightest sidewalls, filter out excessive energy below 350nm.

Catastrophic adhesion failure, severely negative sidewalls and excessive cracking are often indications of an under cross-linking condition. To correct the problem, increase your exposure dose and or increase your post exposure bake (PEB) time.

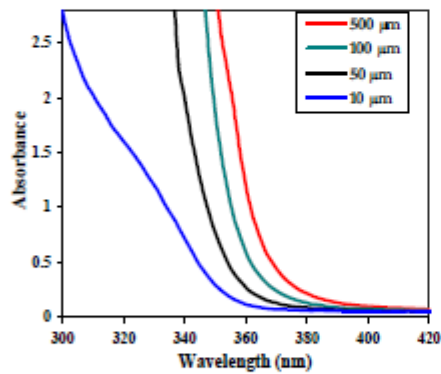


Figure 2. SU-8 absorbance vs. film thickness

Product	Thickness $\mu\text{m}$	Expose Dose $\text{mJ}/\text{cm}^2$
SU-8 50	40	250-300
	50	400-500
	100	500-650
SU-8 100	100	500-650
	150	600-675
	250	625-700

Table 3. Recommended expose dose processes.

### Post Expose Bake

Following exposure, a post exposure bake (PEB) must be performed to selectively cross-link the exposed portions of the film. SU-8 can be post exposure baked (PEB) either on a hot plate or in a convection oven. Optimum cross-link density is realized through careful adjustments of the exposure and PEB process conditions. The bake recommendations below are based on results obtained on a contact hot plate.

**PEB Tip:** SU-8 is readily cross-linked and can result in a highly stressed film. To minimize stress, wafer bowing and resist cracking, a slow ramp or TWO STEP contact hot plate process, as shown in Table 4, is recommended. Avoid rapid cooling after PEB.

Product	Thickness $\mu\text{m}$	PEB Time (minutes)	
		STEP 1 65°C	STEP 2 95°C
SU-8 50	40	2	4
	50	2	5
	100	3	10
SU-8 100	100	3	10
	150	12	15
	250	15	25

Table 4. Recommended PEB processes.

### Develop

SU-8 resists have been optimized for use with MicroChem's SU-8 Developer. Immersion, spray or spray-puddle processes can be used. Other solvent developers such as ethyl lactate and diacetone alcohol may also be used. Strong agitation is recommended for high aspect ratio and/or thick film structures. Recommended develop times are given in Table 5. for immersion processes. These proposed develop times are approximate, since actual dissolution rates can vary widely as a function of agitation rate, temperature and resist processing parameters.

Product	Thickness $\mu\text{m}$	Development minutes
SU-8 50	40	6
	50	6
	100	10
SU-8 100	100	10
	150	15
	200	15
	250	25

Table 5. Recommended develop processes.

### Rinse and Dry

Following development, the substrate should be rinsed briefly with isopropyl alcohol (IPA), then dried with a gentle stream of air or nitrogen.

**Rinse tip:** If a white film is produced during rinse, this is an indication that the substrate has been under developed. Simply immerse or spray the substrate with SU-8 developer to remove the film and complete the development process. Repeat the rinse step.

### Hard Bake (cure)

SU-8 has good mechanical properties, therefore hard bakes are normally not required. For applications where the imaged resist is to be left as part of the final device, the resist may be ramp/step hard baked between 150-200°C on a hot plate or in a convection oven to further cross link the material. Bake times vary based on type of bake process and film thickness.

### Remove

SU-8, after expose and PEB, is a highly cross-linked epoxy, which makes it extremely difficult to remove with conventional solvent based resist strippers. MicroChem's Remover PG will swell and lift off minimally cross-linked SU-8. It will not remove fully cured or hard baked SU-8. Alternate removal processes include immersion in oxidizing acids such as piranha etch/clean, RIE, laser ablation and pyrolysis.

To remove minimally cross-linked SU-8 with Remover PG, heat the bath to 50-80° C and immerse the substrates for 30-90 minutes. Actual strip time will depend on resist thickness and cross-link density.

### Storage

Store SU-8 resists upright in tightly closed containers in a cool dry environment away from direct sunlight at a temperature of 40-70°F (4-21°C). Store away from light, acids, heat and sources of ignition. Shelf life is twelve months from date of manufacture.

### Disposal

SU-8 resist may be included with other waste containing similar organic solvents to be discarded for destruction or reclaim in accordance with local state and federal regulations. It is the responsibility of the customer to ensure the disposal of SU-8 resists and residues made in observance all federal, state, and local environmental regulations.

### Environmental, Health and Safety

Consult product Material Safety Data Sheet before working with SU-8 resists. Handle with care. Wear chemical goggles, chemical gloves and suitable protective clothing when handling SU-8 resist. Do not get into eyes, or onto skin or clothing. Use with adequate ventilation to avoid breathing vapors or mist. In case of contact with skin, wash affected area

with soap and water. In case of contact with eyes, rinse immediately with water and flush for 15 minutes lifting eyelids frequently. Get emergency medical assistance.

The information is based on our experience and is, we believe to be reliable, but may not be complete. We make no guarantee or warranty, expressed or implied, regarding the information, use, handling, storage, or possession of these products, or the application of any process described herein or the results desired, since the conditions of use and handling of these products are beyond our control.

© MicroChem Corp. copyright 2001.  
All rights reserved.

**MICRO CHEM**

1254 Chestnut Street  
Newton, MA 02464

tel: (617)965-5511 fax: (617)965-5818

email: [mcc@microchem.com](mailto:mcc@microchem.com) [www.microchem.com](http://www.microchem.com)  
Rev. 1/01

*First Design*

**GLASS HARDMASK FOR PATTERNING**

<b>Step 1:</b> Substrate Cleaning and Preparation	Time: 1 h 10 min Date: 15/09
Location: Grey area : wet bench	Responsible: User / Eng. Virgínia Soares
<p>1) <b>Substrate:</b> 1 Glass sample of 0.7 mm thickness (50x50 mm<sup>2</sup>)</p> <p>2) <b>Procedure:</b>                      Acetone to remove the glue + IPA to remove acetone residues + DI water + blow dry.                      - If not clean, dip in Alconox for 30 min (65°C + ultrasounds) + IPA + DI water + blow dry                      -Dry carefully with compressed air</p> <p><b>Observations/Comments:</b></p>	

<b>Step 2:</b> Al deposition – 3000 Å thickness film	Time: 20 min Date:15/09															
Location: Cleanroom ISO 5	Responsible: Eng. Fernando Silva															
<p>1) <b>Substrate:</b> 1 Glass sample (50x50 mm<sup>2</sup>)</p> <p>2) <b>Equipment:</b> Nordiko 7000 (clean-room)</p> <p>3) <b>Conditions:</b></p> <table border="1" style="width: 100%; border-collapse: collapse; margin: 10px 0;"> <thead> <tr> <th></th> <th>Mode</th> <th>Power (W)</th> <th>Ar flux (sccm)</th> <th>Pressure (mTorr)</th> </tr> </thead> <tbody> <tr> <td>Set</td> <td>MOD4 F8 Al 3000 Å</td> <td>2000</td> <td>50</td> <td>3</td> </tr> <tr> <td>Read</td> <td>-</td> <td>-</td> <td>-</td> <td>-</td> </tr> </tbody> </table> <p><b>Observations/Comments:</b> some defects in the deposition layer</p>			Mode	Power (W)	Ar flux (sccm)	Pressure (mTorr)	Set	MOD4 F8 Al 3000 Å	2000	50	3	Read	-	-	-	-
	Mode	Power (W)	Ar flux (sccm)	Pressure (mTorr)												
Set	MOD4 F8 Al 3000 Å	2000	50	3												
Read	-	-	-	-												

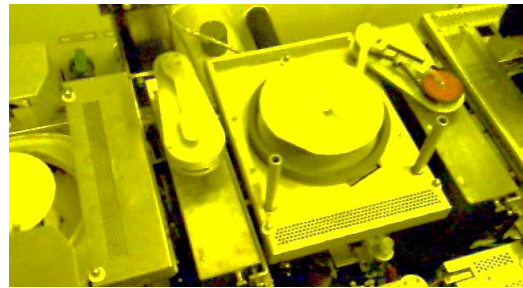
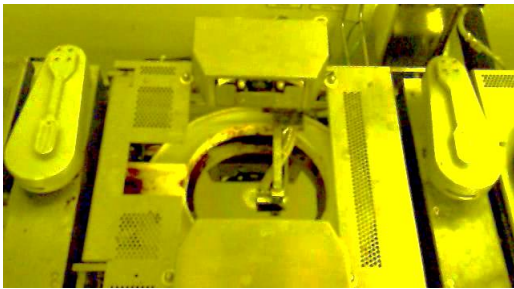
<b>Step 3:</b> Photolithography	Time: 1 h 30 min Date:17/09
Location: Cleanroom ISO 4	Responsible: Eng. José Bernardo
<p>1) <b>Substrate:</b> 1 Glass sample with Al Layer (50x50 mm<sup>2</sup>)</p> <p>2) <b>Equipment and Conditions:</b></p> <p>2.1. <b>Pre Treatment:</b> Vapor Prime 30 min (Recipe 0) — 40 min before lithography</p>	
Step description	Conditions
Wafer dehydration	Vacuum, 10 Torr, 2 min N <sub>2</sub> inlet, 760 Torr, 3 min Heating to 130 °C
Priming	Vacuum, 1 Torr, 3 min HDMS, 6 Torr, 5 min

Purge prime exhaust	Vacuum, 4 Torr, 1 min. N <sub>2</sub> inlet, 500 Torr, 2 min Vacuum, 4 Torr, 2 min
Return to atmosphere	N <sub>2</sub> inlet, 3 min

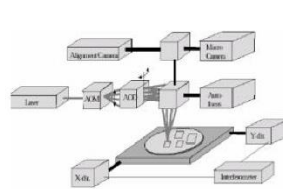
**Observations/Comments:**  
No need for Vapour priming as the minimum feature size of the design is >10 µm

2.2. **Coating:** 1.5 µm PR (Recipe 6/2) @ SGV track Photoresist: PFR7790G27cP

Step description	Coating Parameters
First Step	Dispense photoresist on the sample and spinning at 500 rpm for 10 s
Second step	Spin at 2500 rpm for 30 sec. to obtain ~1.45 µm thickness
Third step	Soft bake at 85 °C for 60 s



### Direct write laser (DWL)



*Heidelberg Instruments Direct Write Laser Lithography System:*  
Direct write lithography system  
HeCd laser (λ=442 nm (g-line) / write lens NA= 0.85) => critical dimensions down to 0.8 µm.  
System works with mask designs in GDS2 format.

### Observations/Comments:

2.3. **Exposing:** @ DWL, Heidelberg Instruments Direct Write Laser Lithography System

#### Conditions:

Map: AMSION\_C

Mask: \_\_\_\_\_ (@ h\_, non-inverted)

Sample Size: 37044 × 37236 µm

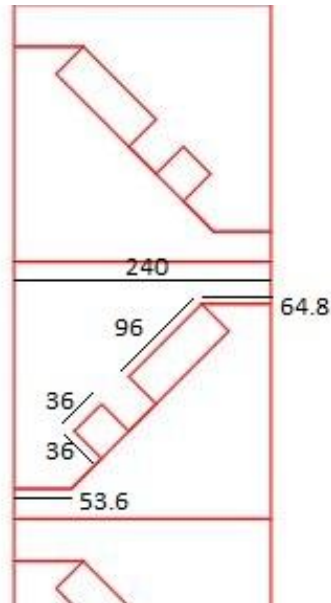
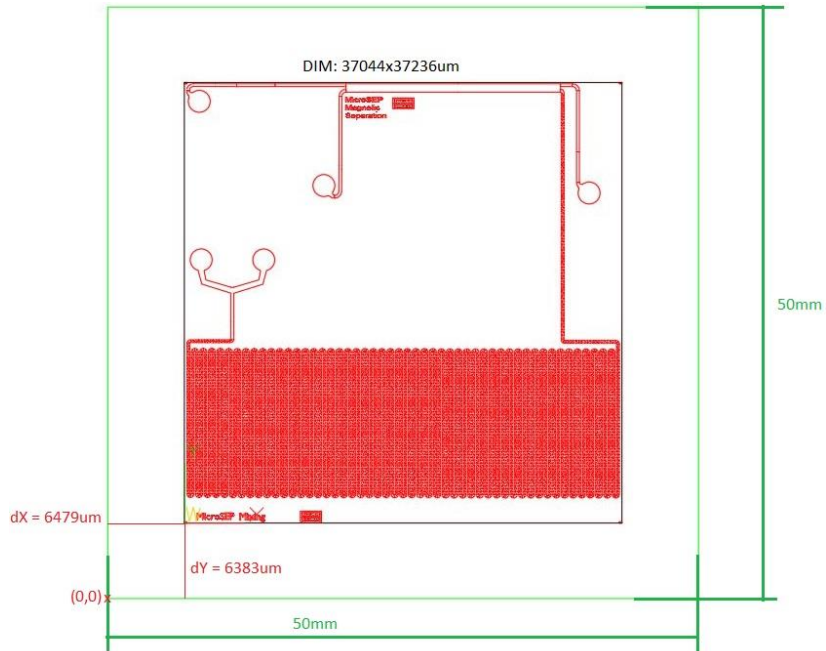
Energy: 95

Power:110mW

Focus:10



Mask (0,0) → Substrate ( 50000 , 50000 ) μm



(measures in μm if not specified differently)

**Observations/Comments:**

**Map MUST BE exposed (6479x6383) μm away from the substrate (60 x 60 mm) border**

**2.4. Microscope verification of PR exposure**

**After lithography and development, the sample must be covered as follows: Structures: without PR**

**Observations/Comments:**

2.5. <b>Development:</b> Recipe 6/2 @ SVG track		Developer: TMA238WA
Step description	Development Parameters	
First Step	Bake at 110 °C for 60 s	
Second step	Cool for 30 s	
Third step	Developer for 60 s	
<p><b>Observations/Comments:</b>  Check the feature size and shape under the optical microscope; check if resist is in expected areas  Check the resist thickness using the profilometer (Eng. José Bernardo)  Save all data/images in Transfer. Keep all originals with the runsheet</p>		

<b>Step 4:</b> Al Wet Etching	<b>Time:</b> 10 min	<b>Date:</b> 17/09								
<b>Location:</b> Cleanroom ISO 5 : wet bench	<b>Responsible:</b> User / Eng. Virgínia Soares									
<ol style="list-style-type: none"> <li><b>Substrate:</b> 1 Glass sample with Al Layer</li> <li><b>Equipment:</b> beakers, automatic agitation</li> <li><b>Conditions:</b></li> </ol> <table border="1"> <thead> <tr> <th>Solvent</th> <th>T (°C)</th> <th>Time</th> <th>Notes</th> </tr> </thead> <tbody> <tr> <td>TechniEtch Al 80 MOS Aluminum etchant</td> <td>RT</td> <td>5min</td> <td></td> </tr> </tbody> </table> <ol style="list-style-type: none"> <li><b>Substrate washing with DI water and drying with compressed air</b></li> <li><b>Microscope verification</b></li> </ol> <p><b>Observations/Comments:</b>  <b>Completely etch exposed Al features until glass substrate</b></p>			Solvent	T (°C)	Time	Notes	TechniEtch Al 80 MOS Aluminum etchant	RT	5min	
Solvent	T (°C)	Time	Notes							
TechniEtch Al 80 MOS Aluminum etchant	RT	5min								

<b>Step 5:</b> Resist Strip	<b>Time:</b> 1 h 10 min	<b>Date:</b> 17/09								
<b>Location:</b> Grey area : wet bench	<b>Responsible:</b> User / Eng. Virgínia Soares									
<ol style="list-style-type: none"> <li><b>Substrate:</b> 1 Glass sample with Al Layer + Photoresist (after etching)</li> <li><b>Equipment:</b> Thermal bath + Ultrasounds</li> <li><b>Conditions:</b></li> </ol> <table border="1"> <thead> <tr> <th>Solvent</th> <th>T (°C)</th> <th>Time</th> <th>Notes</th> </tr> </thead> <tbody> <tr> <td>Microstrip 3001 (Acetone)</td> <td>RT</td> <td>2min</td> <td></td> </tr> </tbody> </table> <ol style="list-style-type: none"> <li><b>Substrate washing with IPA, followed by rinsing DI water and drying with compressed air</b></li> <li><b>Microscope verification</b></li> </ol> <p><b>Observations/Comments:</b></p>			Solvent	T (°C)	Time	Notes	Microstrip 3001 (Acetone)	RT	2min	
Solvent	T (°C)	Time	Notes							
Microstrip 3001 (Acetone)	RT	2min								

## SOFT LITHOGRAPHY

**Step 1:** Substrate Cleaning and Preparation

**Time:** 1 h 10 min **Date:** 07/10/20

**Location:** Grey area : wet bench

**Responsible:** User / Eng. Virgínia Soares

- 1) **Substrate:** 1 Si sample of 0.7 mm thickness (60x60 mm<sup>2</sup>)
- 2) **Procedure:**  
Acetone to remove the glue + IPA to remove acetone residues + DI water + blow dry.  
- If not clean, dip in Alconox for 3 h (65°C + ultrasounds) + IPA + DI water + blow dry  
- Place at UVO cleaner for 15 min including 5 min exhaust time  
- Substrate must not have any visible residues.

**Observations/Comments:**

**Step 2:** Equipment check

**Time:** 10 min **Date:** 07/10/20

**Location:** PDMS room

**Responsible:** User / Eng. Virgínia Soares

- 1) **Procedure:**  
Assure that all required equipments are ON (laminar flow hood, vacuum pump, spinner and UV light;

**Observations/Comments:**

**Step 3:** Soft lithography

**Time:** 1 h 30 min **Date:** 07/10/20

**Location:** PDMS room

**Responsible:** User / Eng. Virgínia Soares

- 1) **Substrate:** 1 Si sample of 0.7 mm thickness (60x60 mm<sup>2</sup>)
- 2) **Equipment:** Aluminium foil, Hotplate (inside laminar flow hood), Spinner, UV lamp, glass beaker, tweezers, profilometer, microscope
- 3) **Procedure: for 100 µm**
  1. Substrate cleaning and preparation
  2. Substrate dehydration at **110 °C** for **5 min**
  3. Cool down to RT (**ramp as wanted**)
  4. Dispense **SU-8 50** photoresist (1 mL for each 1" substrate diameter = **2.75ml**)
  5. Spin coating **500 rpm** for **10 s** at **100 rpm.s<sup>-1</sup>**
  6. Spin coating **900 rpm** for **30 s** at **300 rpm.s<sup>-1</sup>**
  7. Pre-bake at **65 °C** for **10 min** (**ramp 2°C/min**)
  8. Soft bake at **95 °C** for **30 min** (**ramp 2°C/min**)
  9. Cool to room temperature before next step (**ramp 3°C/min**)
  10. Expose to **UV light** for **30 s**. UV Lamp energy intensity 5.55 W.cm<sup>-2</sup> @ slot 2

11. Post exposure bake at **65 °C** for **1 min. (ramp 2°C/min)**
  12. Post exposure bake at **95 °C** for **10 min. (ramp 2°C/min)**
  13. Cool to room temperature before next step (**ramp 3°C/min**)
  14. Develop with PGMEA with strong agitation for **15 min**, could be useful to be helped through a Pasteur pipette and could be necessary to add extra time:  
*Extra 5 min development after PGMEA solution substitution with fresh one*
  15. Clean with IPA and blow dry
- Perform dehydration bake on an aluminum foil topped hotplate (5 min) at 110°C. If using aluminum foil, bear in mind that the temperature of the top of aluminum foil is about 10 °C lower than the hotplate.
  - Try to keep SU-8 out of the bowl, chuck or any other part of the spinner tool. After usage, clean the spinner carefully
  - In case the tweezers get SU-8 on them, try to clean as best as you can with wipes and acetone/IPA after you finished
  - UV-Exposure: Make contact between the hard mask and the SU-8 sample with the **METAL SIDE IN CONTACT** with SU-8 minimizing the gap between them. Ensure that both pieces are mounted in the UV light center.
  - Post exposure bake: Polymer shrinkage of 7.5% with postbaked at 95°C (<http://memscyclopedia.org/su8.html>)
  - Developing step: If SU-8 is still undeveloped, a white precipitate will show at SU-8 surface. If this occurs put the substrate back in SU-8 developer for longer developing time

**Observations/Comments:**

Step 5. Coating speed chosen according to previous experiments

**USED MASK VERSION 3 (17/09/20)**

## PDMS CASTING

**Step 1:** PDMS preparation

**Time:** 1 h 10 min **Date:** 01/11/20

**Location:** PDMS room

**Responsible:** User / Eng. Virgínia Soares

- 1) Place the plastic cup in the analytical balance and tare (zero) the scale
- 2) Pour the dimethyl siloxane into the plastic cup and register the weight. Tare (zero) the scale
- 3) The quantity of curing agent is added in a proportion of 10:1 as depicted in the table

<b>Lot name</b>	<b>10:1 (for 2 parts)</b>	<b>Mass measured [g]</b>
Dimethyl siloxane	15 g	16.92g
Curing agent	1.5 g	1.693g

- 4) Add the desired amount of curing agent. Remove from balance and carefully mix with the spatula. Bubbles will form with agitation
- 5) Place the plastic cup with the mixture in the desiccator for 1 h to allow bubbles to be removed

- a. To *open the vacuum-sealed desiccator*, proceed as follows: first close the vacuum tap and open the air inlet. This will release the vacuum and stabilize the air pressure inside. This step must be performed slowly and carefully so the samples inside the desiccator do not spill nor fall. When the chamber is full with air, remove the top part of the desiccator by sliding it horizontally.
  - b. To *close the vacuum-sealed desiccator*, proceed as follows: first attach the top part of the desiccator to close it. Make sure it is well aligned with the bottom part. Next, close the air inlet. Then slowly open the vacuum tap to form a vacuum seal and remove any air from inside the desiccator.
- 6) Clean and organize the PDMS table
  - 7) If after 1 h bubbles are still present, leave the cup in the desiccator for another 30 min. Repeat until no bubbles are present
  - 8) If necessary, cover the cup with cling film and keep it in the fridge no longer than 15 h

**Observations:**

**Step 2:** Mold filling

**Time:** 30 min    **Date:** 01/11/20

**Location:** PDMS room

**Responsible:** User / Eng. Virgínia Soares

- 1) Carefully pour the PDMS into the molds. Proceed gently to avoid the formation and trapping of bubbles.

**Observations:**

**Step 3:** Baking and peeling

**Time:** 1 h    **Date:** 01/11/20

**Location:** PDMS room

**Responsible:** User / Eng. Virgínia Soares

- 1) Place the mold filled with PDMS and the membrane in the oven to bake at 70 °C for 1 h
- 2) Remove the mold from the oven
- 3) Peel the baked PDMS off from the bottom layer by using a scalpel and tweezers
- 4) Stow the PDMS device in a new/clean plastic box with molded features facing up. Prevent the PDMS from getting dirty (no fingertips, no dust, ..., use a clean box).

**Observations:**

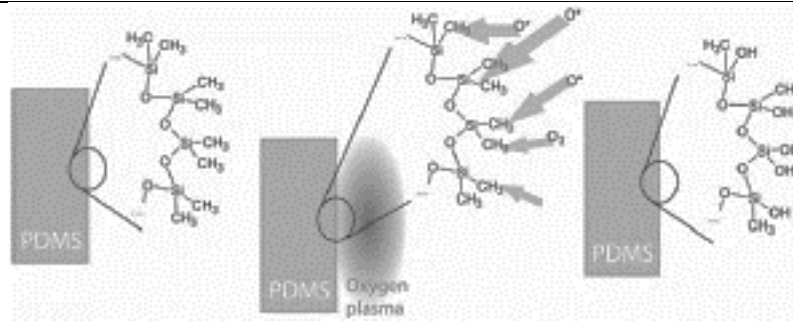
**Step 4:** Permanent bonding

**Time:** 30 min    **Date:** 01/11/20

**Location:** Grey Area

**Responsible:** User / Eng. Virgínia Soares

- 1) Take the molded PDMS to the Plasma Cleaner, in the Grey Area
- 2) Oxygen plasma treatment for 60 s @ MED (follow Plasma Cleaner Protocol), with the contact surface for bonding (exposed surface) facing up;



- 3) After the program finishes, quickly remove the PDMS and align face-to-face: the exposed glass surface onto the exposed PDMS microchannels surface;
- 4) Store it carefully, and use only after 24h
- 5) Blow dry

**Observations:**

## *Second Design*

# GLASS HARDMASK FOR PATTERNING

**Step 1:** Substrate Cleaning and Preparation

**Time:** 1 h 10 min    **Date:** 15/09

**Location:** Grey area : wet bench

**Responsible:** User / Eng. Virginia Soares

- 3) **Substrate:** 1 Glass sample of 0.7 mm thickness (50x50 mm<sup>2</sup>)
- 4) **Procedure:**  
 Acetone to remove the glue + IPA to remove acetone residues + DI water + blow dry.  
 - If not clean, dip in Alconox for 30 min (65°C + ultrasounds) + IPA + DI water + blow dry  
 -Dry carefully with compressed air

**Observations/Comments:**

**Step 2:** Al deposition – 3000 Å thickness film

**Time:** 20 min    **Date:** 15/09

**Location:** Cleanroom ISO 5

**Responsible:** Eng. Fernando Silva

- 4) **Substrate:** 1 Glass sample (50x50 mm<sup>2</sup>)
- 5) **Equipment:** Nordiko 7000 (clean-room)
- 6) **Conditions:**

	Mode	Power (W)	Ar flux (sccm)	Pressure (mTorr)
Set	MOD4 F8 Al 3000 Å	2000	50	3
Read	-	-	-	-

**Observations/Comments:** some defects in the deposition layer

--

**Step 3: Photolithography** **Time: 1 h 30 min** **Date:20/07**  
**Location: Cleanroom ISO 4** **Responsible: Eng. José Bernardo**

- 3) **Substrate: 1 Glass sample with Al Layer (60x60mm<sup>2</sup>)**
- 4) **Equipment and Conditions:**

~~2.6. Pre Treatment: Vapor Prime 30 min (Recipe 0) — 40 min before lithography~~

<b>Step description</b>	<b>Conditions</b>
Wafer dehydration	Vacuum, 10 Torr, 2 min N <sub>2</sub> inlet, 760 Torr, 3 min Heating to 130 °C
Priming	Vacuum, 1 Torr, 3 min HDMS, 6 Torr, 5 min
Purge prime exhaust	Vacuum, 4 Torr, 1 min. N <sub>2</sub> inlet, 500 Torr, 2 min Vacuum, 4 Torr, 2 min
Return to atmosphere	N <sub>2</sub> inlet, 3 min

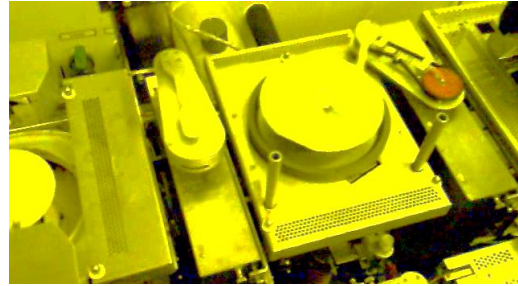
**Observations/Comments:**  
No need for Vapour priming as the minimum feature size of the design is 50 µm

2.7. **Coating:** 1.5 µm PR (Recipe 6/2) @ SGV track  
PFR7790G27cP

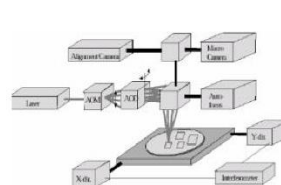
Photoresist:

<b>Step description</b>	<b>Coating Parameters</b>
First Step	Dispense photoresist on the sample and spinning at 500 rpm for 10 s
Second step	Spin at 2500 rpm for 30 sec. to obtain ~1.45 µm thickness
Third step	Soft bake at 85 °C for 60 s

**Observations/Comments:**



## Direct write laser (DWL)



*Heidelberg Instruments Direct Write Laser Lithography System:*

Direct write lithography system

HeCd laser ( $\lambda=442$  nm (g-line) / write lens NA= 0.85)  $\Rightarrow$  critical dimensions down to 0.8  $\mu\text{m}$ .

System works with mask designs in GDS2 format.

### 2.8. Exposing: @ DWL, Heidelberg Instruments Direct Write Laser Lithography System

#### Conditions:

Map: AMSION\_C

Mask: 100 $\mu\text{m}$ \_new\_V19p0 (@ h6, non-inverted)

Sample Size: 41000  $\times$  22000  $\mu\text{m}$

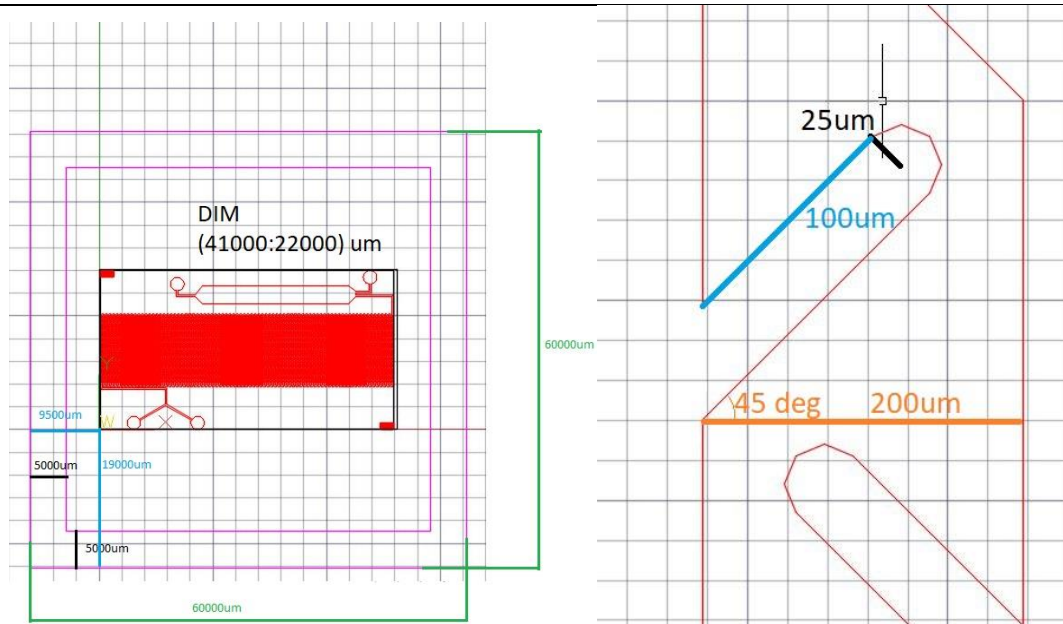
Energy: 95

Power:110 mW

Focus:10

Mask (0,0)  $\rightarrow$  Substrate ( 60000 , 60000 )  $\mu\text{m}$





**Observations/Comments:**

Map **MUST BE** exposed (9500x19000)  $\mu\text{m}$  away from the substrate (60 x 60  $\text{mm}^2$ ) border

**2.9. Microscope verification of PR exposure**

After lithography and development, the sample must be covered as follows: Structures: without PR

**Observations/Comments:**

**2.10. Development:** Recipe 6/2 @ SVG track

Developer: TMA238WA

Step description	Development Parameters
First Step	Bake at 110 °C for 60 s
Second step	Cool for 30 s
Third step	Developer for 60 s

**Observations/Comments:**

Check the feature size and shape under the optical microscope; check if resist is in expected areas  
 Check the resist thickness using the profilometer (Eng. José Bernardo)  
 Save all data/images in Transfer. Keep all originals with the runsheet

**Step 4:** Al Wet Etching

**Time:** 10 min **Date:**17/09

**Location:** Cleanroom ISO 5 : wet bench

**Responsible:** User / Eng. Virgínia Soares

6) **Substrate:** 1 Glass sample with Al Layer

7) **Equipment:** beakers, automatic agitation

8) **Conditions:**

Solvent	T (°C)	Time	Notes
TechniEtch Al 80 MOS Aluminum etchant	RT	5min	

9) **Substrate washing with DI water and drying with compressed air**

10) **Microscope verification**

**Observations/Comments:**

Completely etch exposed Al features until glass substrate

**Step 5: Resist Strip**

**Time: 1 h 10 min Date:17/09**

**Location:** Grey area : wet bench

**Responsible: User / Eng. Virgínia Soares**

6) **Substrate: 1 Glass sample with Al Layer + Photoresist (after etching)**

7) **Equipment:** Thermal bath + Ultrasounds

8) **Conditions:**

Solvent	T (°C)	Time	Notes
Microstrip (Acetone)	300± RT	2min	

9) **Substrate washing with IPA, followed by rinsing DI water and drying with compressed air**

10) **Microscope verification**

**Observations/Comments:**

## SOFT LITHOGRAPHY

**Step 1: Substrate Cleaning and Preparation**

**Time: 1 h 10 min Date:07/10/20**

**Location:** Grey area : wet bench

**Responsible: User / Eng. Virgínia Soares**

3) **Substrate: 1 Si sample of 0.7 mm thickness (60x60 mm<sup>2</sup>)**

4) **Procedure:**

Acetone to remove the glue + IPA to remove acetone residues + DI water + blow dry.

- If not clean, dip in Alconox for 3 h (65°C + ultrasounds) + IPA + DI water + blow dry

- Place at UVO cleaner for 15 min including 5 min exhaust time

- Substrate must not have any visible residues.

**Observations/Comments:**

<b>Step 2:</b> Equipment check	<b>Time:</b> 10 min <b>Date:</b> 07/10/20
<b>Location:</b> PDMS room	<b>Responsible:</b> User / Eng. Virgínia Soares
<p>2) <b>Procedure:</b> Assure that all required equipments are ON (laminar flow hood, vacuum pump, spinner and UV light);</p> <p><b>Observations/Comments:</b></p>	

<b>Step 3:</b> Soft lithography	<b>Time:</b> 1 h 30 min <b>Date:</b> 07/10/20
<b>Location:</b> PDMS room	<b>Responsible:</b> Eng. Virgínia Soares
<p>4) <b>Substrate:</b> 1 Si sample of 0.7 mm thickness (70x70mm<sup>2</sup>)</p> <p>5) <b>Equipment:</b> Aluminium foil, Hotplate (inside laminar flow hood), Spinner, UV lamp, glass beaker, tweezers, profilometer, microscope</p> <p>6) <b>Procedure: for 100 µm</b></p> <ol style="list-style-type: none"> <li>1. Substrate cleaning and preparation</li> <li>2. Substrate dehydration at <b>110 °C</b> for <b>5 min</b></li> <li>3. Cool down to RT</li> <li>4. Dispense <b>SU-8 50</b> photoresist (1 mL for each 1" substrate diameter)</li> <li>5. Spin coating <b>500 rpm</b> for <b>10 s</b> at <b>100 rpm.s<sup>-1</sup></b></li> <li>6. Spin coating <b>900 rpm</b> for <b>30 s</b> at <b>300 rpm.s<sup>-1</sup></b></li> <li>7. Pre-bake at <b>65 °C</b> for <b>10 min (ramp 2°C/min)</b></li> <li>8. Soft bake at <b>95 °C</b> for <b>30 min (ramp 2°C/min)</b></li> <li>9. Cool to room temperature before next step (<b>ramp 5°C/min</b>)</li> <li>10. Expose to <b>UV light</b> for <b>30 s</b>. UV Lamp energy intensity 5.55 W.cm<sup>-2</sup> @ slot 2</li> <li>11. Post exposure bake at <b>65 °C</b> for <b>1 min. (ramp 2°C/min)</b></li> <li>12. Post exposure bake at <b>95 °C</b> for <b>10 min. (ramp 2°C/min)</b></li> <li>13. Cool to room temperature before next step (<b>ramp 5°C/min</b>)</li> <li>14. Develop with PGMEA during <b>15 min</b> with strong agitation</li> <li>15. Clean with IPA and blow dry</li> </ol> <ul style="list-style-type: none"> <li>- Perform dehydration bake on an aluminum foil topped hotplate (5 min) at 110°C. If using aluminum foil, bear in mind that the temperature of the top of aluminum foil is about 10 °C lower than the hotplate.</li> <li>- Try to keep SU-8 out of the bowl, chuck or any other part of the spinner tool. After usage, clean the spinner carefully</li> <li>- In case the tweezers get SU-8 on them, try to clean as best as you can with wipes and acetone/IPA after you finished</li> <li>- UV-Exposure: Make contact between the hard mask and the SU-8 sample with the <b>METAL SIDE IN CONTACT</b> with SU-8 minimizing the gap between them. Ensure that both pieces are mounted in the UV light center.</li> <li>- Post exposure bake: Polymer shrinkage of 7.5% with postbaked at 95°C (<a href="http://memscyclopedia.org/su8.html">http://memscyclopedia.org/su8.html</a>)</li> </ul>	

- Developing step: If SU-8 is still undeveloped, a white precipitate will show at SU-8 surface. If this occurs put the substrate back in SU-8 developer for longer developing time

**Observations/Comments:**

**Step 5 chosen depending on results on MicroSEP**

**USED MASK VERSION II 17/09/20**

## PDMS CASTING

**Step 1: PDMS preparation**

**Time: 1 h 10 min Date: 01/11/20**

**Location: PDMS room**

**Responsible: User / Eng. Virgínia Soares**

- 9) Place the plastic cup in the analytical balance and tare (zero) the scale
- 10) Pour the dimethyl siloxane into the plastic cup and register the weight. Tare (zero) the scale
- 11) The quantity of curing agent is added in a proportion of 10:1 as depicted in the table

<i>Lot name</i>	<b>10:1 (for 2 parts)</b>	<b>Mass measured [g]</b>
Dimethyl siloxane	15 g	15.33g
Curing agent	1.5 g	1.541g

- 12) Add the desired amount of curing agent. Remove from balance and carefully mix with the spatula. Bubbles will form with agitation
- 13) Place the plastic cup with the mixture in the desiccator for 1 h to allow bubbles to be removed
  - a. To *open the vacuum-sealed desiccator*, proceed as follows: first close the vacuum tap and open the air inlet. This will release the vacuum and stabilize the air pressure inside. This step must be performed slowly and carefully so the samples inside the desiccator do not spill nor fall. When the chamber is full with air, remove the top part of the desiccator by sliding it horizontally.
  - b. To *close the vacuum-sealed desiccator*, proceed as follows: first attach the top part of the desiccator to close it. Make sure it is well aligned with the bottom part. Next, close the air inlet. Then slowly open the vacuum tap to form a vacuum seal and remove any air from inside the desiccator.
- 14) Clean and organize the PDMS table
- 15) If after 1 h bubbles are still present, leave the cup in the desiccator for another 30 min. Repeat until no bubbles are present
- 16) If necessary, cover the cup with cling film and keep it in the fridge no longer than 15 h

**Observations:**

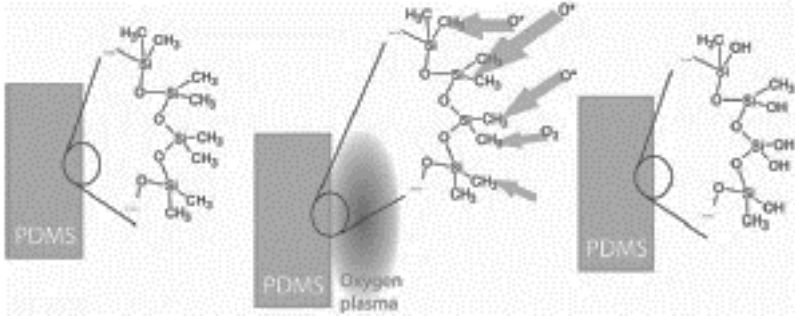
**Step 2: Mold filling**

**Time: 30 min**

**Date: 01/11/20**

<b>Location:</b> PDMS room	<b>Responsible:</b> User / Eng. Virgínia Soares
2) Carefully pour the PDMS into the molds. Proceed gently to avoid the formation and trapping of bubbles. <b>Observations:</b>	

<b>Step 3:</b> Baking and peeling	<b>Time:</b> 1 h	<b>Date:</b> 01/11/20
<b>Location:</b> PDMS room	<b>Responsible:</b> User / Eng. Virgínia Soares	
5) Place the mold filled with PDMS and the membrane in the oven to bake at 70 °C for 1 h 6) Remove the mold from the oven 7) Peel the baked PDMS off from the bottom layer by using a scalpel and tweezers 8) Stow the PDMS device in a new/clean plastic box with molded features facing up. Prevent the PDMS from getting dirty (no fingertips, no dust, ..., use a clean box).  <b>Observations:</b>		

<b>Step 4:</b> Permanent bonding	<b>Time:</b> 30 min	<b>Date:</b> 01/11/20
<b>Location:</b> Grey Area	<b>Responsible:</b> User / Eng. Virgínia Soares	
6) Take the molded PDMS to the Plasma Cleaner, in the Grey Area 7) Oxygen plasma treatment for 60 s @ MED (follow Plasma Cleaner Protocol), with the contact surface for bonding (exposed surface) facing up;   8) After the program finishes, quickly remove the PDMS and align face-to-face: the exposed glass surface onto the exposed PDMS microchannels surface; 9) Store it carefully, and use only after 24h 10) Blow dry  <b>Observations:</b>		

7.6. Appendix F: Antibodies AbCam Datasheets  
*ab68539 Rb pAb to Pseudomonas aeruginosa (biotin)*



## Product datasheet

# Anti-Pseudomonas antibody (Biotin) ab68539

★★★★☆ 2 Abreviews

### Overview

<b>Product name</b>	Anti-Pseudomonas antibody (Biotin)
<b>Description</b>	Rabbit polyclonal to Pseudomonas (Biotin)
<b>Host species</b>	Rabbit
<b>Conjugation</b>	Biotin
<b>Tested applications</b>	<b>Suitable for:</b> ICC/IF, IHC-Fr
<b>Species reactivity</b>	<b>Reacts with:</b> Other species
<b>Immunogen</b>	Tissue/ cell preparation - whole cells of Pseudomonas aeruginosa
<b>General notes</b>	<p>Reproducibility is key to advancing scientific discovery and accelerating scientists' next breakthrough.</p> <p>Abcam is leading the way with our range of recombinant antibodies, knockout-validated antibodies and knockout cell lines, all of which support improved reproducibility.</p> <p>We are also planning to innovate the way in which we present recommended applications and species on our product datasheets, so that only applications &amp; species that have been tested in our own labs, our suppliers or by selected trusted collaborators are covered by our Abpromise™ guarantee.</p> <p>In preparation for this, we have started to update the applications &amp; species that this product is Abpromise guaranteed for.</p> <p>We are also updating the applications &amp; species that this product has been "predicted to work with," however this information is not covered by our Abpromise guarantee.</p> <p>Applications &amp; species from publications and Abreviews that have not been tested in our own labs or in those of our suppliers are not covered by the Abpromise guarantee.</p> <p>Please check that this product meets your needs before purchasing. If you have any questions, special requirements or concerns, please send us an inquiry and/or contact our Support team ahead of purchase. Recommended alternatives for this product can be found below, as well as customer reviews and Q&amp;As.</p>

### Properties

<b>Form</b>	Liquid
<b>Storage instructions</b>	Shipped at 4°C. Store at +4°C short term (1-2 weeks). Store at -20°C or -80°C. Avoid freeze /

	thaw cycle.
<b>Storage buffer</b>	pH: 7.2 Preservative: 0.1% Sodium azide Constituent: 0.0268% PBS
<b>Purity</b>	Protein A purified
<b>Clonality</b>	Polyclonal
<b>Isotype</b>	IgG

### Applications

Our [Abpromise guarantee](#) covers the use of **ab68539** in the following tested applications.

The application notes include recommended starting dilutions; optimal dilutions/concentrations should be determined by the end user.

Application	Abreviews	Notes
ICC/IF		Use at an assay dependent concentration.
IHC-Fr		Use at an assay dependent concentration.

### Target

<b>Relevance</b>	Pseudomonas are Gram-negative rod bacteria commonly found in soil, ground water, plants and animals. The most common form is Pseudomonas aeruginosa which is an opportunistic pathogen of both humans and plants.
------------------	---

**Please note:** All products are "FOR RESEARCH USE ONLY. NOT FOR USE IN DIAGNOSTIC PROCEDURES"

### Our Abpromise to you: Quality guaranteed and expert technical support

- Replacement or refund for products not performing as stated on the datasheet
- Valid for 12 months from date of delivery
- Response to your inquiry within 24 hours
- We provide support in Chinese, English, French, German, Japanese and Spanish
- Extensive multi-media technical resources to help you
- We investigate all quality concerns to ensure our products perform to the highest standards

If the product does not perform as described on this datasheet, we will offer a refund or replacement. For full details of the Abpromise, please visit <https://www.abcam.com/abpromise> or contact our technical team.

### Terms and conditions

- Guarantee only valid for products bought direct from Abcam or one of our authorized distributors



## Product datasheet

# Anti-*Klebsiella* spp antibody (Biotin) ab69468

### Overview

---

<b>Product name</b>	Anti- <i>Klebsiella</i> spp antibody (Biotin)
<b>Description</b>	Rabbit polyclonal to <i>Klebsiella</i> spp (Biotin)
<b>Host species</b>	Rabbit
<b>Conjugation</b>	Biotin
<b>Specificity</b>	ab69468 reacts with <i>Klebsiella</i> sp. in bacterial and infected tissue samples.
<b>Tested applications</b>	<b>Suitable for:</b> IHC-Fr, WB, ELISA, ICC/IF
<b>Species reactivity</b>	<b>Reacts with:</b> Species independent
<b>Immunogen</b>	Whole cell <i>Klebsiella pneumoniae</i>
<b>General notes</b>	<p>Reproducibility is key to advancing scientific discovery and accelerating scientists' next breakthrough.</p> <p>Abcam is leading the way with our range of recombinant antibodies, knockout-validated antibodies and knockout cell lines, all of which support improved reproducibility.</p> <p>We are also planning to innovate the way in which we present recommended applications and species on our product datasheets, so that only applications &amp; species that have been tested in our own labs, our suppliers or by selected trusted collaborators are covered by our Abpromise™ guarantee.</p> <p>In preparation for this, we have started to update the applications &amp; species that this product is Abpromise guaranteed for.</p> <p>We are also updating the applications &amp; species that this product has been "predicted to work with," however this information is not covered by our Abpromise guarantee.</p> <p>Applications &amp; species from publications and Abreviews that have not been tested in our own labs or in those of our suppliers are not covered by the Abpromise guarantee.</p> <p>Please check that this product meets your needs before purchasing. If you have any questions, special requirements or concerns, please send us an inquiry and/or contact our Support team ahead of purchase. Recommended alternatives for this product can be found below, as well as customer reviews and Q&amp;As.</p>

### Properties

---

<b>Form</b>	Liquid
<b>Storage instructions</b>	Shipped at 4°C. Store at +4°C short term (1-2 weeks). Store at -20°C or -80°C. Avoid freeze /



	thaw cycle.
<b>Storage buffer</b>	pH: 7.2 Preservative: 0.1% Sodium azide Constituent: 0.0268% PBS
<b>Purity</b>	Affinity purified
<b>Clonality</b>	Polyclonal
<b>Isotype</b>	IgG

### Applications

Our [Abpromise guarantee](#) covers the use of **ab69468** in the following tested applications.

The application notes include recommended starting dilutions; optimal dilutions/concentrations should be determined by the end user.

Application	Abreviews	Notes
IHC-Fr		Use at an assay dependent dilution.
WB		Use at an assay dependent dilution.
ELISA		Use at an assay dependent dilution.
ICC/IF		Use at an assay dependent dilution.

### Target

**Relevance** Klebsiella is a genus of non-motile, Gram-negative, Oxidase-negative bacteria with a prominent polysaccharide-based capsule. Frequent human pathogens, Klebsiella organisms can lead to a wide range of disease states, notably pneumonia, urinary tract infections, septicemia, Ankylosing spondylitis, and soft tissue infections. Klebsiella pneumoniae is clinically the most important member of the Klebsiella genus of Enterobacteriaceae. New antibiotic resistant strains of K. pneumoniae are appearing, and it is increasingly found as a nosocomial infection.

**Please note:** All products are "FOR RESEARCH USE ONLY. NOT FOR USE IN DIAGNOSTIC PROCEDURES"

### Our Abpromise to you: Quality guaranteed and expert technical support

- Replacement or refund for products not performing as stated on the datasheet
- Valid for 12 months from date of delivery
- Response to your inquiry within 24 hours
- We provide support in Chinese, English, French, German, Japanese and Spanish
- Extensive multi-media technical resources to help you
- We investigate all quality concerns to ensure our products perform to the highest standards

If the product does not perform as described on this datasheet, we will offer a refund or replacement. For full details of the Abpromise, please visit <https://www.abcam.com/abpromise> or contact our technical team.